AD 606569

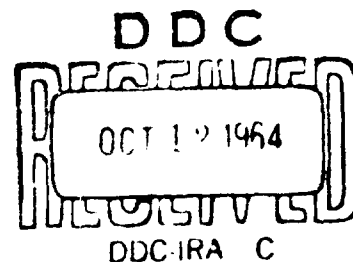# STUDY AND EXPLORATORY FREE-FLIGHT INVESTIGATION OF DEPLOYABLE AERODYNAMIC DECELERATORS OPERATING AT HIGH ALTITUDES AND AT HIGH MACH NUMBERS

D D C

OCT 1 ? 1964

DDC-IRA   C

FOREWORD

This report was prepared by the Cook Research Laboratories, Tech-Center Division of the Cook Electric Company, Morton Grove, Illinois, in compliance with Contract No. AF 33(657)-8423, Project No. 6065, Task No. 606505. The Recovery and Crew Station Branch of the Air Force Flight Dynamics Laboratory, Research and Technology Division, was the initiating agency with Mr. Charles A. Babish III serving as Project Officer. The work at the Cook Research Laboratories was under the supervision of Mr. R. C. Edwards; Director, Mr. L. J. Lorenz, Manager; and Dr. R. J. Benjamin, Director of Engineering of the Aerospace Technology Section. The program was directed by Mr. W. M. Gran, Program Manager and Mr. W. E. Nickel, Project Engineer.

Staff members who contributed to the project include: F. A. Ruprecht, Executive Engineer; L. W. Sims, Staff Engineer; L. J. Richter, Staff Engineer; J. Elliott, Senior Engineer; E. C. Gregory, Senior Engineer; P. A. Minerva, Senior Engineer; R. D. Turner, Senior Engineer; R. Goldbach, Design; H. J. Loellbach, Junior Engineer; G. L. Williams, Engineering Specialist; B. Lund, Modelmaker; G. Hausler, Technician; E. Rosiak, Technician; and J. Wilbanks, Technician.

REPRODUCTION QUALITY NOTICE

This document is the best quality available. The copy furnished to DTIC contained pages that may have the following quality problems:

- Pages smaller or larger than normal.

- Pages with background color or light colored printing.

- Pages with small type or poor printing; and or

- Pages with continuous tone material or color photographs.

Due to various output media available these conditions may or may not cause poor legibility in the microfiche or hardcopy output you receive.

☐ If this block is checked, the copy furnished to DTIC contained pages with color printing, that when reproduced in Black and White, may change detail of the original copy.

ABSTRACT

Thirteen parachute decelerator tests were performed at the Gulf Test Range of the Air Proving Ground Center at Eglin Air Force Base, Florida. These tests were accomplished through the use of multistage rocket boosters. The Cree payload vehicle was used as the test platform and data gathering system. These tests were conducted using both Hyperflo and Hemisflo parachutes which were deployed at predetermined Mach number-altitude regimes. Tests were accomplished over a Mach number range of 0.2 to 4.4 and an altitude range of 45,000 to 190,000 feet.

The data presented includes drag coefficients versus Mach number, dynamic pressure, Reynolds number and velocity, canopy angles of oscillation, canopy temperatures and general design considerations.

From this parachute decelerator test program, it may be concluded that Perlon mesh roof Hyperflo parachutes perform satisfactorily through Mach 2.1, that Nomex ribbon Hyperflo parachutes perform satisfactorily through Mach 4.0 and that Nomex Hemisflo parachutes perform satisfactorily through Mach 3.4. These Mach numbers apply in an altitude regime of 80,000 to 140,000 feet. The stainless steel mesh roof Hyperflo parachutes were unsatisfactory, and the Perlon mesh roof Hyperflo at a Mach number of 3.1 suffered complete canopy destruction due to aerodynamic heating.

iii

TABLE OF CONTENTS

iv

TABLE OF CONTENTS (Cont'd)

v

ILLUSTRATIONS

ILLUSTRATIONS (Cont'd)

ILLUSTRATIONS (Cont'd)

ILLUSTRATIONS (Cont'd)

ILLUSTRATIONS (Cont'd)

TABLES

SYMBOLS AND NOMENCLATURE

A   -   area (ft^2)

C   -   canopy factor (dimensionless)

C_D -   drag coefficient (dimensionless)

C_r -   root chord (ft)

C_L -   lift curve slope (per radian)

C_N -   normal force curve slope (per radian)

C_p -   fluid specific heat at constant pressure $(\frac{BTU\text{-}ft}{lb\ sec^2\ °R})$,

                material specific heat $(\frac{BTU}{lb\ °R})$

D   -   parachute diameter (ft)

                body diameter (ft)

F_o -   parachute opening shock (lbs)

L   -   lift force (lbs)

L_C -   canopy stress (lb/in)

L_S -   suspension line load (lbs)

M   -   material factor (dimensionless)

N   -   normal force (lbs)

P_r -   Prandtl number (dimensionless)

R   -   reefing factor (dimensionless)

S   -   canopy area (ft^2)

                planform area (ft^2)

T — temperature (^{O}R)

T_a — radiation sink temperature (^{O}R)

T_r — recovery temperature (^{O}R)

T_w — wall temperature (^{O}R)

V — velocity (ft/sec)

W — weight (lbs)

X — decreasing factor (dimensionless)

- -

a — body radius (ft)

Δa — relative acceleration (ft/sec^2)

b — body radius plus semi-span (ft)

d_B — vehicle base diameter (ft)

g — local acceleration of gravity (ft/sec^2)

h — heat transfer coefficient (BTU/ft^{2}sec^{O}R)

n — number of suspension lines

q — dynamic pressure, $(\rho/2) V^2$ (lb/ft^2)

r — recovery factor (dimensionless)

rps — angular velocity (revolutions/sec)

t_f — parachute filling time (sec)

u   -   velocity (ft/sec)

x   -   distance aft of forebody base (ft)

- -

β -   stagnation point velocity gradient $(\frac{ft\ sec^{-1}}{ft})$

ϵ -   emissivity (dimensionless)

Λ -   angle of sweep (degrees)

γ -   angle between two diametrically opposite suspension

lines (degrees)

μ -   coefficient of fluid viscosity $(\frac{lb\text{-}sec}{Ft^2})$

ρ -   fluid density $(\frac{lb\text{-}sec^2}{ft^4})$

σ -   Stefan-Boltzman constant $(\frac{BTU}{ft^2\ sec\,^\circ R^4})$

- -

Subscripts

δ -   condition outside boundary layer

∞ -   free-stream conditions

comp-   compressibility correction

inc -   refers to incompressible

1   -   forward vehicle

2   -   rear vehicle

p   -   projected (frontal)

o   -   total

1. INTRODUCTION

1.1 General

This report contains the objectives, results, and conclusions of the test program entitled "Study and Exploratory Free-Flight Investigation of Deployable Aerodynamic Decelerators Operating at High Altitudes and at High Mach Numbers", in accordance with the provisions of Contract AF 33(657)-8423. A total of 13 ground-launched test missions were accomplished at the Air Proving Ground Center, Eglin Air Force Base, Florida. A typical three-stage booster-Cree configuration is shown in Figure 1-1.

1.2 Objectives

The objectives of this test program were two-fold; first, to further advance the state of the art of textile parachutes in the regime of high Mach numbers at high altitude, and second, to substantiate wind tunnel data. Test Mach numbers and altitudes were to vary from 2.5 to 4.4 and from 70,000 to 190,000 feet, respectively. All the parachutes tested, except for Tests 1 and 8, were 2.71 and 3.69 feet D_o Hyperflos. Tests 1 and 8 employed a 4.12 ft D_o Hemisflo.

Among the major parameters to be measured or obtained were parachute force, parachute oscillation, parachute temperature, parachute C_D, vehicle Mach number, vehicle velocity, vehicle altitude, dynamic pressure and Reynolds number. All of the above parameters were to be obtained versus time.

1.3 Background

Parachute testing, using the Cree vehicle as a test platform, has been accomplished by the Tech-Center Division of Cook Electric Company, under Air Force Contracts AF 33(616)-3664, AF 33(616)-5507, and AF 33(616)-7016. Forty-one test missions have occurred during these past test programs. An additional 13 tests were accomplished under the current Air Force Contract, AF 33(657)-8423, for a total of 54 free-flight decelerator tests. Of these 54 tests, 20 have taken place from aircraft-launched Crees, six from balloon-launched Crees, and 38 from ground-launched Crees (see Table 1-1 for field test summary).

Manuscript released by the authors January 1964 for publication as an RTD Technical Documentary Report.

1
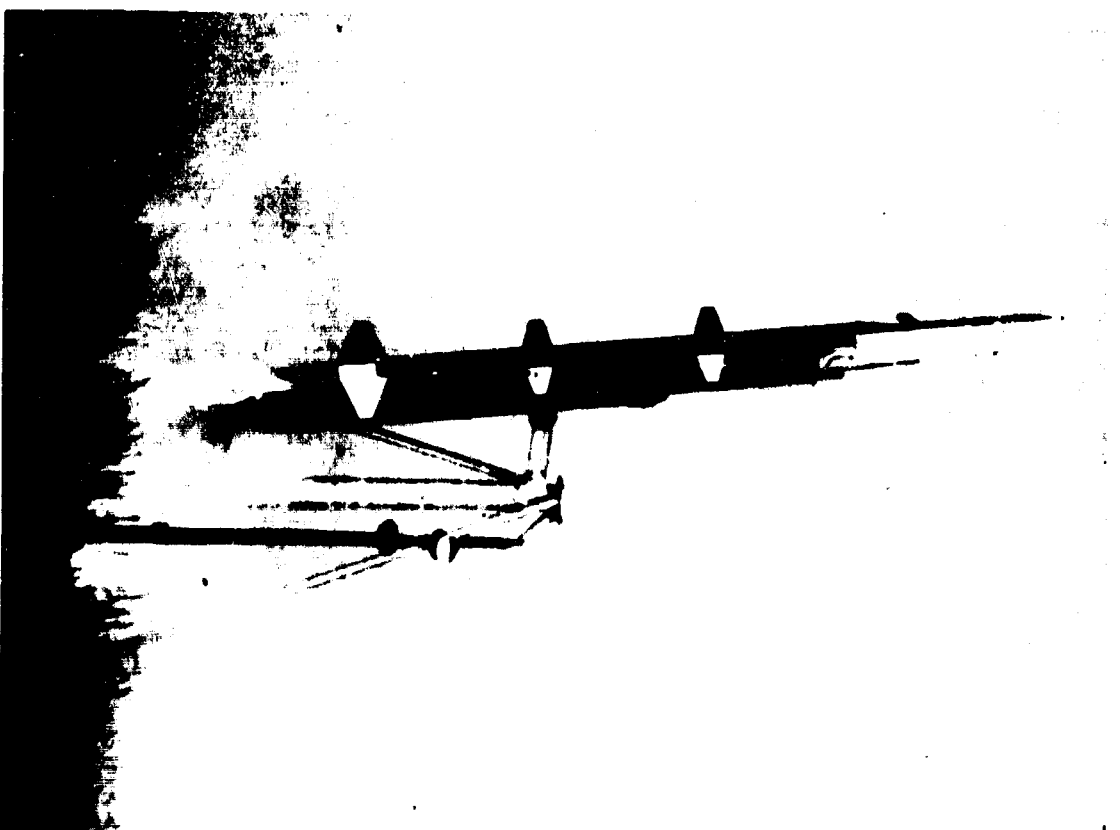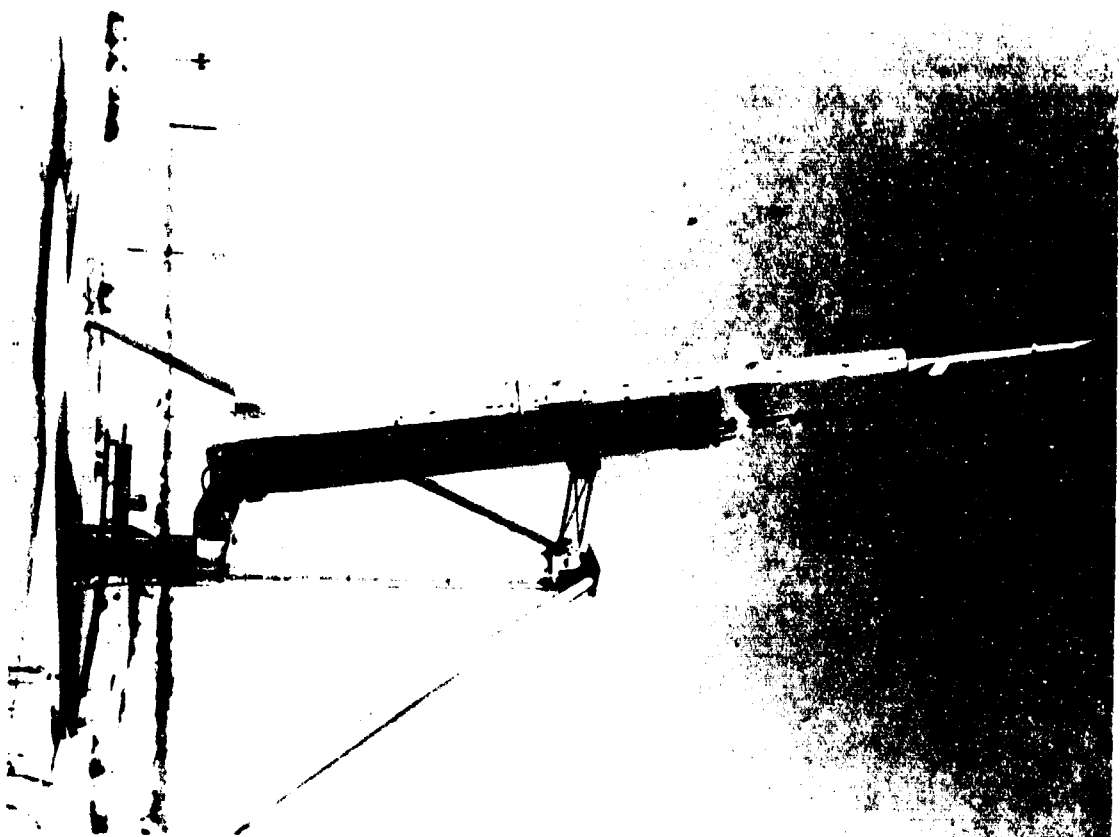
Figure 1.1 Typical Cree Three Stage Launch Configurations

TABLE 1-1

FIELD TEST PROGRAM SUMMARY

Mission No.	Mach No.	Altitude in Feet	Test Site	Type Launch	Vehicle Test Weight (lbs.)
1	0.5	15,000	El Centro	Aircraft	170
2	0.75	15,000	El Centro	Aircraft	500
3	0.75	15,000	El Centro	Aircraft	500
4	0.75	15,000	El Centro	Aircraft	170
5	0.75	15,000	El Centro	Aircraft	170
6	0.5	15,000	El Centro	Aircraft	170
7	0.5	15,000	El Centro	Aircraft	170
8	0.5	15,000	El Centro	Aircraft	170
9	0.5	30,000	El Centro	Aircraft	500
10	0.5	30,000	El Centro	Aircraft	800
11	0.75	30,000	El Centro	Aircraft	170
12	0.75	30,000	El Centro	Aircraft	800
13	0.5	30,000	El Centro	Aircraft	500
14	0.75	15,000	El Centro	Aircraft	500
15	0.75	30,000	El Centro	Aircraft	500
16	0.75	30,000	El Centro	Aircraft	500
17	0.75	15,000	El Centro	Aircraft	Cluster*
18	0.75	15,000	El Centro	Aircraft	Cluster*
19	0.5	70,000	Holloman	Balloon	Cluster*
20	0.5	70,000	Holloman	Balloon	Cluster*
21	0.75	70,000	Holloman	Balloon	Cluster*
22	2.0	30,000	El Centro	Aircraft	Cluster*
23	2.0	30,000	El Centro	Aircraft	Cluster*
24	0.75	70,000	Holloman	Balloon	Cluster*
25	0.75	100,000	Holloman	Balloon	Cluster*
26	2.0	30,000	El Centro	Aircraft	Cluster*
27	0.5	100,000	Holloman	Balloon	Cluster*
28	1.5	25,000	Eglin	Ground	800
29	1.5	66,000	Eglin	Ground	800
30	1.5	66,000	Eglin	Ground	800
31	1.87	50,000	Eglin	Ground	800
32	1.87	50,000	Eglin	Ground	800
33	1.705	68,800	Eglin	Ground	800
34	1.44	122,000	Eglin	Ground	500
35	2.77	74,800	Eglin	Ground	800
36	2.45	60,000	Eglin	Ground	230
37	1.52	123,000	Eglin	Ground	500
38	3.0	70,000	Eglin	Ground	230
39	0.43	8,950	Eglin	Ground	800
40	1.02	162,990	Eglin	Ground	800
41	3.0	59,200	Eglin	Ground	800
42	2.4	82,800	Eglin	Ground	820
43	2.8	101,000	Eglin	Ground	540
44	2.1	100,000	Eglin	Ground	540
45	3.0	121,000	Eglin	Ground	540
46	3.2	84,500	Eglin	Ground	540
47	4.0	122,700	Eglin	Ground	540
48	0.5	44,000	Eglin	Ground	540
49	3.56	109,000	Eglin	Ground	840
50	0.4	30,000	Eglin	Ground	540
51	3.0	190,000	Eglin	Ground	680
52	4.4	100,000	Eglin	Ground	540
53	3.2	79,000	Eglin	Ground	540
54	2.95	154,000	Eglin	Ground	600

*Cluster consists of one each, 200, 500 and 800 pound Cree Vehicles.

3

Under the above past contracts, Hemisflo parachutes performed satisfactorily up to a Mach number of about 2.0. Beyond Mach 2.0, the parachutes tested exhibited erratic performance which resulted in considerable canopy damage. Under the present contract, the state of the art for ribbon-roofed Hyperflo parachutes has been advanced to Mach 4.0 and for Hemisflo parachutes to Mach 3.5.

Wind tunnel tests were accomplished by the Tech-Center Division of Cook Electric Company under Air Force Contract AF 33(616)-8459. During these tests the canopy shape called "Hyperflo" evolved. This parachute performed satisfactorily in the wind tunnel up to a maximum tested Mach number of 4.65. Tests later performed by the Flight Dynamics Laboratory extended this Mach number range to 6.0.

2.   DISCUSSION OF RESULTS

The following is a discussion of the test canopies, results of the test program and associated analyses. A summary of the test data may be found in Appendix A of this report.

Thirteen tests were accomplished under the present contract. Of these 13 tests, 2 were with Hemisflo canopies and 11 were with Hyperflo canopies. Test data were gathered at Mach numbers and altitudes that varied from 0.2 to 4.4 and from 44,000 to 190,000 feet, respectively.

Table 2-1 shows the deployment conditions, general parachute design parameters, general performance data and an over-all evaluation of each parachute. Noted in this table is a column entitled "General Parachute Performance Evaluation". This column represents a rating which is considered to be an evaluation of the overall canopy performance as observed from the on-board movies taken during the test. Such characteristics as inflation stability, stability about the point of suspension, and structural integrity of the fabrication technique serve as the bases for this evaluation. The performances of various model canopies in wind tunnel tests (Ref. 1) serve as the criteria for the ratings shown in Table 2-1. In these wind tunnel tests, some model canopies performed with negligible inflation instabilities, or instabilities about the point of suspension. Such canopy performances serve to define the "Excellent" rating, where shown, in Table 2-1. "Fair", "Poor", and "Very Poor" represent proportionate reductions in performance rating.

4.

TABLE 2-1

SUMMARY OF TEST RESULTS

Test No.	Parachute Type	Roof Construction	Mach No.	Altitude (ft)	q (psi)	So (ft²)	Roof Porosity (%)	Ave. Load 1st sec (lb)	Max. Load (lb)	Load Factor	Ave. Test CD₀ 1-5 sec	Ave. Re-entry CD₀	Ave. Angular Osc. 1st 5 sec (deg.) Ave.	Max.	Max. Temp. (°F)	General Parachute Performance Evaluation	Post-Flight Parachute Condition
1	Hemisflo	(Not Applicable)	2.4	82,600	206	13.3	14.3 [1/]	1000	1713	1.30	0.48	0.39	8	12	210	Fair	No damage to test chute
2	Hyperflo	Ribbon	2.84	100,500	120	5.78	28.5	215	364	1.87	0.28	0.27	8	18	330	Poor-Fair	No damage to test chute
3	Hyperflo	Perlon Mesh	2.1	101,200	79	5.78	26.0	-	-	-	0.28	-	4.5	6	105	Excellent	No damage to test chute
4	Hyperflo	Ribbon	2.53	122,000	61	10.68	27.5	150	245	1.25	0.30	0.31	11	20	350	Fair	Tensionmeter failed, chute lost during re-entry
5	Hyperflo	Ribbon	3.22	86,400	345	10.68	22.0	800	1732	1.57	0.30	0.32	7	14	550	Fair	No damage to test chute
6	Hyperflo	Ribbon	3.98	122,700	113	10.68	14.9	250	385	1.23	0.26	-	5	10	-	Good	Chute lost during re-entry (lines cut)
7	Hyperflo	Perlon Mesh	0.2-0.5	44,200	8-150	10.68	33.8	-	-	-	0.37	-	7	10	-	Excellent	No damage to test chute
8	Hemisflo	(Not Applicable)	3.44	108,700	148	13.3	14.3 [1/]	480	1050	1.56	0.34	0.25	6	13	660	Fair	No damage to test chute
9	Hyperflo	Steel Mesh	0.25	29,200	75	10.68	29.1	-	-	-	-	-	-	-	-	Very poor	Test chute damaged at deployment
10	Hyperflo	Perlon Mesh	2.98	188,200	5	10.68	33.8	-	16	1.5	0.2	-	-	-	-	Unknown	Test chute destroyed during or prior to re-entry
11	Hyperflo	Steel Mesh	4.4	94,200	430	5.78	24.7	225	333	1.34	0.1	-	-	-	930	Poor	Test chute destroyed during test
12	Hyperflo	Perlon Mesh	3.12	77,100	494	10.68	33.8	290	350	-	0.035	-	-	-	550	Very poor	Test chute destroyed early in test
13	Hyperflo	Perlon Mesh	2.95	154,000	16	10.68	31.0	50	136	3.69	0.22	-	-	-	-	Unknown	Test chute destroyed during or prior to re-entry

1/ Total Porosity of Hemisflo

2.1 Strength Analysis

The selection of test parachute materials was, in many ways, based up-
on a desire to recover an undamaged canopy rather than upon the expected test
environment. Thus, in cases where the deployment dynamic pressure was
low, the parachute stresses were based upon expected re-entry conditions.
The use of the word "re-entry" refers to the descent portion of the test
trajectory. In this program parachute tests were programmed for the ascent
leg of the trajectory. It was recognized that there might be some change in
aerodynamic characteristics caused by the greatly overstrength parachute
operating in a low "q" regime. However, this effect, since unknown, was
not considered in the parachute design.

In general, aerodynamic heating was not considered when stressing the
parachute. The materials selection for the parachute canopy, nylon versus
Nomex (duPont trade name for a high temperature material also known as
HT-1) was based upon a general consideration of whether or not severe heat-
ing was expected. The Nomex yarn retains about 50% of its tensile strength
near 600°F. Because canopy test temperatures were unknown and the zero
strength temperature of Nomex is about 700°F, a minimum margin of safety
of 2 was considered adequate compensation for aerodynamic heating. In the
case of mesh roofs where Perlon (a type of nylon mesh) was considered to be
submarginal for the expected aerodynamic heating, a stainless steel mesh
was used. (It was desired to use a Nomex mesh; however, none existed at
the time the tests were accomplished.)

A very limited choice of materials was available for fabrication of the
test parachutes, due to the lack of experience in weaving the new high
temperature Nomex yarn.

Materials were selected by means of the parachute stress analysis
developed by Cook Electric Company several years ago.

Suspension line load is simply

$$L_S = \frac{F_O}{n \cos \gamma/2}$$

where

F_O = opening shock (lb)

n = number of suspension lines

6.

γ = angle between two diametrically opposite suspension lines (degrees)

The results has the unit of pounds per line.

The canopy stress is given as

$$L_c = \frac{CRMF_o}{D_o}$$

where

D_o = nominal parachute diameter in inches

C = dimensionless canopy factor

R = dimensionless reefing factor

M = dimensionless material factor

The results has the units of pounds tensile stress per linear inch.

The canopy, reefing, and material factors have been determined for conventional parachutes and materials from subsonic test data. For example,

C = 2.5 for solid flat

C = 1 for ribbon parachutes

R = 1 for an unreefed parachute or for disreef shock of a previously reefed parachute.

R = 2 for a reefed parachute

M = 1 for nylon

The factors applicable to Hyperflo parachutes constructed of Nomex were approximated as follows. Since none of the test configurations were reefed, R = 1. The material factor M is dependent upon the stress-strain relationship of the material under consideration. At the time the test parachutes were designed, the stress-strain relationships for nylon and Nomex could not be accurately compared. A material factor of 2 for Nomex was assumed, although more recent data on this material appears to indicate that this factor was conservative.

The choice of a canopy factor (C) of 1 was based more on porosity consideration than on shape. The canopy factors of solid parachutes are distinctly higher than those pertaining to ribbon canopies. Based on the fact that the Hyperflo roof approximates a ribbon parachute, at least with respect to porosity, the factor 1 was chosen.

Opening shock is given in the USAF Parachute Handbook as

$$F_o = C_D A q X K$$

where

$C_D A$ = effective drag area (ft^2)

q = dynamic pressure = $\dfrac{\rho V^2}{2}$ (lb/ft^2)

K = dimensionless canopy factor

X = dimensionless decreasing factor

The dynamic pressure, q, was determined from initial conditions. The reference area A was represented by S_o, the total canopy area. C_D was represented by C_{D_o}, the drag coefficient based upon total area. These values of C_{D_o} were determined from steady state supersonic wind tunnel Hyperflo drag data recorded by Sims, Reference 1. It was noted from this wind tunnel program that the Hyperflo C_D varies with Mach number and thus C_D's were selected from average values determined in this program (Fig. 2-1).

In the absence of adequate supersonic Hemisflo data, a subsonic $C_{D_o} = 0.50$ was assumed for the design of this canopy.

The K factor is a canopy factor and is believed to be dependent upon shape and porosity. It ranges from 1 for a ribbon canopy to 1.4 for a solid flat. Again, since no later Hyperflo data were available, the K factor had to be assumed and was selected as $K = 1.3$. For similar reasons, a K factor of 1.3 was also used for the Hemisflo parachute.

The X factor compensates for system deceleration during parachute inflation. With the high velocity and $W/C_D A$ factors involved, the X factor was assumed to equal 1 for both Hyperflo and Hemisflo parachutes.

8.
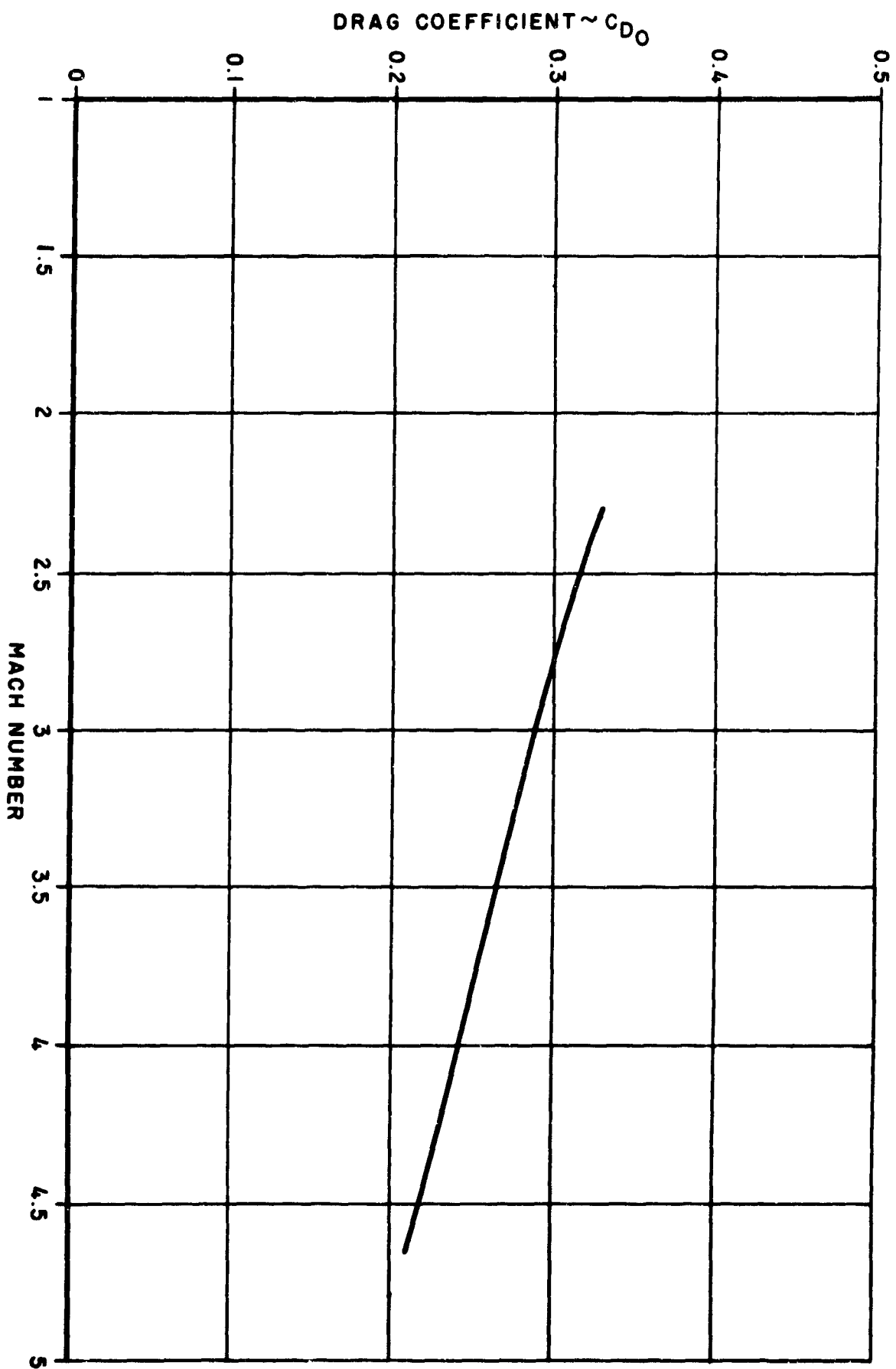
Figure 2-1 Drag Coefficient vs Mach Number,
Average Hyperflo Wind Tunnel Data (Ref.1)

Re-entry stresses were checked by the same means using $F_o = C_D A \ q$ (re-entry).

The anticipated opening shock loads calculated in the manner described above are listed as such in Appendix A. Since the opening shock load was assumed to be the maximum load, no additional "maximum load" was anticipated.

The stresses resulting from the above calculations methods are without safety factors. Compared to the materials chosen, no structural elements (with the exception of some mesh roofs) had a margin of safety less than 2 in either deployment or re-entry conditions. Some elements in some of the configurations had margins of safety as high as 5. The Perlon mesh has a relatively low tensile capability (85 lb/in) and was treated as a special case when, based upon the above calculations, was predicted to fail. In these instances, it was compared to the results obtained from sled parachute data, Ref. 2 which successfully tested Perlon roof Hyperflo's at much higher q's than any existing in this Cree program. These tests showed little or no Perlon damage. Not considering aerodynamic heating, the Perlon was thus assumed to be more than adequate for all tests in which it was to be used.

2.2   Aerodynamic Heating

2.2.1   General Considerations

Some work has been performed in past programs to determine heat transfer coefficients to parachute component shapes immersed in a subsonic airstream, with component shapes such as conventional ribbons oriented either parallel or perpendicular to the stream direction. Measurements of heat transfer to various areas of a parachute in either a subsonic or supersonic airstream, however, have apparently not been performed.

Heat transfer in supersonic flow to a blunt body is determined by the shock wave shape ahead of the body and the shock stand off distance. These parameters affect the velocity gradients on the body surface which, in turn, affect the local heat transfer coefficients.

A parachute may be considered to be a blunt body, although flow through the canopy prescribes local flow conditions which are, perhaps, at variance with those conditions for a similarly shaped non-porous body. However, if the flow is choked by the parachute, it would be expected (apparently confirmed by wind tunnel tests) that the flow is subsonic through the parachute. Hence, flow conditions outside the boundary layer of

10.

parachute components are not unlike those near the surface of a similarly shaped solid non-porous body. These local flow conditions are determined, however, not by the consideration of a given canopy component (such as a ribbon) as an isolated body in the supersonic stream, but as a part of a body over which flow conditions are prescribed by the entire canopy shock wave.

In several of the Cree tests, Test No. 11 in particular, extreme evidence of heating was apparent from the on-board camera coverage during the test. This was confirmed by examination of the test canopy after recovery. However, as was apparent also from the test film, structural failure of the steel mesh roof occurred 1. 5 seconds after test parachute deployment. Failure of the roof resulted in increased heating rates due to the reduced effective parachute diameter. Progressive and ultimately complete failure of the roof resulted in continued increases in heating rates and ultimate failure due to heating of the remainder of the canopy. The parachute had seen little benefit from the reduction in thernal environmental conditions normally expected when a drag device is deployed.

Examination of canopies after tests have shown the significance of the parachute material mass. Areas remote fron over-lapped seams, for example, have attained higher temperatures than in the higher-mass seam areas. It is apparent that the thermal heat sink of a given parachute component is significant in determining the final temperature attained by that component. This is found to be the case in both low and high deceleration environments, although apparently more significantly in the latter case. In the high deceleration cases, material conductivity rates and thermal masses provide a lag in temperature rise, allowing significant decelerations to take place during temperature build-up with attendant lower heat input rates and lower maximum radiation equilibrium temperatures.

2.2.2 Test Results

Efforts were made to determine temperatures in various parts of the test canopy by the use of temperature-sensitive paints and crayons, and are recorded in the test results of Appendix A. Such a temperature study would have greatest significance when color changes could be detected from the on-board camera film made during the test. This technique would eliminate the necessity of reading temperatures from the recovered test item which might have encountered a more severe heating environment on re-entry than during the test. In some cases (Tests 1, 3, 4) examination of the test film resulted in a reasonable indication of the maximum temperatures attained during the tests. In other cases, the maximum temperature attained was not conclusively established by this procedure. Reliance on the examination of the test item after recovery for maximum temperature indication, as

mentioned previously, may reflect a thermal environment other than that corresponding to the test condition.

It is expected that temperature indications such as those provided by temperature-sensitive paints or crayons which are affixed to the outer surface of a parachute component may indicate surface temperatures which are higher than those seen by the bulk of the material. This is particularly true in areas of relatively high density under high heating rate conditions.

In the following subsection, an analytical approach to the determination of parachute material temperatures is presented. Where possible, temperatures predicted by this procedure are compared with previously discussed measured values.

2.2.3 Analytical Approach

In the absence of confirmed formalized procedures for the prediction of heat transfer coefficients at supersonic speeds to a trailing parachute, heat transfer coefficients are predicted by the method outlined in Ref. 3, assuming stagnation point heating to a sphere with appropriate stagnation point velocity gradients. No consideration is given to the presence of the forebody wake, although it is felt unquestionably that the presence of the forebody wake and corresponding modifications of the canopy shock wave caused by the viscous wake (Ref. 1) will affect the heat transfer coefficients and possibly the recovery temperatures.

Schlieren photographs of supersonic wind tunnel tests have indicated that the strong normal shock which would be expected to exist ahead of a blunt body such as a parachute in free stream is diffracted into a conical shock by the non-uniform forebody wake. Further, as discussed in Ref. 1, the low energy wake is apparently diverged by this shock to the inlet of the canopy. Drag coefficients measured in wind tunnel tests appear to confirm this flow field characteristic ahead of the canopy. Since the drag coefficients realized by the Hyperflo canopy result from such a reduced internal pressure distribution, and not by the stagnation pressures which would result behind a normal shock-free stream immersed canopy condition, the heating conditions in the canopy would be expected to be much less severe. Calculations which account for the presence of the wake result in the prediction of heat transfer coefficients which are from 50 to 60 percent oᵢ those predicted for the canopy in free stream conditions. However, in the absence of test data to confirm the predictions of the "wake method", the free stream assumption is made. Fair agreements with measured data is realized by this procedure. However, as will be discussed later, the parachute in test 6 would have been

12.

predicted to fail, although film coverage of this test did not show any sign of canopy damage. This particular test parachute was not recovered and temperature measurements from this test film were inconclusive.

To express the laminar stagnation heat transfer coefficient to the parachute, the following relation is used from Ref. 3.

$$h = \frac{0.763}{Pr^{0.6}} \left(\frac{\beta D}{u_\infty}\right)^{1/2} \left(\frac{\mu_\infty}{\rho_\infty u_\infty D}\right)^{1/2} \left(\frac{\rho_\delta}{\rho_\infty}\right)^{1/2} X$$

$$\left(\frac{\mu_\delta}{\mu_\infty}\right)^{1/2} \qquad \rho_\infty u_\infty c_p \qquad (1)$$

where

h = heat transfer coefficient, $BTU/ft^2 sec\, ^\circ R$

Pr = Prandtl number

u = velocity, ft/sec

μ = coefficient of fluid viscosity, $\dfrac{lb\text{-}sec}{ft^2}$

ρ = fluid density, $\dfrac{lb\text{-}sec^2}{ft^4}$

β = stagnation point velocity gradient, ft/sec-ft

D = body diameter, ft.

c_p = fluid specific heat at constant pressure, $\dfrac{BTU\text{-}ft}{lb\text{-}sec^2\text{-}^\circ R}$

The subscript ∞ refers to free stream conditions, and the subscript δ refers to local conditions outside the boundary layer.

Temperature-time histories are determined using the assumption of infinite material conductivity and by considering the heat sink capability of the parachute material. Heat transfer coefficients are assumed

13.

uniform over the inner surface of the canopy, and equal to the stagnation heating to a sphere whose diameter is the parachute projected diameter. Recovery temperatures on the outer surface of the canopy are expected to be comparable to the recovery temperature on the inner surface (assuming small differences in recovery factors) hence significant aerodynamic heating rates may be anticipated on the outer canopy surfaces. In Ref. 4, heating rates over the base of a body have been related to the heating rates at the body side ahead of the base. Values from 33 percent to 100 percent of this heating rate were shown to represent the distribution over the base region in the test condition of Ref. 4. The calculations performed in this report assume the heating rate on the outside of the canopy to be 50 percent of the heating rate on the inside of the canopy.

A turbulent flow recovery factor of 0.9 is assumed on both inner and outer surfaces of the canopy. Radiation shape factors of 1.0 and 0.5 are used for the canopy assuming an inflated hemispherical canopy contour. In consideration of the condition that the parachute is tested on the ascent leg of the trajectory, a shape factor of 1.0 is assumed relative to radiation to the earth, and a factor of 0.5 relative to space. A radiation sink temperature of 520 $^{\mathrm{o}}$R is assumed for both earth and space.

$$\Delta T_w = \frac{1.5}{\rho\, c_p} \left[h\, (T_r - T_w) - \epsilon \sigma\, (T_w^4 - T_a^4) \right] \Delta t \quad (2)$$

where

T_w = wall surface temperature, $^{\mathrm{o}}$R

σ = Stefan-Boltzman constant, $\dfrac{BTU}{ft^2 sec\, ^{\mathrm{o}}R^4}$

ϵ = wall emissivity, (0.8 used for Nomex)

T_a = radiation sink temperature, $^{\mathrm{o}}$R

h = defined by equation (1), BTU/ft^2 sec $^{\mathrm{o}}$R

ρ = material density, lb/ft^2

c_p = material specific heat, $\dfrac{BTU}{lb\, ^{\mathrm{o}}R}$
  (0.30 used for Nomex)

t = time (sec)

Tr = recovery temperature, $^{\mathrm{o}}$R

14.

Calculations were performed by this procedure to compare calculated maximum temperatures attained in several tests with those measured, where applicable, from the temperature-sensitive paints or crayons.

In Test 2, the maximum measured temperature which appeared to exist on the horizontal ribbons of the roof was 330°F. Calculations employing the density of these 3/4 x 400 Nomex ribbons or 0.0594 pounds per square foot predict a maximum temperature of 410°F.

In Test 8, a similar calculation was performed to compare a temperature of 660°F measured on the roof horizontal ribbons constructed of 1 1/4 x 300 Nomex. The calculation predicts a temperature of 610°F.

In the case of Test 6, no conclusive temperature measurements were made as mentioned previously, and the parachute was not recovered. However, the test film coverage revealed no evidence of structural damage throughout the duration of the film coverage. Calculations to determine the maximum temperature of the lightest component of this canopy predict a temperature of approximately 700°F, at which temperature the strength of Nomex should be at or near zero. The component examined in the analysis was the vertical ribbon constructed of 2 ply 3/8 x 58 material with a total density of 0.049 pounds per square foot.

Test 4 provided a temperature measurement of from 350°F to 390°F, as indicated by the test film coverage. Calculations indicate a maximum temperature of 400°F on the 1-1/4 x 300 Nomex horizontal roof ribbons having a density of 0.0396 pounds per square foot.

Although reasonable agreement is realized in the calculation of maximum canopy local temperatures with those measured, it is considered that the heating calculations are conservative. This is especially evidenced in the Test 6 calculation described previously. Maximum temperatures in all calculations occurred in less than 10 seconds after parachute deployment. Although, the calculation of the maximum temperature of the Test 6 canopy indicated zero strength in less than 10 seconds, film coverage revealed nearly 20 seconds of undamaged operation.

A plot of measured canopy temperatures is shown in Figure 2-2. Superimposed on this plot are several predicted maximum temperatures which were calculated by the method described above. Due to the relatively small altitude range associated with the test points plotted (85,000 to 125,000 feet), the Mach number effect on maximum temperature predominates. However, since both altitude and material densities have a strong influence on the maximum material temperature, this variation should not be generally

interpreted as a strictly Mach number-temperature relation. For example, a Mach 3 maximum temperature at 10,000 feet altitude would be much larger than indicated on this plot for the high altitude conditions represented.
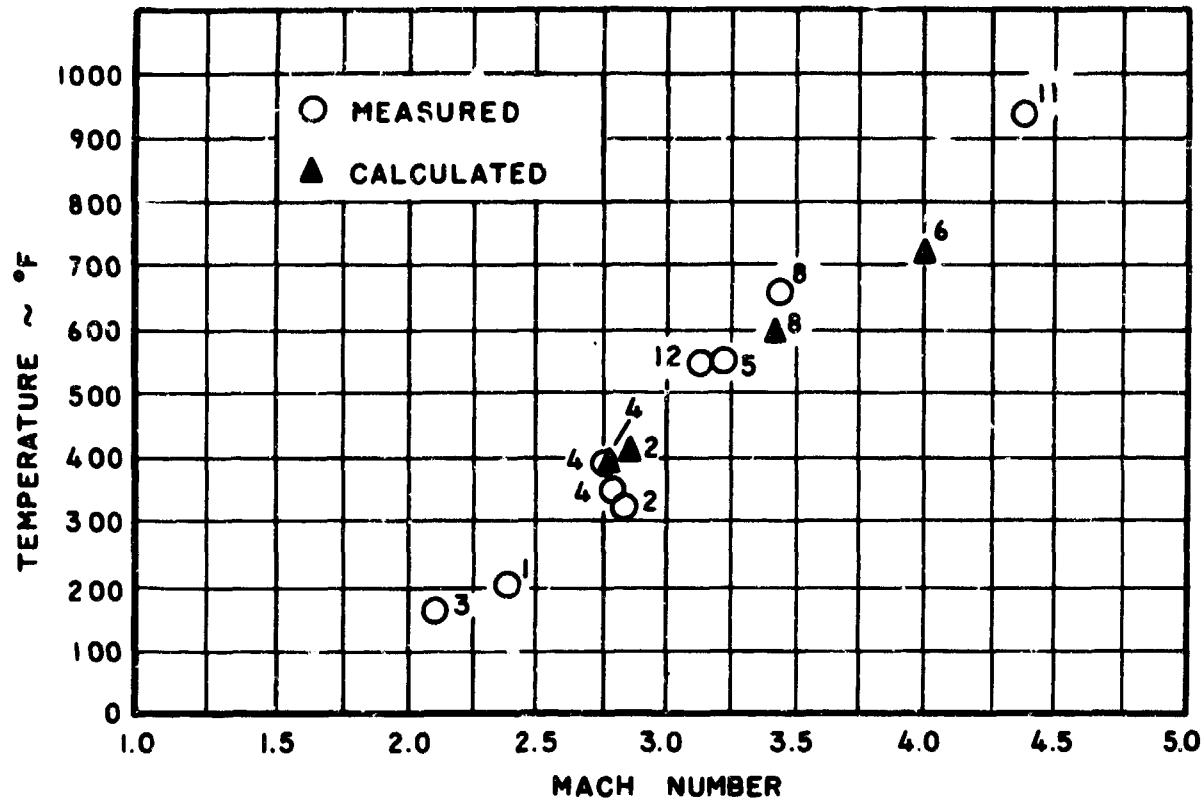
Figure 2-2 Measured and Calculated Canopy Temperature

2.3 The Hemisflo Parachute

2.3.1 Test Summary

Tests conducted using the Hemisflo parachute design were aimed at the flight evaluation of this canopy, the design of which incorporated a significant reduction in porosity from that normally employed in past supersonic tests. This is described in more detail in Section 2.3.2.

In the conduct of this test program, two Hemisflo tests were completed. Both of these tests used the same canopy. Test No. 1 (Mach 2.4 at 82,600 feet) was selected to duplicate a wind tunnel test condition (Ref. 1). Test No. 8 (Mach 3.44 at 108,700 feet) was selected to provide higher Mach data on this canopy design. The results of these tests are given in Section 2.3.3 and Appendix A, and are discussed in detail in subsequent sections of this report.

16.

2.3.2 Design Configuration

2.3.2.1 General

Hemisflo parachutes have been subjected to both wind tunnel model tests and full scale tests in past programs on the Cree vehicle and on the Tomahawk sled. Wind tunnel tests resulted generally in unsatisfactory parachute performance at Mach numbers above 2. Incomplete canopy inflation proved to be the primary malfunction in these tests. The total porosity employed in these wind tunnel tests was considered to be too high (25%) as compared to Hyperflo parachutes (9% to 18%). Since certain isolated full scale tests on past Cree programs indicated fair performance of the Hemisflo, it was considered appropriate to retest this configuration. However, the normally high porosity which had been considered necessary in past practice to achieve stability about the point of suspension was reduced to improve inflation characteristics in the present Hemisflo test canopy design. A porosity comparable to the average porosity employed in the Hyperflo designs (14.3%) was selected for this test canopy. In addition, the diameter (projected) was selected so as to provide a ratio of inflated diameter to forebody diameter which was within the range of ratios employed in the wind tunnel tests of this and the Hyperflo canopies conducted under Contract AF 33(616)-8459. It was in this latter program that the significance of this parameter on supersonic parachute performance was indicated.

2.3.2.2 The Hemisflo Design

The Hemisflo canopy is designed as a hemisphere with a truncated cone extension beginning at the periphery of the hemisphere. The slant height of the truncated cone is equal to one-twentieth of the circumference of a great circle of the hemisphere. The included angle of the cone is equal to the angle between two diametrically opposite suspension lines. The suspension lines have a free length (canopy skirt to confluence point) equal to the circumference of a great circle of the hemisphere. The hemisphere and truncated cone actually have a lateral cross section of a regular polygon of n sides where n equals the number of suspension lines. As such, they are not truly hemispherical or conical. The entire canopy is of ribbon construction.

2.3.3 Parachute Performance

2.3.3.1 Drag Force Measurements

Force measurements were provided by the Cree on-board tensiometer. These measurements were then transmitted on two

17.

telemetry channels. Since all Cree test conditions were selected such that parachute deployment occurred on the ascending leg of the trajectory, dynamic pressure decreased rapidly during the test. Since the test parachutes were generally designed to survive the entire trajectory re-entry (descent) force data were obtained in many tests. These re-entry force data in some cases covered ranges of both increasing and decreasing dynamic pressure environments.

Test parachute data reduction has enabled the plotting of force versus Mach number, dynamic pressure and Reynolds number. From these data, parachute drag coefficients based upon the total canopy cloth area (C_{D_o}) have been determined. These are shown in Figures 2-3, 2-4, 2-5, for both test and re-entry. It may be noted that the drag data during test have been shown on these figures for at most the first five seconds after test parachute deployment. Since force reduces rapidly after parachute deployment to values which may have large percent errors, it is felt that data derived beyond the first five seconds may be misleading or misinterpreted and is therefore not included on the above plots. Complete data for each test is shown in the detailed test resumes in Appendix A.

2.3.3.2 Parachute Deployment and Filling Time

Examination of the telemetered force data during the initial time from parachute deployment has resulted in the determination of the deployment and opening load time histories of the test canopies. The force-time histories for the test parachutes are shown in Appendix A. Close inspection of the various force records after parachute deployment has indicated that, in general, three peak loads are indicated. In order of time from deployment, the first of these is associated with the full line stretch of the parachute (normally called snatch force) and is labeled (1) on the force plots, the second spike is associated with the full-open time of the parachute (normally called the opening shock) and is labeled (2), and a third point is labeled (3) on these plots. In most cases, it was determined that the maximum load is associated with point (3) rather than point (2). Point (2), which represents the parachute opening shock, has normally been considered in past practice to represent the maximum parachute loading condition.

A complete analysis of these phenomena is beyond the scope of this program; however, it appears that the succession of spikes of increasing magnitude after the parachute is fully open may be attributed to parachute suspension system stiffness. Since in all cases, the test parachutes were designed overstrength for the test condition, the suspension system may be compared to a spring with a high spring constant. Simplifying the para-

18.
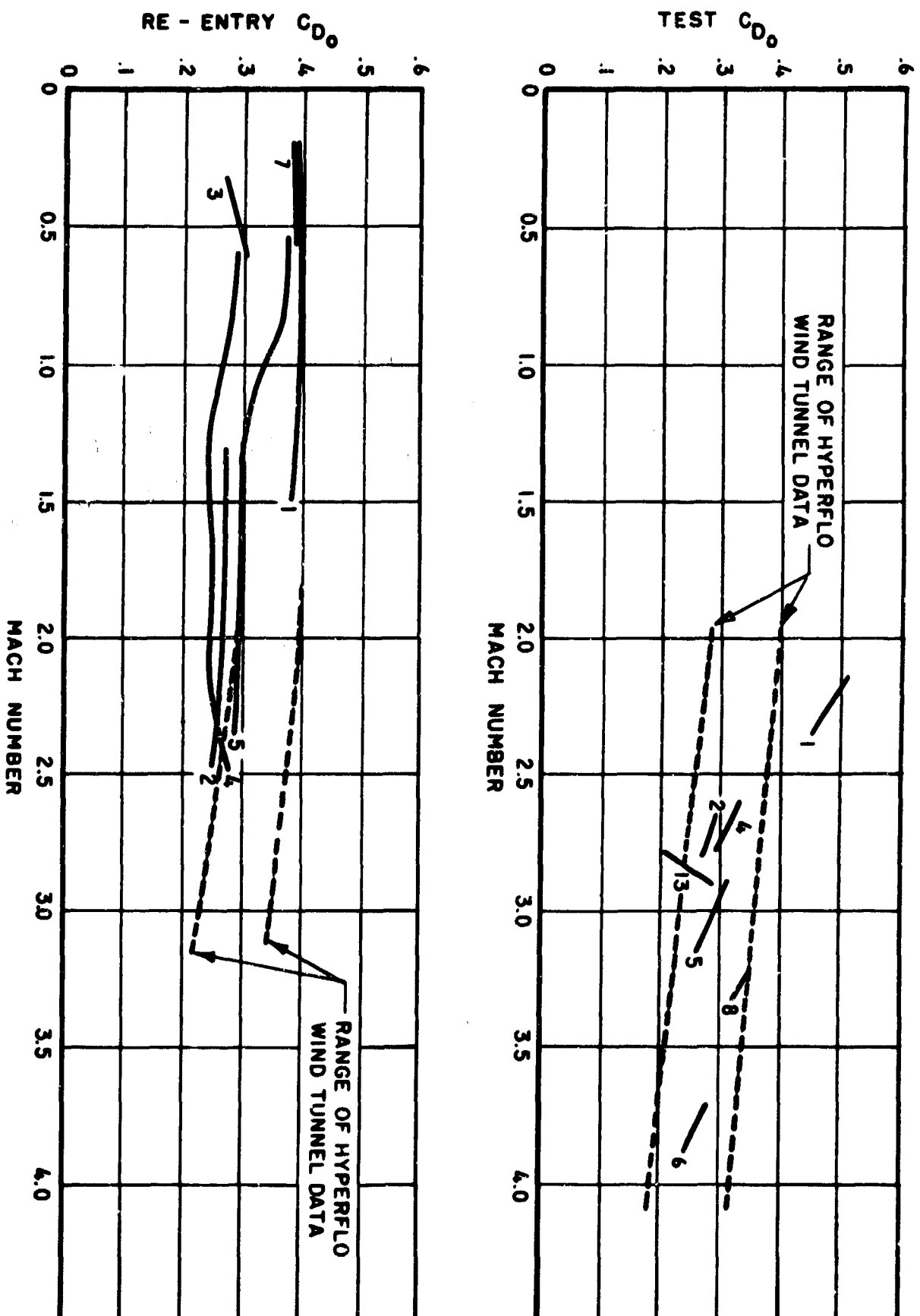
Figure 2-3 Test and Re-entry C_{D_O} vs. Mach Number
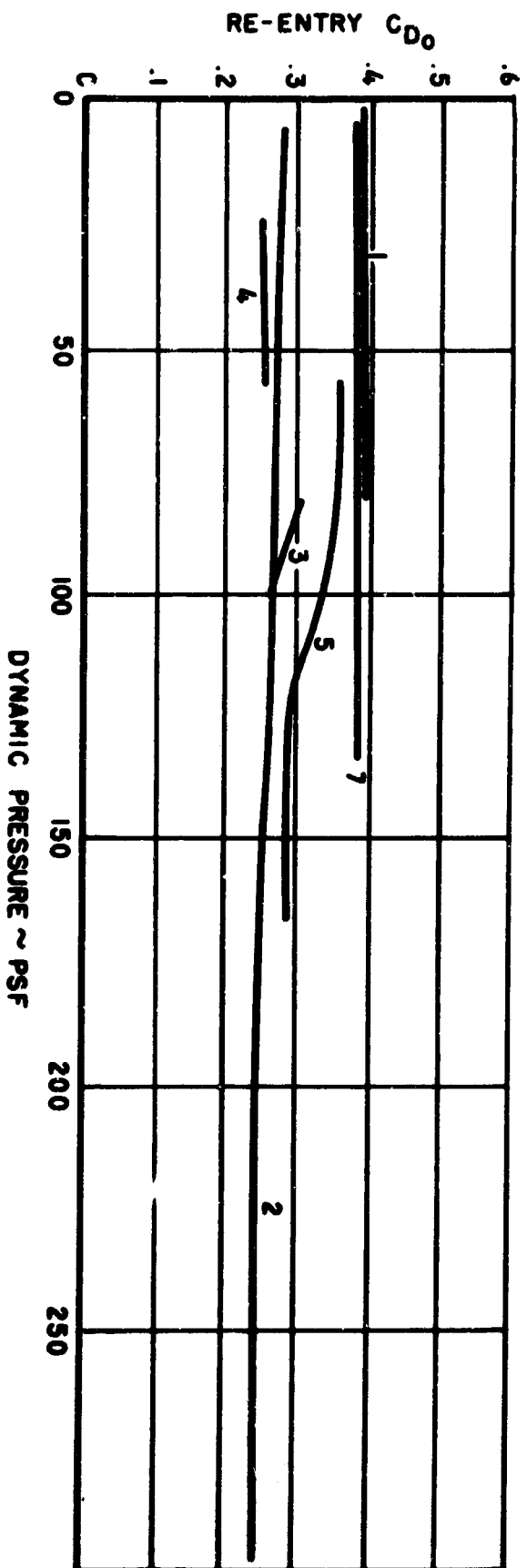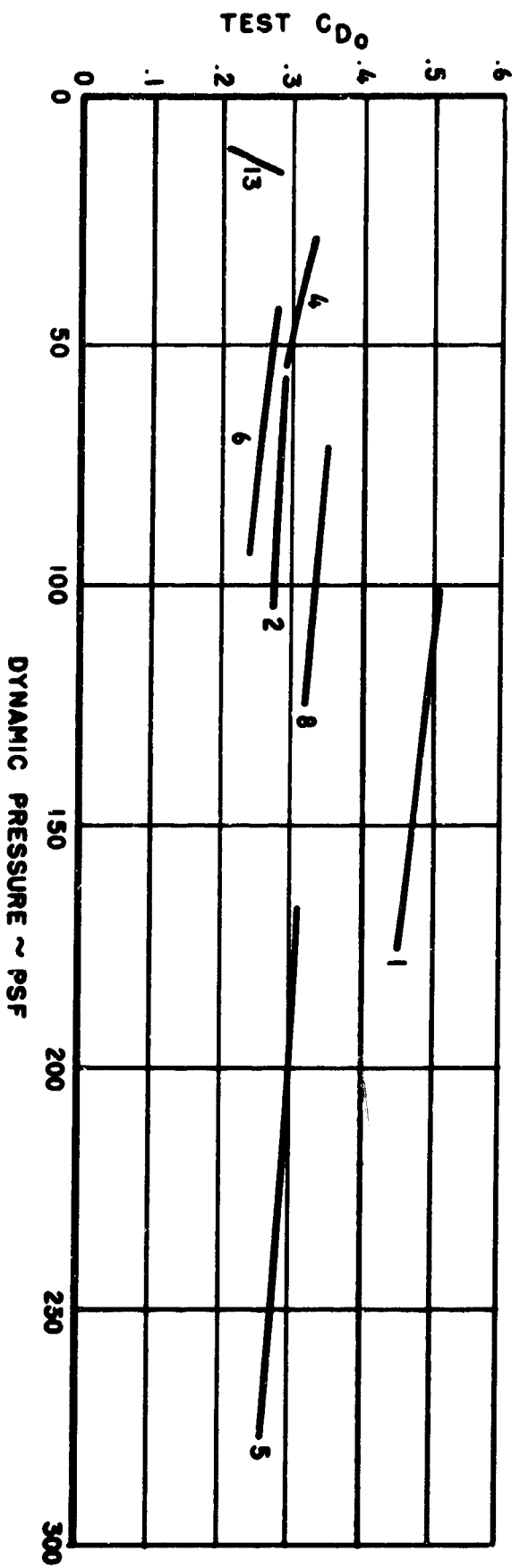
Figure 2-4 Test and Re-entry C_{D_0} vs. Dynamic Pressure
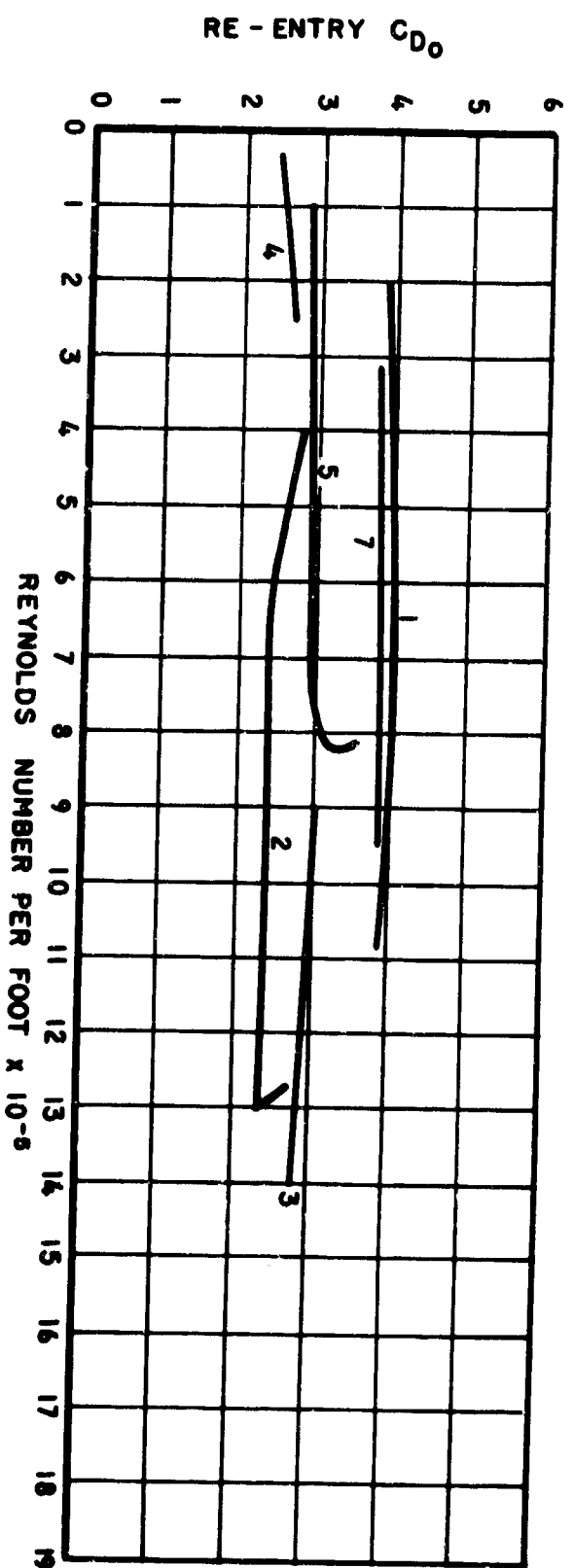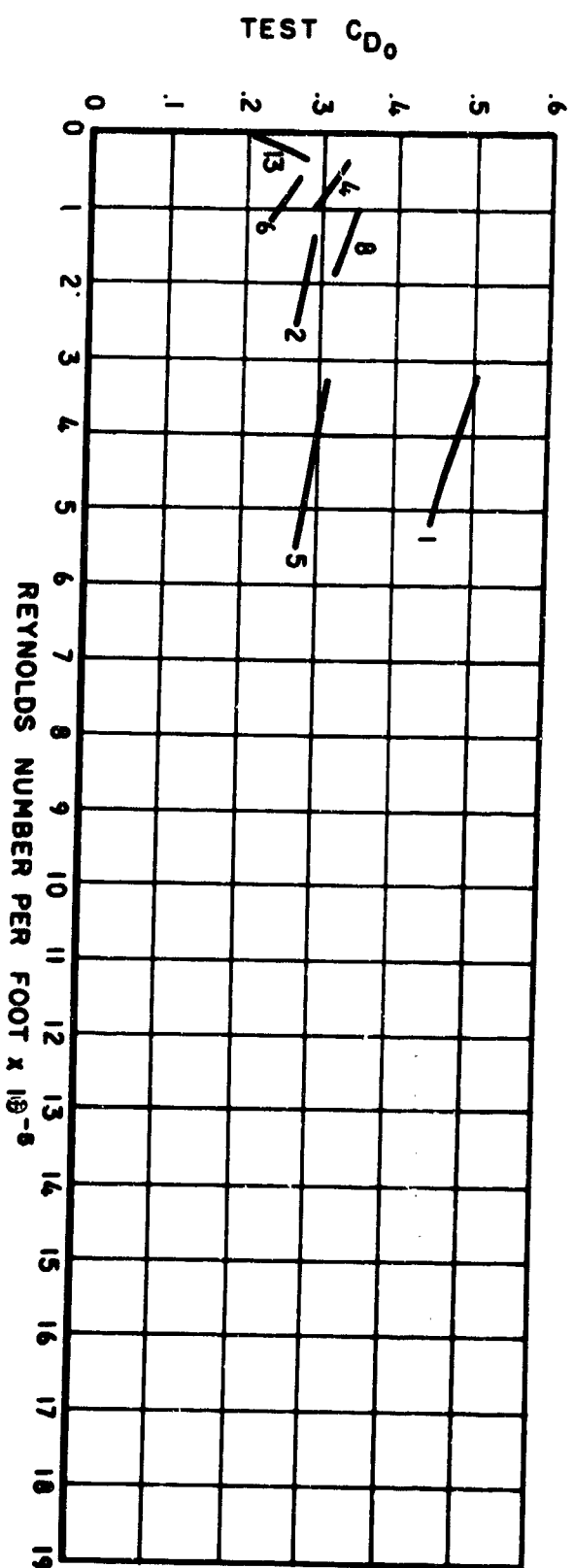
Figure 2-5 Test and Re-entry C_{D_o} vs. Reynolds Number

chute system to a simple spring-mass system with a high spring constant indicates that during an energy absorption cycle high force levels may be encountered. Based on the above simple analogy, a given energy absorption requirement specifies that the maximum force exerted on the suspended mass is proportional to the spring constant to the one-half power. This analogy is to some extent justified since during the time that the point (3) is encountered, a definite loading and unloading of the suspension lines is occurring based upon on-board photograph coverage.

Consistent with the discussion above, Table 2-2 shows a summary of the force-time derived from the Hemisflo tests 1 and 8. Δt_1 represents the time from deployment to full line stretch, Δt_2 represents the time from full line stretch to parachute fully open (filling time), and Δt_3 represents the time from parachute fully open to the (generally) maximum load condition. The column in this table labeled "load factor" represents the ratio of the maximum load attained in the first second after deployment to the steady state load expected under the initial deployment conditions. The steady state load is determined using the actual C_{D_o} average (1-5 sec.) for each test.

TABLE 2-2

HEMISFLO DEPLOYMENT TIMES AND LOAD FACTOR

Test	Δt_1 (Sec.)	$\Delta t_2 = t_f$ (Sec.)	Δt_3 (Sec.)	Load Factor
1	0.209	0.05	0.313	1.3
8	0.39	0.09	0	1.56

In Test No. 8 it may be noted that $\Delta t_3 = 0$. Although examination of the force record for this test in Appendix A revealed the existence of a point (3), the load at point (2) is the same. Hence, the maximum load is repeated, occurring first at the parachute fully open condition. A more complete tabulation of data obtained during the parachute deployment and opening process may be found in the individual test resumes in Appendix A.

2.3.3.3 Drag Coefficient

As discussed previously, the Hemisflo configuration tested in the free-flight test program was constructed with a considerably lower porosity (14.3 percent) than the previous wind tunnel model (25 percent) to improve the relatively poor inflation characteristics exhibited by the wind tunnel model. Fair inflation of this canopy was exhibited in Test No. 1, with excellent drag coefficients indicated by the telemetered force data. The drag coefficients, C_{D_o}, are shown plotted versus Mach number, dynamic pressure, and Reynolds number in Figures 2-3, 2-4, and 2-5. In the majority of free-flight tests in this test program, quite reasonable correlation with wind tunnel data under steady state conditions is indicated. However, in this test as well as in Test No. 8 with the same canopy, it is difficult to explain the high drag coefficients attained even upon consideration of the relative porosities of this full scale canopy with the wind tunnel model and the relative degrees of inflation of these canopies. The drag coefficient attained by a supersonic parachute has generally been indicated to vary inversely with its porosity, although a reduction of one-half in porosity will not result in an increase in drag by factor of 2. However, assuming this proportionate increase to take place and considering that the wind tunnel model was inflated only to 0.43 of its theoretical projected diameter, a factor of 6.28 is indicated to be the multiplier on the wind tunnel C_{D_o} = 0.05 to convert it to the maximum expected C_{D_o} for this free-flight test canopy. A drag coefficient of approximately 0.31 might be expected in this case for the optimistic assumption made. Actual measured drag coefficients in this test indicated a minimum of C_{D_o} = 0.44 during test.

Upon examination of Figures 2-3, 2-4, and 2-5, it may be seen that a drag coefficient of approximately C_{D_o} = 0.38 to 0.4 was indicated for transonic and subsonic speeds on the re-entry of the Test 1 parachute. Since most parachute data indicate a supersonic drag coefficient less than the transonic-subsonic value, the test drag coefficients of C_{D_o}=0.46 and greater are questionable for this parachute.

Test 8 (Mach 3.44 at 108,700 feet) force data indicates an initial drag coefficient of C_{D_o} = 0.31 (C_{D_p} = 0.81) for this Hemisflo canopy. This is within the range of wind tunnel test data obtained with Hyperflo canopies of comparable porosities. The apparent increase in drag coefficient with decreasing Mach number, dynamic pressure, and Reynolds number substantiates similar trends indicated in wind tunnel tests. This trend is clearly indicated in most tests shown in Figures 2-3, 2-4, and 2-5.

2.3.3.4   Canopy Stability

Photographic coverage obtained by the on-board movie camera permitted the determination of the parachute oscillation angle. The decreasing dynamic pressure environment during the test represents a relatively severe basis on which to measure the canopy stability about the point of attachment to the Cree vehicle, since dynamic instability generally increases in such an environment.

The canopy stability is represented in Figures A. 3. 4 and A. 10. 4, Appendix A, for the two Hemisflo tests. No attempt was made, in the reduction of angular oscillation data, to establish polar coordination. A parachute which would "cone" at a constant angle about the point of suspension would be represented by a line parallel to the abscissa (time) on the oscillation plots. Also, the stability data presented show both an average oscillation curve which represents a time-weighted average oscillation condition, and also a maximum oscillation curve representing relatively infrequent high angle excursions.

The Hemisflo Test 1 indicated average excursion angles about the point of attachment of from approximately 8 to 9 degrees, and maximum oscillations of from 11 to 18 degrees. Test 8 shows an average oscillation of from 6 to 8 degrees and maximum oscillations of from 12 to 17 degrees. The variations of average and maximum excursion angles stated above are seen in Figures A. 3. 4 and A. 10. 4 to represent generally increasing angular excursions with time (decreasing dynamic pressure).

Wind tunnel tests conducted with a Hemisflo model constructed with a higher (25 percent) porosity had maximum angular excursions about the point of suspension of less than 1 degree (often typical with underinflated parachutes) for all test Mach numbers from 2. 3 to 3. 5. In general, conventional parachutes (prior to the Hyperflo) have indicated a decrease in stability with a decrease in porosity at supersonic speeds. The subject full scale Hemisflo canopy, constructed with a porosity which is 57 percent of that used in the wind tunnel model, would be expected to be less stable. The increase of instability with time however, is not unique with the Hemisflo in a decreasing dynamic pressure environment.

2.4   The Hyperflo Parachute

2.4.1   Test Summary

Tests conducted using the Hyperflo parachute design were aimed in several cases to validate wind tunnel test data and in others to provide as

24.

wide a Mach number-altitude coverage as possible with the booster units available in this program. As discussed previously, Hyperflo canopies were designed and fabricated so as to simulate as closely as possible the design parameters of the wind tunnel models, while employing materials which were readily available and appropriate for the flight test environment in a specific case.

In the conduct of this test program, eleven Hyperflo tests were completed. Tests 2, 3, 9, and 12 were aimed at validation of wind tunnel Mach number and dynamic pressure conditions. The remaining Hyperflo tests were closely comparable to wind tunnel Mach number conditions, but reflected wide variations in dynamic pressure conditions as compared to the wind tunnel tests.

2.4.2 Design Considerations

The Hyperflo canopies tested in this program were designed to provide roof porosities, inlet porosities, total porosities, and over-all canopy geometry similar to those models which performed satisfactorily in the basic wind tunnel program. Numerous practical design and fabrication problems were introduced, however, which necessitated deviations from desired designs in many cases. The problems which were introduced in these free-flight tests were primarily caused by the high aerodynamic heating environments encountered in most of the free-flight test conditions.

Model Hyperflo canopies performed in an outstanding manner in wind tunnel tests up to Mach 6. However, wind tunnel stagnation temperatures did not exceed values which would prohibit the use of conventional nylon materials in the fabrication of the models. Free-flight applications of parachutes at Mach numbers of 3 or above, and an altitude of 100,000 feet or below may require the use of materials other than conventional nylon. This operational limit is not rigid since the limiting heating environment is determined not only by the materials but also by the thermal mass ($\rho\ C_p$) of canopy components employed and the size of the parachute, as discussed in Section 2.2. However, for the test conditions and the parachute size range of this program, the conditions cited above did represent an approximate limitation on the use of conventional nylon parachute components.

For test conditions with greater aerodynamic heating conditions, Nomex materials with a melting temperature near 800°F were considered. Serious problems were imposed, however, by the limitations of types of weave available in this material at the time of this program. Since the Hyperflo parachutes tested in wind tunnels had shown optimum performance

25.

with high porosity mesh roofs and since no Nomex mesh of satisfactory geometry had yet been fabricated, less optimum ribbon roof designs were necessary. To pursue high Mach number evaluation of high porosity mesh-roof geometries, however, stainless steel meshes were used in the parachute designs of tests 9 and 11 for anticipated high heating environments. The use of a steel mesh roof coupled with the use of Nomex for the remainder of the canopy imposed severe fabrication problems in these test canopies.

2.4.3 Parachute Performance

2.4.3.1 Drag Force Measurements

All drag data were reduced from force measurements provided by telemetry from the on-board tensiometer during the test period, and in many instances, during the re-entry phase of the trajectory. The force data from each test are presented in the individual test resumes in Appendix A. The drag coefficients, C_{D_o}, reduced from these data are presented in Figures 2-3, 2-4, and 2-5 where they are plotted versus Mach number, dynamic pressure, and Reynolds number.

2.4.3.2 Parachute Deployment and Filling Time

The reduction of Hyperflo test deployment and filling time data has been performed as described in Section 2.3.3.2 above. Since it is necessary to correlate parachute deployment and opening load force-time data with the test film coverage, those tests in which the vehicle was not recovered are not included in the discussion of data in the following section. Also, those tests in which early canopy structural failure was observed on the test film are not considered applicable in transient load data analysis.

In accordance with the previously defined parameters Δt_1, Δt_2, Δt_3 and load factor, the results of the Hyperflo tests are summarized in the following tabulation:

TABLE 2-3

HYPERFLO DEPLOYMENT TIMES AND LOAD FACTOR

Test No.	Δt_1 (Sec.)	$\Delta t_2 = t_f$ (Sec.)	Δt_3 (Sec.)	Load Factor
2	0.104	0.036	0.36	1.87
4	0.23	0.07	0.18	1.25
5	0.14	0.042	0.048	1.57
6	0.26	0.09	0.31	1.23

26.

The maximum parachute opening load was generally found to be after the canopy full open condition. In all of the cases listed above, maximum loading occurred at the time Δt_3 after canopy opening and hence, are subject to the considerations discussed in Section 2. 3. 3. 2 above, where the effects of suspension system stiffness were suggested as an explanation of the high loadings evidenced in the data after full canopy inflation.

Of the four tests tabulated above, the Test 6 canopy performed the best from the standpoint of inflation and oscillation stability. It may be noted that this test canopy demonstrated the lowest load factor. It is possible that inflation instabilities may contribute to successive loading spikes occurring at instants of full inflation. This behavior coupled with (and possibly in phase with) high loadings caused by suspension system stiffness, as discussed previously, may contribute to the relatively high load factors evidenced by the less stable canopies.

2.4.3.3 Drag Coefficient

Drag coefficients obtained from the force data are plotted versus Mach number, dynamic pressure and Reynolds number in Figures 2-3, 2-4, and 2-5. These drag coefficients are shown for both test and re-entry conditions where applicable.

In Test 2, a drag coefficient of C_{D_o} = 0.28 to 0.29 representing C_{D_R} = 0.58 to 0.61 was indicated shortly after deployment. These are well within the range of data from wind tunnel tests. The on-board camera coverage indicated only fair canopy performance since full inflation of the canopy was not maintained. The effects of Mach number after test parachute deployment indicate a relatively rapid rise of drag coefficient during the first few seconds, although the Mach number decrease during this time is small. This appears to be true for most test conditions as shown in Figure 2-3. As in the case of the Hemisflo test data described previously, this seems to be explainable only through the increases in drag coefficient corresponding with decreases in dynamic pressure and Reynolds number indicated in Figures 2-4 and 2-5. This variation is not apparent from the re-entry data.

In Test 3, the telemetry signal was lost during the test, hence no force data were obtained during this period. However, drag data was obtained during re-entry and is shown in Figure 2-3 for a short subsonic speed range. The average drag coefficient in this range is indicated to be about C_{D_o} = 0.28, which is lower than the values of 0.38 to 0.41 indicated by sled and wind tunnel tests in this speed range for the supersonic

27.

Hyperflo configurations. Even though data were obtained from the tele-metry, these data were of questionable quality. Figure 2-6 shows the deployment and opening sequence of this mesh roof parachute as recorded by the on-board camera.

The Test 4 drag coefficients during test and re-entry are shown in Figures 2-3, 2-4, and 2-5. Test drag coefficients of $C_{D_o} = 0.29$ to 0.32 agree well with wind tunnel data. Again, decreases in Mach number, dynamic pressure, and Reynolds number during test result in indications of an increasing drag coefficient. The re-entry data shown in Figures 2-3, 2-4, and 2-5 indicate little variation in drag coefficient with Mach number, Reynolds number, or dynamic pressure. Drag coefficients on re-entry ($C_{D_o} = 0.25$ to 0.27) are less than those during test at higher Mach numbers.

The Test 5 drag coefficients for both test and re-entry conditions are shown in Figures 2-3, 2-4, and 2-5. Slightly lower drag coefficients are indicated during the test as compared with the Test 4 results, although higher drag coefficients are indicated during re-entry than obtained with the Test 4 parachute. The same general trend of drag coefficient with decreasing Mach number, dynamic pressure, and Reynolds number indicated by previous tests is shown. The subsonic drag coefficient is quite consistent with other subsonic and transonic data mentioned previously. The general range of drag coefficients for this parachute is within the band of wind tunnel test data throughout the test and re-entry Mach number ranges.

The Test 6 drag coefficients are shown in Figures 2-3, 2-4, and 2-5. No re-entry data were obtained on this test; however, the drag coefficients in the early seconds of test ($C_{D_o} = 0.24$ to 0.28 are within the range of wind tunnel results. Figure 2-7 shows the deployment and open-ing sequence of this ribbon roof parachute as recorded by the on-board camera.

Due to booster system malfunction in Test 7, the test condition was not achieved. The launch did provide an excellent subsonic test prior to water impact, and the drag coefficient is shown on the re-entry por-tion of Figure 2-3. A value of $C_{D_o} = 0.38$ agrees well with previous data in this speed range.

Also, due to a booster system malfunction, the Test 9 conditions were not achieved and the parachute was damaged on deployment. No force data were obtained. The individual test resume in Appendix A may be referred to for further details.

28.
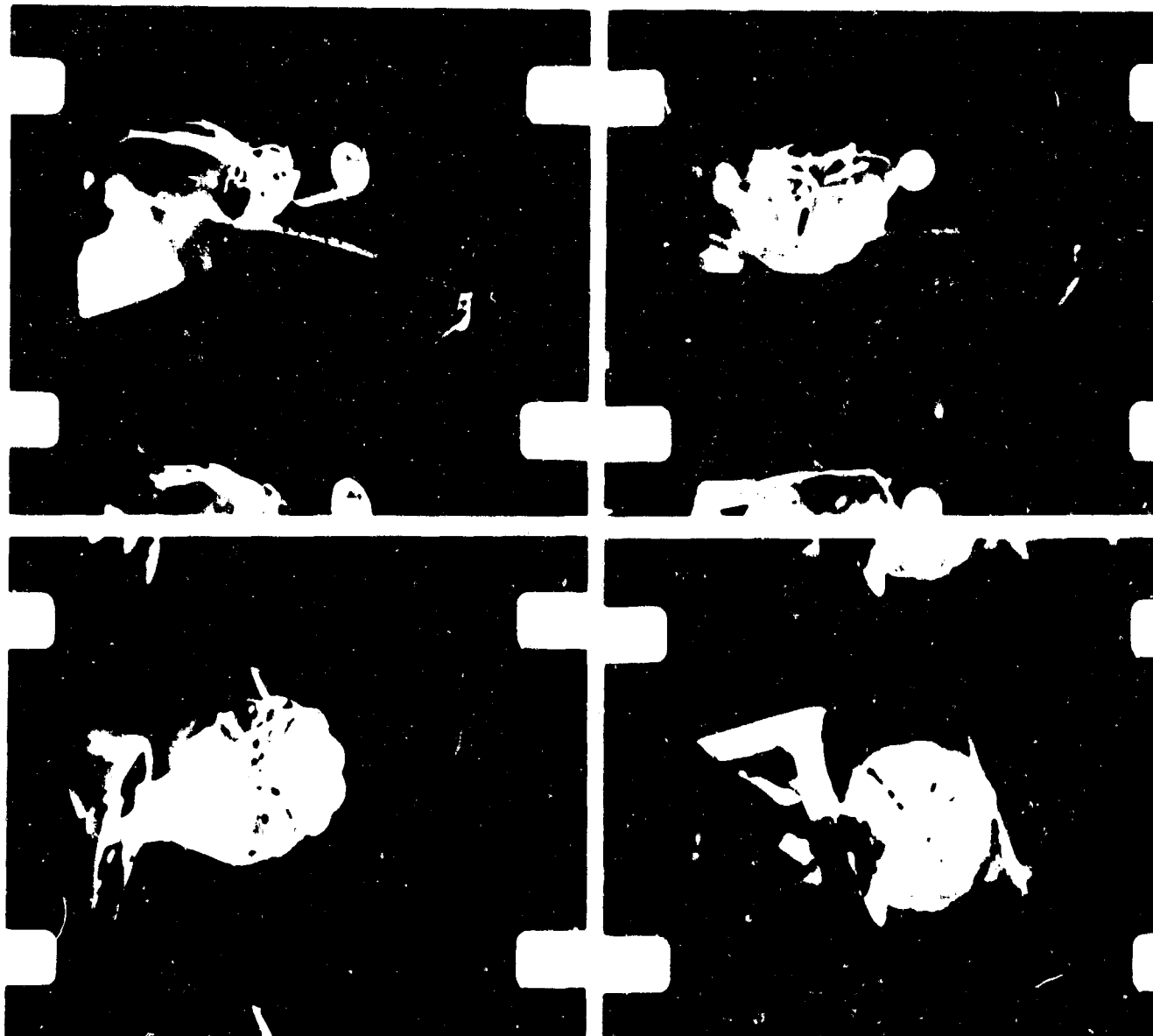
Figure 2-6   Mesh Roof Hyperflo Deployment Sequence,
Mach 2.1 at 101,000 feet - Test 3

29
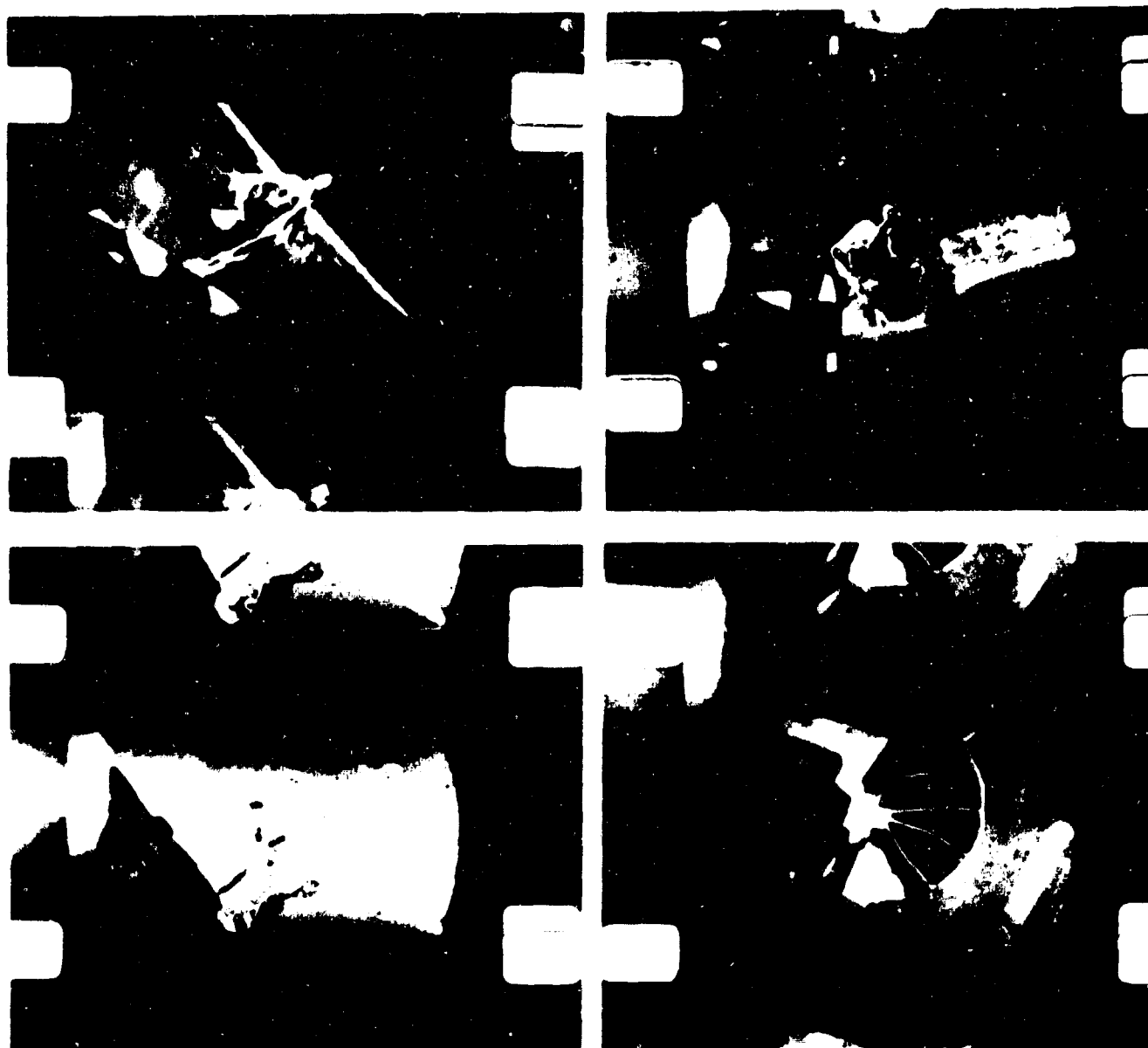
Figure 2-7 Ribbon Roof Hyperflo Deployment Sequence,
Mach 4. 0 at 123, 000 Feet - Test 6

30

In Test 10, the vehicle was not recovered and no photographic coverage was obtained. The force data recorded from this test, though presented in the test resume in Appendix A, are not considered reliable for reasons explained in the resume.

In Test 11 rather violent inflation instabilities were evidenced during this test and no attempt was made to present drag coefficient data. A plot of the force record, however, is shown in the test resume in Appendix A.

Due to deviation from the planned trajectory, the Number 12 Test condition was much more severe (M $=$ 3.12 at 77,000 feet) than the planned test condition (M = 2.8 at 100,000 feet). Although a force record was obtained during test and re-entry, the on-board camera coverage indicated a complete roof failure by 0.2 seconds after parachute deployment. This failure is considered to have occurred as a result of aerodynamic heating on the Perlon mesh roof. Force data are shown in the test resume in Appendix A.

Since for Test 13 the vehicle was not recovered, film coverage was not available for analysis. Reduction of the force data indicates that the canopy may have survived at least the first 2 to 3 seconds after deployment. A drag coefficient (C_{D_O}= 0.28 to 0.2) is shown in Figures 2-3, 2-4, and 2-5. The rapid drop off in this drag coefficient with time after deployment is contrary to other test data shown. This may indicate progressive structural failure during this time. Sampling of force data during the re-entry indicated that the parachute must have failed prior to re-entry.

2.4.3.4   Canopy Stability

Examination of the on-board motion picture film has permitted the determination of the parachute angular excursions about the point of suspension. A general discussion concerning both the interpretation of this data in a decreasing dynamic pressure environment and the manner of plotting was presented in Section 2.3.3.4.

Angular oscillation data for Tests 2, 3, 4, 5, 6, and 7 are shown in Figures A.4.4, A.5.3, A.6.4, A.7.4, A.8.3, and A.9.3 in Appendix A. In all cases, it may be observed that both the average oscillation angles and the maximum oscillation angles increase generally with time. No general trend of stability as a function of canopy porosity is apparent from these data. However, it may be noted that the best operating parachutes from the standpoint of inflation stability, namely test canopies 3, 6, and 7, had the lowest average and maximum oscillation angles. It seemed

apparent from test films that those canopies which were not stably inflated were most subject to large excursions. Larger excursions seemed to be associated with the asymmetries which resulted, in most cases, from partial canopy collapse. In the cases of test canopies 2, 4, and 5, examination of the test films indicated varying degrees of inflation instability. The inflation instability in these canopies is attributed to improper ribbon grid geometry which resulted in an increased effective porosity and resultant marginal inflation characteristics.

In particular, the wide ribbons used in the designs of test canopies 2 and 4 are considered responsible for some of the canopy instability. The successive ribbon grid design changes involved in canopies 5 and 6 were considered necessary since the use of narrow ribbons and reduced size openings would tend to minimize ribbon instabilities. These instabilities result from the tendency of ribbons to distort or tilt under load. The random ribbon distortions introduce local porosity changes in the canopy roof causing asymmetric loadings and excessively large open spaces. The performance of test canopy 6 appeared to illustrate the improvement in performance resulting from the small ribbon-small open space design of the roof.

3.   TEST CONCLUSIONS

3.1   General Considerations

In the following paragraphs, performances of the test canopies are summarized. Such factors as aerodynamic heating, parachute opening characteristics, parachute stability, drag, canopy construction, and canopy porosity are considered. Where possible, canopy performance characteristics are compared to past wind tunnel scale model test data.

3.1.1 Aerodynamic Heating

Canopy temperatures, which were measured by employing temperature sensitive paints and crayons, were predicted by analytical techniques. It was apparent from both measurement and calculation, that the material density is significant in the maximum temperature seen by a given canopy component. Under flight test conditions of from slightly above Mach 2 at approximately 100,000 feet altitude to Mach 4.4 at 94,000 feet, canopy temperature measurements ranged from $165^{\circ}F$ to $930^{\circ}F$.

3.1.2 Opening Characteristics

The canopy opening load-time histories, correlated with test movies, revealed in most cases a maximum load condition which was

32.

recorded at a significant time interval after the full open condition of the test canopy. This phenomenon appears to be associated with high suspension system stiffness resulting from over-strength parachute design characteristics. Such designs resulted from a requirement that the test parachute survive the entire trajectory. The highest load factors were exhibited by canopies which indicated inflation instabilities, hence a coupling of canopy full inflation with suspension system "bounce" may have been demonstrated in such cases.

3.2   The Hemisflo Parachute

3.2.1   Parachute Performance

The Hemisflo parachute performance exceeded the general performance of model canopies in wind tunnel tests above Mach 2. The wind tunnel model canopies were constructed with a much higher porosity (25 percent) than that of the flight test canopy (14.3 percent) hence no direct performance comparison could be made. Excellent inflation was realized with this canopy at Mach numbers of 2.4 and 3.44. Average oscillation angles of from 6° to 9° were evidenced in the Mach number ranges tested. Drag coefficients of $C_{D_o} = 0.48$ at Mach 2.4 and $C_{D_o} = 0.34$ at Mach 3.44 were realized with this canopy.

3.2.2   Effect of Geometric Porosity

Design studies (Ref. 1) of the Hyperflo parachute configurations revealed the importance of a low total porosity for successful high supersonic speed operation. By employing a porosity comparable to that associated with the Hyperflo designs, the Hemisflo parachute tested in this program proved to have excellent inflation characteristics. However, a reduced stability about the point of suspension resulted. Past studies involving supersonic tests of conventional ribbon parachute designs have indicated this trend of reduced stability with reduced porosity. The Hyperflo design, however, results in excellent stability while employing the necessary low total porosity required for good inflation characteristics at high Mach numbers.

3.3   The Hyperflo Parachute

3.3.1   Parachute Performance

In general, recorded drag data agreed with wind tunnel test data for the Hyperflo parachutes under flight environments which were comparable to the wind tunnel test conditions. The effects of varying dynamic

33.

pressure or Reynolds number for approximately constant Mach numbers appear to confirm a general trend of increasing drag coefficient values during test with decreases in these parameters. This trend had been indicated in previous wind tunnel model tests. These phenomena were not apparent in the flight re-entry data, however.

The Hyperflo stability data about the point of suspension (5°-7° average) appear, in general, to be comparable to those recorded in wind tunnel tests (5° average). The angles of excursion tend to increase during the decreasing dynamic pressure environment of the free-flight tests.

3.3.2 Ribbon Roof Hyperflo Canopies

Hyperflo tests indicate, in some cases, canopy inflation instabilities. These appear to be dependent upon the ribbon grid construction (ribbon size, open space size, etc.) in those canopies constructed with ribbon roofs. Such instabilities may be a function of either the individual ribbon stabilities or the effective porosity, or both. Due to the satisfactory performance of a ribbon roof canopy at Mach 3.98, it is apparent that this type of construction can provide a satisfactory high Mach number decelerator.

It was considered that a ribbon grid composed of narrow ribbons would provide a satisfactory roof construction, since such a grid geometry proved satisfactory in scale model wind tunnel tests. The successful full scale performance of such a construction at Mach 3.98 appeared to confirm this assumption.

3.3.3 Mesh Roof Hyperflo Canopies

In the basic wind tunnel program from which the Hyperflo canopies evolved, the Perlon mesh roof models performed in an outstanding manner compared to models with other types of roof constructions. This was confirmed in free-flight by the Test 3 canopy which was constructed with the identical Perlon to that used in the wind tunnel models. Tests involving other Perlon weave canopies did not provide sufficient supersonic data for evaluation of this particular weave, although the Test 7 canopy performed well subsonically. The canopies which were designed to evaluate the mesh roof design at high Mach numbers employed stainless steel mesh which had geometric porosities similar to the wind tunnel tested Perlon; however, hole size and filament sizes differed considerably from that of the Perlon. In Test 9, almost immediate structural failure prevented an aerodynamic evaluation of the first steel mesh canopy. In Test 11, a sufficient time was available for performance evaluation, and severe inflation instability was apparent.

Upon examination of wind tunnel Schlieren photographs, and track-side sled camera pictures of inflated Hyperflo canopies, it is apparent that the inflated roof shape requires an elastic roof construction. This is based upon the observation and measurement of inflated canopy geometries which indicate that although the roof profile is curved, the inflated diameter is essentially the same as the design projected diameter (sometimes greater). The use of a flat steel mesh roof may not have sufficient elasticity to allow the canopy to assume its preferred inflated shape. Inflation instabilities noted in free-flight tests of such configurations may be attributed to such possible inelastic roof problems. Should this be true, then some degree of roof shaping may be necessary for satisfactory performance if an inelastic roof material is used.

Other factors such as the actual mesh grid geometry may also have contributed to the malfunction in these tests. The mesh geometry, although equivalent in porosity to the previous satisfactory performing Perlon mesh, was markedly different in filament and open space sizes.

4. DATA ACQUISITION PROBLEMS

There are many data acquisition problems which affect the accuracy of the data. These problems range from extreme test environment conditions to telemetry limits, recording limits and data reading accuracies.

4.1 Pressure Measurements

The measurement of accurate pressures, even at subsonic velocities, is a difficult task requiring careful calibration. Add to this a changing altitude rate of 3000 to 4000 feet per second at altitudes of 80,000 to 190,000 feet and the extent of the problem should be apparent. In Test 1, on 18 December 1963, the static pressure measurement lagged the actual altitude, as given by the radar, by approximately 20,000 feet. The differential pressure, when corrected for the radar-given altitude pressure, provided the correct Mach number, thus indicating that the ram pressure measurement was correct. The static pressure error could have been caused by either a lag in the system caused by too large a tubing volume as compared with the pressure ports or more likely to higher than static pressures surrounding the static ports.

Because of these problems, the Mach number and altitude values for each test were obtained from the radar data. This data is generally considered to be accurate enough for our purposes to be used without correction. However, there were times that Mach number did have to be corrected due to errors in the temperature input.

It was normal for Eglin Air Force Base to launch a weather balloon prior to each test. These balloons ascended to altitudes of 80,000 to 120,000 feet. Temperature and pressure data were quite accurate at the altitudes reached by the weather balloons; however, above this altitude, both temperature and pressure had to be obtained from standard atmosphere data. It does not seem unreasonable that the dynamic pressures used above weather balloon heights could be in error by at least 10 to 20 percent. Since the dynamic pressure data is used for the determination of the drag coefficient, the C_D data also could be in error by this amount.

4.2 Telemetry

The telemetry system had very few problem areas. The telemetry channels had high enough frequency response so that no data was lost due to low response time. The only real problem with the telemetry was a zero shift that occurred on some tests after transducer restore. This shift appeared to be a function of time. That is, the longer power was on the bridge the less the zero shift. What made the zero shift such a problem was that once the test parachute was deployed, it was almost impossible to determine the new zero position with time. This had little effect when the loads were high so that an error in the zero position of 2-3 hundredths of an inch meant only a very small percent change in load. But when loads were small, such as 10-20 seconds after parachute deployment, a small zero shift could mean a 50-100 percent load error.

Efforts were made during data analysis to correct for obvious zero shifts. One procedure used, was to establish a time when the test parachute load should be near or at zero. Then, assuming this load reading to be zero, a zero shift correction was applied to the test regime area. It is, of course, impossible to know the accuracy of this correction. However, it has definitely increased confidence in the accuracy of the data.

It presently seems that to eliminate this zero shift the bridge power should be left on from about T_o-10 minutes until water impact. This would prevent any cooling of the bridge circuit and corresponding resistance changes.

4.3 Receiving and Recording Equipment

The receiving, recording and data processing equipment was operated by Eglin Gulf Test Range. Thus the experimenter had no control over possible built-in system or operational errors. Sometimes the analog force data was received lacking the base reference line necessary to get accurate

deviation readings and therefore required rerun of the analog record. In other cases, two separate records of the same flight had small but obvious differences.

4.4 Low Loads

Normally, the tensiometer selection was based upon a deployment load equaling its approximate mid-range output. Since load data were being read for a full 15-20 seconds after deployment, the vehicle may have increased its altitude by 60,000 to 70,000 feet in that period. The dynamic pressure may have decreased from 100 psf to 5 psf and the parachute loads would have decreased correspondingly. Assuming the deployment load was 50 percent of full range, then the final load would be about 3 percent. These 3 percent loads are not considered very accurate.

However, many times the deployment conditions were other than expected and the deployment loads were as low as 10 percent of full scale. In these cases, the final load dropped to 1/2 of 1 percent of full scale. For this condition, the load was well below the accuracy of the telemetry, receiving and recording system. The practical accuracy of the electronic system is considered to be 2-3 percent of the tensiometer full range.

4.5 Data Reading

The force data are obtained in analog form from the Testing Facility. A typical pound per inch of deviation for a 1000 pound tensiometer is approximately 700 pounds per inch. Therefore, each 0.01 inch of deviation is equal to 7 pounds of parachute drag. It was not unusual for the parachute loads to drop to 10-20 pounds during the 18 seconds for which data were reduced. The trace provided on the analog record is typically 0.01 to 0.02 inch thick. Reading accuracies better than 0.01 inch are difficult. Thus, the percent error in the low load range of the tensiometer, just due to reading, could be 50-100 percent.

5. RECOMMENDATIONS FOR FUTURE TESTING

5.1 Wind Tunnel Parachute Tests

In order to extend the state of the art of current Hyperflo parachute designs, the significance of certain canopy design parameters must be determined. Many design and performance parameters were found to be significant to canopy performance during supersonic wind tunnel investigations.

The significant aerodynamic parachute performance parameters which should be considered are: Effective porosity of meshes and ribbon grids at supersonic speeds, location of parachute canopy aft of both blunt and pointed forebodies, effects of the ratio of parachute diamter to forebody diameter, and canopy geometry variation effects.

5.2 Parachute Material Studies

In addition to strictly aerodynamic performance parameters, various structural criteria must be established which should be compatible with the aerodynamic criteria. Such factors, for example, as elasticity and material strength properties as a function of temperature are essential to the attainment of proper canopy shape and structural integrity of parachute components in high loading and/or severe thermal environments. In the consideration of high temperature materials for parachute application, it is felt that priority should be given to coated fabrics or coated fibers, such as Teflon or silicone rubber coated nylon and Nomex materials. This is based upon the normally expected short aerodynamic heating periods associated with a first stage decelerator application where an ablative insulating coating would allow the use of conventional internal fibers for parachute component construction. It is considered that the use of metal fiber fabrics would not, in general, be required for most applications of first stage decelerators. The use of such materials for parachutes would be restricted in early orbital re-entry maintained for extended time periods, where ablative type insulating materials could not be effectively applied.

5.3 Full Scale Parachute Tests

Extensive use of high speed sleds are recommended to establish and/or confirm structural design criterial for the Hyperflo type parachute configurations. The controlled test condition and ease, and reliability of data acquisition of the high speed sled type testing would provide an ideal means of evaluating the structural-aerodynamic design parameter compatibilities discussed in 5.1 and 5.2 above. The use of the relatively low speed sled is particularly applicable for such studies in the light of the Mach number insensitivity of the properly designed Hyperflo parachutes in past wind tunnel and flight tests. In particular, the use of the Mach 3 sled now being built by the Air Force would be particularly appropriate for the evaluation of canopies constructed of unconventional materials and fabricated possibly by new techniques.

Evaluation of satisfactory parachute configurations would then be performed in a flight test vehicle in the high Mach number environments.

5.4 Parachute Deployment and Opening Loads

It is recommended that both analytical and experimental studies be performed to evaluate supersonic parachute and parachute suspension system dynamics during the deployment and opening process. The indication of maximum parachute opening load factors at a time which is not coincident with the first full open condition of the deployed parachute has indicated a possible correlation with suspension system stiffness. Since stress analysis techniques rely on the maximum load factor (which is normally associated with the full open canopy, or opening shock) the use of the "opening shock factor" for design calculations may in general result in an understrength design.

REFERENCES

1. "Analytical and Experimental Investigation of Supersonic Parachute Phenomena," L. W. Sims, ASD-TDR-62-844, (CONFIDENTIAL)

2. "Study of Parachute Performance and Design Parameters for High Dynamic Pressure Operation," P. E. Pedersen, FDL-TDR-64-66

3. "The Problem of Aerodynamic Heating," E. R. van Driest, Aeronautical Engineering Review, October 1956

4. "Measurements of Turbulent Heat Transfer Rates on the Aft Portion and Blunt Base of a Hemisphere Cylinder in the Shock Tube," J. Rabinowicz, Jet Propulsion, September 1958

40.

APPENDIX A

FIELD TEST RESUME

A.1 INTRODUCTION

The following sections of this appendix discuss and show the available data from each of the 13 tests accomplished as a result of this program. Each test is discussed separately and no attempt is made to reference data from one test to another or to come to any conclusions except as it may apply to an individual test. A summary of the significant test data is provided in Table 2-1. More detailed information is presented in the individual test resumes.

A.2 GENERAL

In each test section, various graphs are provided. The graph of the payload trajectory covers the area from launch to water impact. This graph is provided as an aid in seeing the entire trajectory and it is not intended that trajectory data of high accuracy can be obtained from it.

A graph of C_D and parachute force is provided for both the test regime and re-entry, where data is available. In general, data has been provided for about 20 seconds in the test regime. Because of this extended time, it is not unusual for the parachute loads to drop below 2% of full range on the tensiometer. Therefore, in areas where data, although available, has appeared somewhat questionable, dashed lines rather than solid have been used for C_D and Force.

Anticipated Hyperflo drag coefficients (C_{D_O}) were determined from Figure 2-1 of this report. A drag coefficient (C_{D_O}) of 0.5 was assumed for the Hemisflo parachute.

The test result summaries specify an anticipated opening shock load which is normally expected to be the maximum canopy load during the opening process. Test data, however, revealed higher loadings after canopy inflation in many instances. To allow for the tabulation of both loadings, both opening shock and "maximum load" are tabulated.

A graph of canopy oscillation is provided where data is available. The oscillation angle is measured from the attachment in reference to the vehicle centerline. No attempt has been made to establish polar coordination. That is, if the parachute were coning about the vehicle centerline at

41.

a constant 5 dgree angle, then the graph would show a constant line at 5 degrees. The curve on the graph marked "Max. Osc." represents the maximum excursions of the parachute. In most cases, these excursions were of very short time durations. The curve marked "Ave. Osc." represents the average time weighted oscillations.

A. 3   TEST MISSION 1

Date: 18 December 1962
Time: 12:30 CST

A. 3. 1   Objective and Test Setup

The objective of Test No. 1 was to test a Hemisflo parachute (Cook Electric P/N 596-8151) at a Mach number of 2.6 and an altitude of 87,000 feet. This 4.12 foot D_o parachute had its roof contructed using 16 gores of 1-1/4 inch by 300 pounds and 3/8 inch by 200 pounds for the horizontals and verticals, respectively. All material was high temperature Nomex. Canopy porosity was 14.3 percent. The line length was 2D, the D_p/d_B ratio was 3.4, the x/d_B was 12.0 and the W/S_o was 61,

where
$$D_p = 2.55 \text{ ft.} \qquad S_o = 13.33 \text{ ft.}^2$$
$$d_B = 0.75 \text{ ft.} \qquad S_p = 5.1 \text{ ft.}^2$$
$$D = \frac{\pi}{2} D_p$$

A 3000 pound tensiometer and an accelerometer rated at ±1 g were used as part of the data gathering components.

The launch vehicle consisted of a 1st stage Honest John, a 2nd stage Nike and an 820 pound Cree payload with a 15 dgree Nike to Cree Adapter. Ignition time for the second stage was 30 seconds. The booster fin angles of incidence were $0.5°$ and $0°$ for first and second stages, respectively.

A. 3. 2   Test Result Summary

The general test results are summarized below:

	Anticipated	Actual
Deployment Mach Number	2.6	2.4
Deployment Altitude (Ft.)	87,000	82,600
Deployment Dynamic Pressure (lb/ft.^{2})	205	206
Vehicle Spin Rate at Deployment (rps)	-	1/4
Deployment Time (sec.)	50.95	50.80
Ejection to Full Line Stretch (sec.)	-	.209
Line Stretch to Full Open (sec.)	-	.05
Full Open to Max Load (sec.)	-	.313
Snatch Force (lbs)	-	460

Opening Shock (lbs)	1780	1101
Max. Load (lbs)	-	1713
C_{D_O} Ave. (1-5 sec.)	0.50	0.48
Max. Temperature (^{O}F)	-	210

A.3.3   Test Discussion

This parachute test was good in all respects. Excellent telemetry data was obtained from test parachute deployment through water impact. The on-board camera functioned properly and good film data was obtained. The tracking radars provided good trajectory information throughout the flight (see Figure A.3.1).

This was a unique Hemisflo in that the total canopy porosity was about one-half that of Hemisflos previously tested. The over-all parachute performance has been judged to be fair. The drag coefficient (see Figure A.3.2) appears somewhat high as compared to Hemisflos previously tested, but this could, to a large extent, be attributed to the decrease in porosity. Points 1, 2, and 3 on the force curve are snatch, full open, and maximum loads, respectively.

Drag data has been reduced covering the re-entry phase of the trajectory. This data covers the suppersonic, transonic and subsonic regimes, (see Figure A.3.3). Canopy oscillation is shown in Figure A.3.4.

The test parachute was recovered undamaged. Crayon type heat sensors were used to record canopy temperatures. Since the low temperature heat sensors fade back to their original color within a short time when in contact with salt water, it was necessary to determine the canopy maximum temperature from the on-board camera film. This maximum temperature was 210°F. Figure A.3.5 shows the parachute after recovery.

The trajectory was close to predicted. When second stage ignited, the trajectory angle changed azimuth by about 40 degrees for some unknown reason. All vehicle functions occurred as planned except for the recovery phase. The recovery parachute charge was ignited as programmed at 10,000 feet; however, the cartridge holder failed structurally, allowing the gases to escape and the recovery parachute was not deployed. The vehicle hit the water at about 200 fps and some structural damage was done. The flotation balloon was inflated but was then cut on a piece of the damaged structure. The vehicle sank in 95 feet of water and was recovered by Navy Recovery Divers three days later. The transducer compartment was the only instrumentation that got wet. The water entered this compartment through the solenoid valve in the pressure lines. This valve opened when the timer was recycled due to the salt water completing the recycle

44.

circuit through the umbilical connector. This condition is expected on all tests unless vehicle power is removed prior to salt water impact.

The sonar beacon, which is located in the recovery parachute riser, was damaged beyond repair.

In reducing the static and ram pressure data used to determine altitude and Mach number, large errors were found. These errors were caused by incorrect static pressure measurements. The static pressure measurements were too high and may have been caused by a lag in the pitot static system. It was decided that all Mach, altitude, and similar information would have to be provided by the tracking radars for this and future tests.
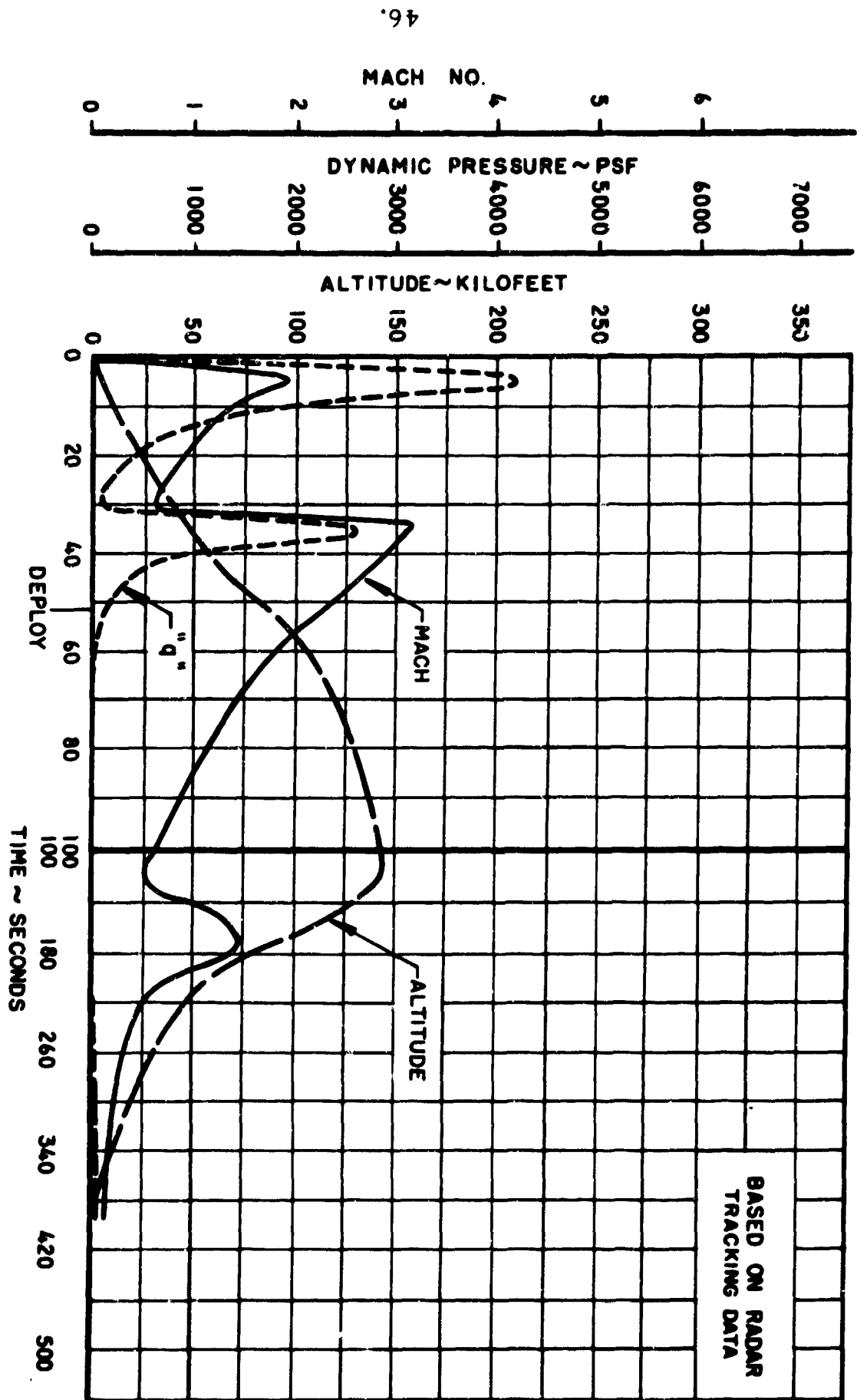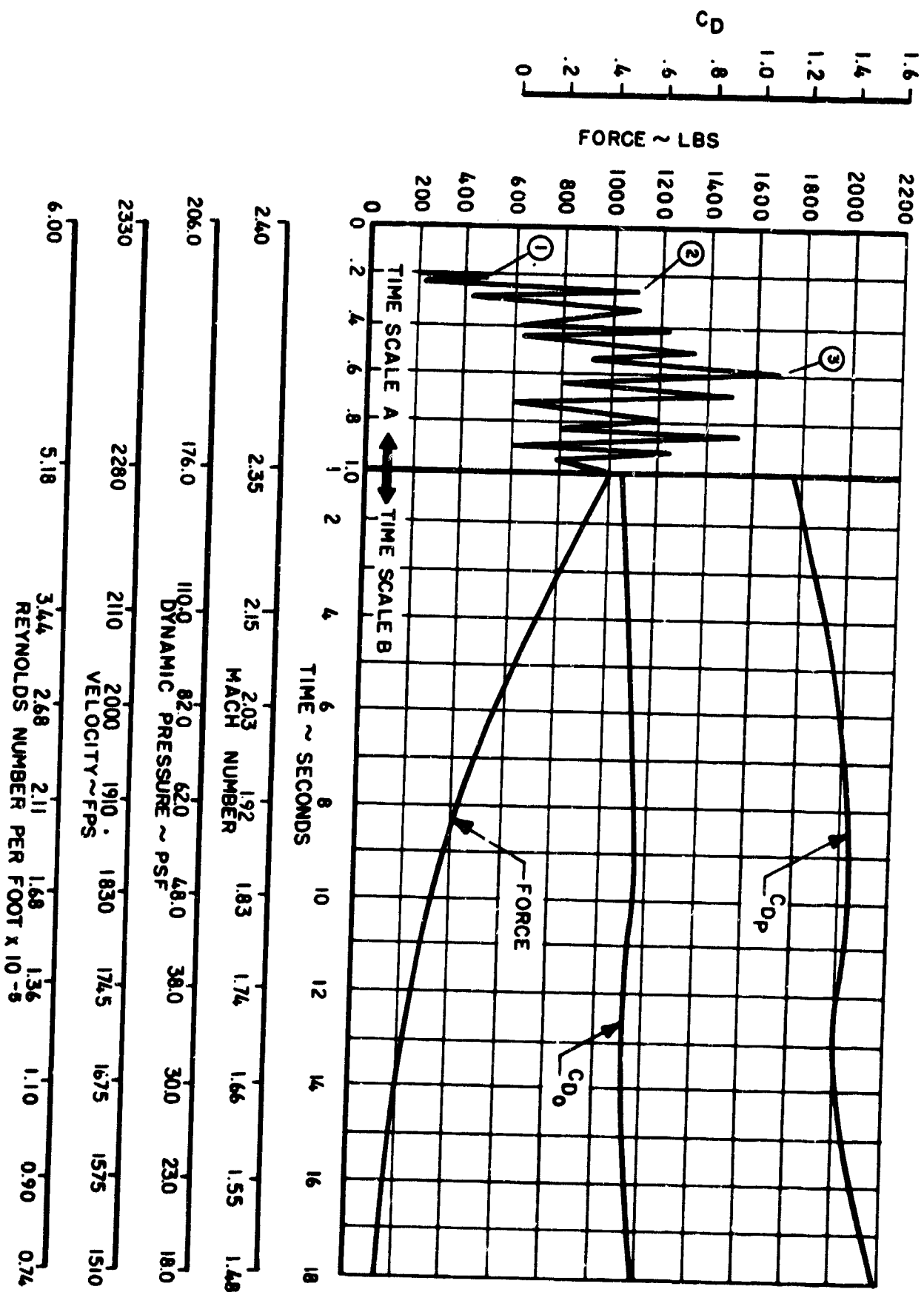
Figure A.3-1 Missile Tracking Data - Test No. 1

Figure A.3-2 C_D and Force Vs. Time, Mach Number, Dynamic Pressure, Velocity and
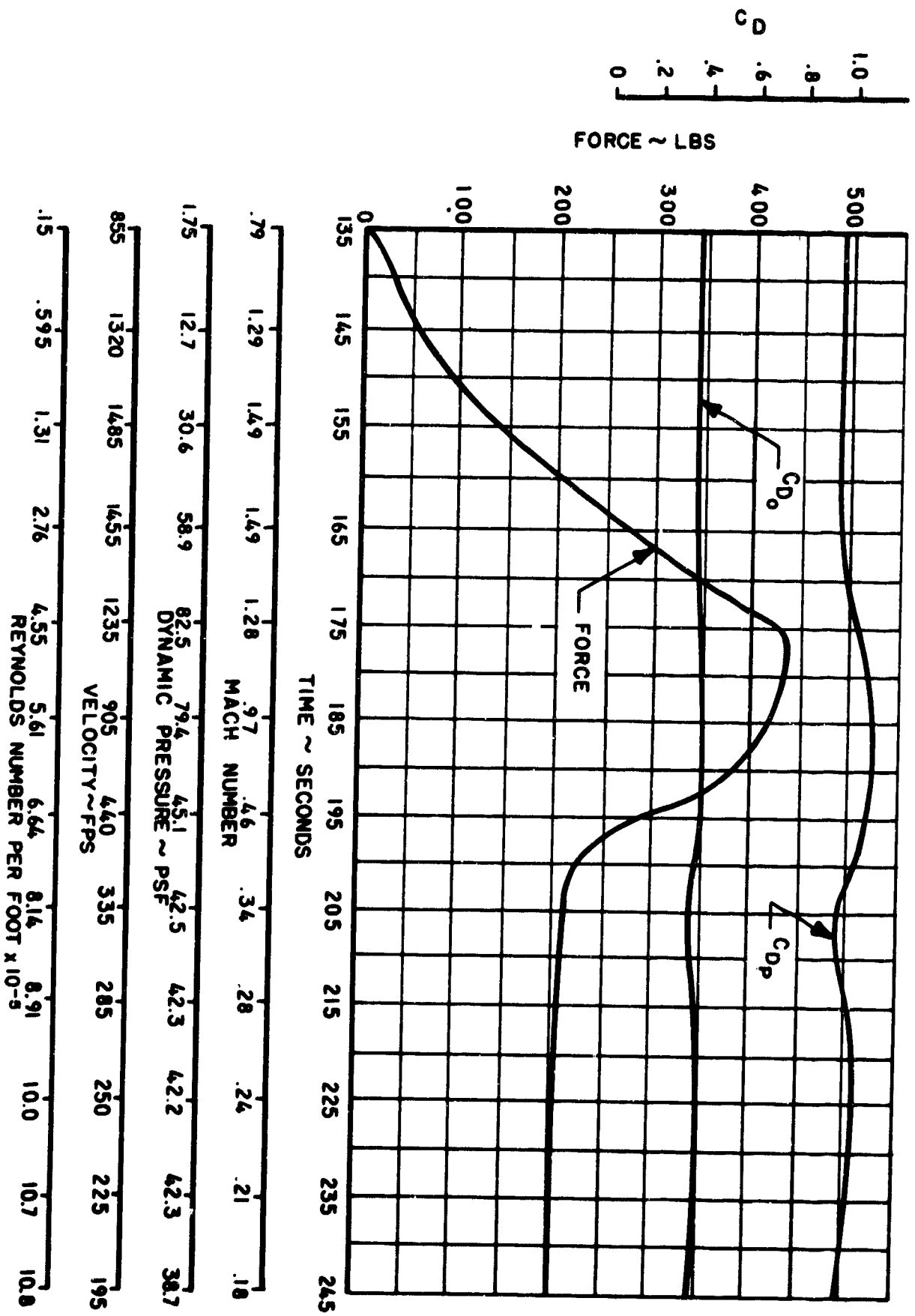Reynolds Number - Test No. 1

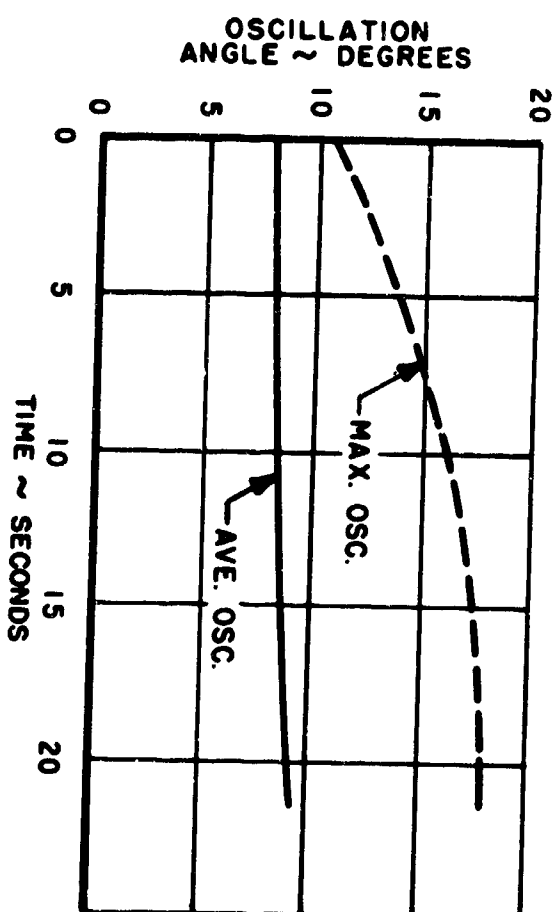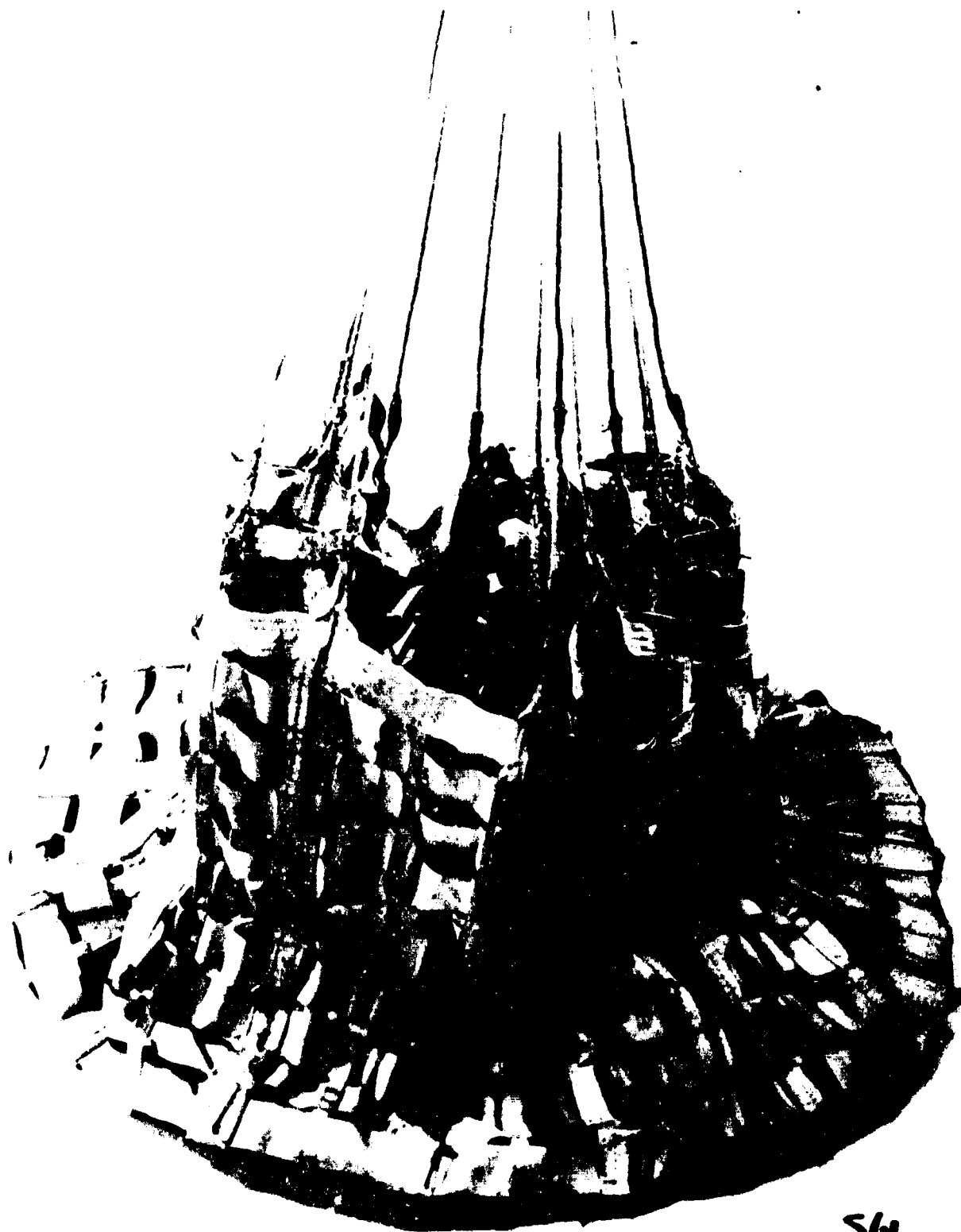Figure A.3-3 CD and Force Vs. Time, Mach Number, Dynamic Pressure, Velocity and Reynolds Number - Re-entry No. 1

Figure. A. 3-4 Oscillation Angle Vs. Time
Test No. 1

S/N
1315

Figure A. 3-5 Recovered Test Parachute - Test No. 1

A.4 TEST MISSION 2

Date: 7 February 1963
Time: 07:11 CST

A.4.1 Objective and Test Setup

The objective of Test No. 2 was to test a Hyperflo parachute (Cook Electric P/N 596-8169) at a Mach number of 3.1 and an altitude of 110,000 feet. This 2.71 foot D_o parachute had its roof constructed using 12 gores of 3/4 inch by 400 pound and 3/8 inch by 200 pound horizontal and vertical ribbons, respectively. All material was high temperature Nomex. Roof porosity was 28.5 percent and total parachute porosity was 14.0 percent. The line length was 2.6 D_p, the D_p/d_B ratio was 2.5, the x/d_B was 7.8 and the W/S_o was 94,

where D_p = 1.87 ft. S_o = 5.78 ft.^{2}

d_B = 0.75 ft. S_p = 2.76 ft.^{2}

A 1000 pound tensiometer and an accelerometer rated at ±1 g were used as part of the data gathering components.

The launch vehicle consisted of a 1st stage Honest John, a 2nd stage Nike and a 540 pound Cree payload with a 15 degree Nike to Cree Adapter. Ignition time for the second stage was 25 seconds. The booster fin angles of incidence were 0.5° and 0° for first and second stages, respectively.

A.4.2 Test Result Summary

The general test results are summarized below:

	Anticipated	Actual
Deployment Mach Number	3.1	2.84
Deployment Altitude (Ft.)	110,000	100,500
Deployment Dynamic Pressure (lbs/ft^2)	103	120
Vehicle Spin Rate at Deployment (rps)	-	1/3
Deployment Time (sec.)	47.5	48.60
Ejection to Full Line Stretch (sec.)	-	.104
Line Stretch to Full Open (sec.)	-	.036
Full Open to Max. Load (sec.)	-	.360
Snatch Force (lbs)	-	84
Opening Shock (lbs)	225	250
Max. Load (lbs)	-	364

51.

C_{D_0} Ave. (1-5 sec.)   .29   .280

Max. Temperature (°F)   -   330

A.4.3   <u>Test Discussion</u>

This parachute test was successful and all objectives of the test were achieved. Excellent telemetry data was obtained from test paracute deployment through water impact. The on-board camera functioned properly and good film data were obtained. Radar tracking was good and the trajectory is shown in Figure A.4.1.

Figures A.4.2 and A.4.3 show force and C_D during the test and re-entry regimes, respectively. Points 1, 2, and 3 on Figure A.4.2 are snatch, full open and maximum loads, respectively.

Parachute oscillation is shown in Figure A.4.4. The over-all performance of this parachute is rated at poor to fair.

The test parachute was recovered undamaged. The temperature-sensitive paints applied to the parachute indicate a maximum temperature of 330°F on both the roof and cone. Figure A.4.5 shows the parachute after recovery.

The vehicle functioned completely as programmed except that it again went off course when second stage ignited. It took the recovery boat 1-3/4 hours to reach the floating recovery package. The recovered vehicle was undamaged except for the loss of the telemetry antenna and the Sonar Beacon was broken beyond repair. The electrical systems were recovered intact except that the differential pressure transducer had an open bridge.

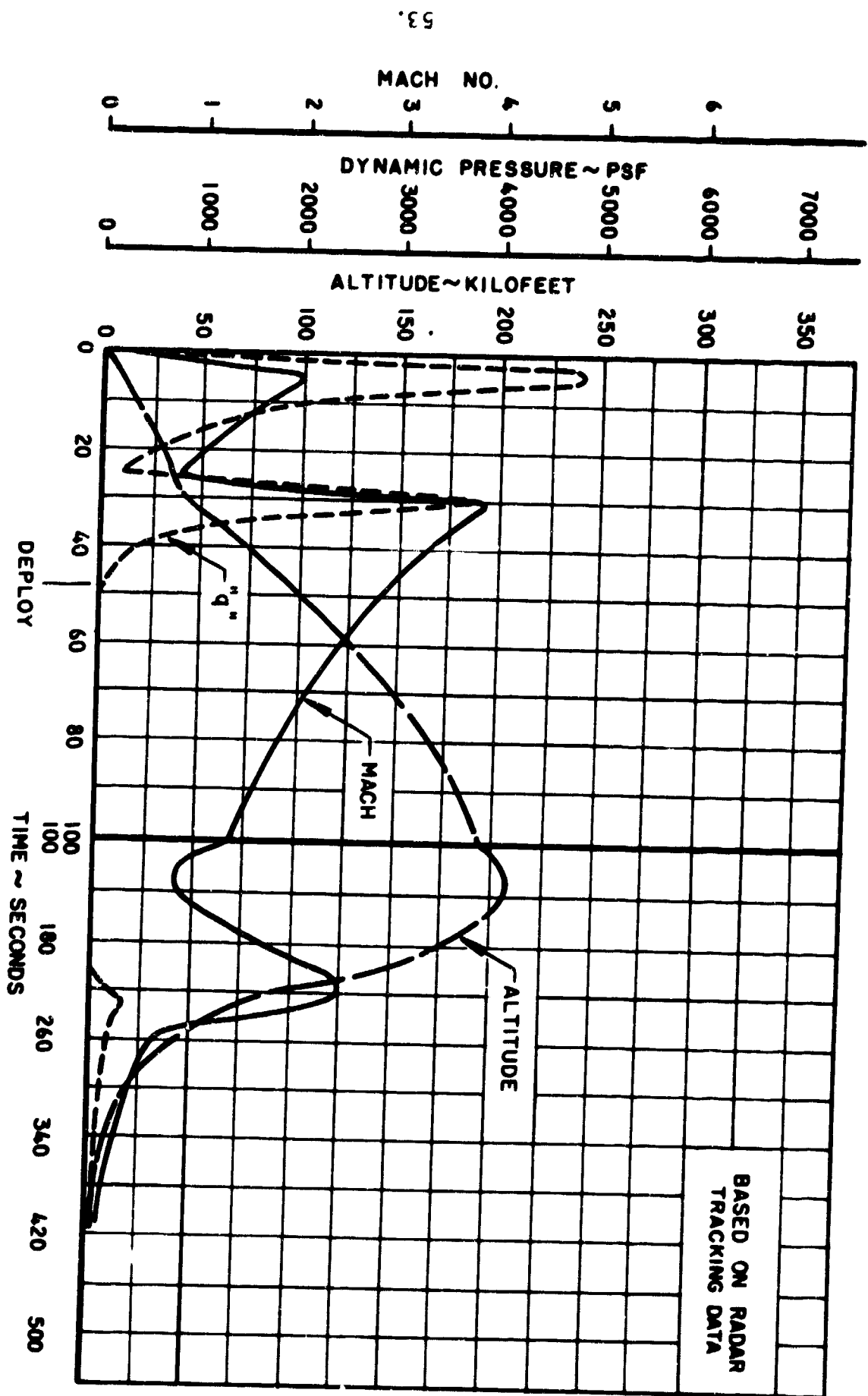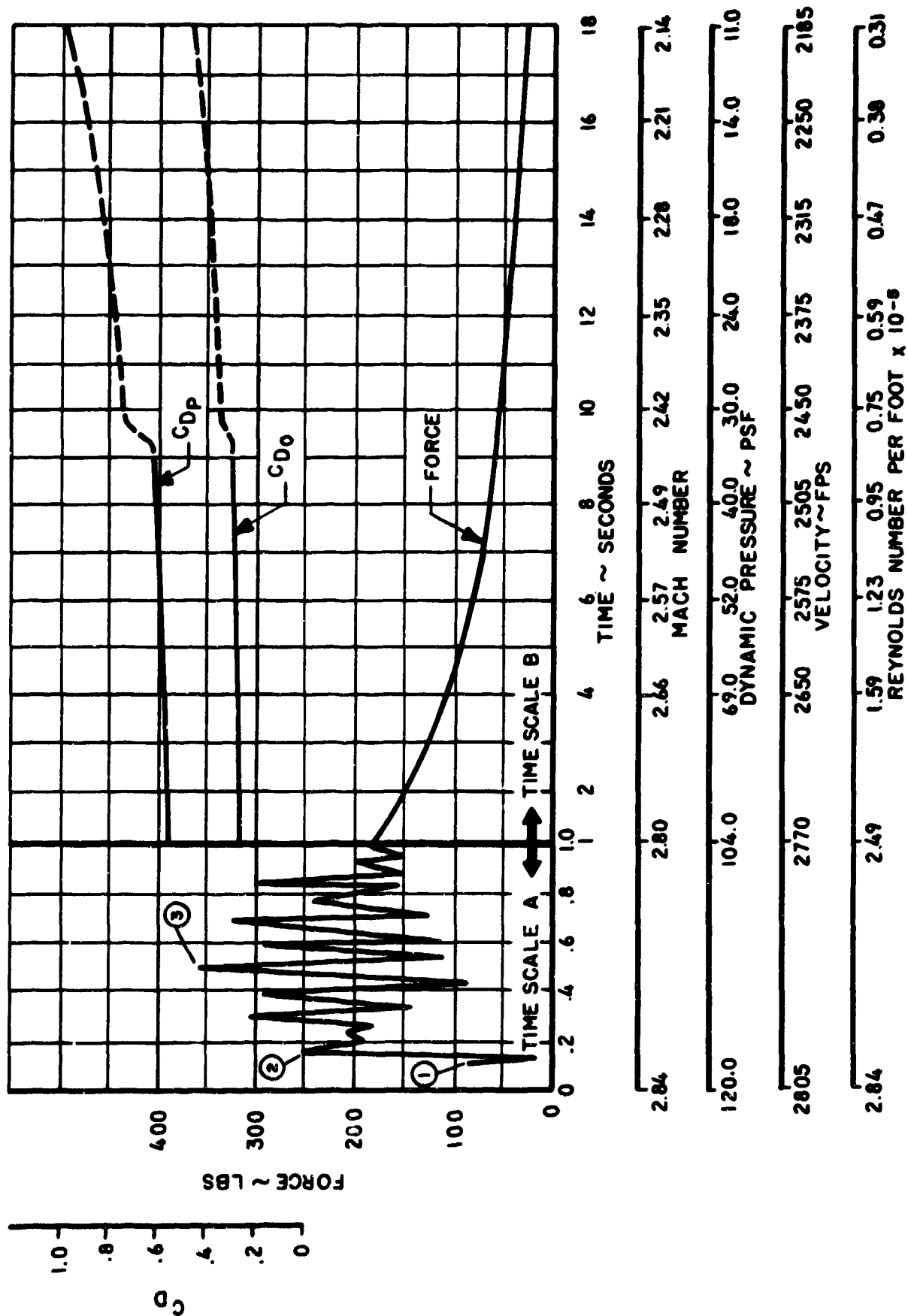Figure A.4-1   Missile Tracking Data - Test No. 2

Figure A.4-2 C_D and Force Vs. Time, Mach Number, Dynamic Pressure, Velocity and Reynolds Number - Test No. 2
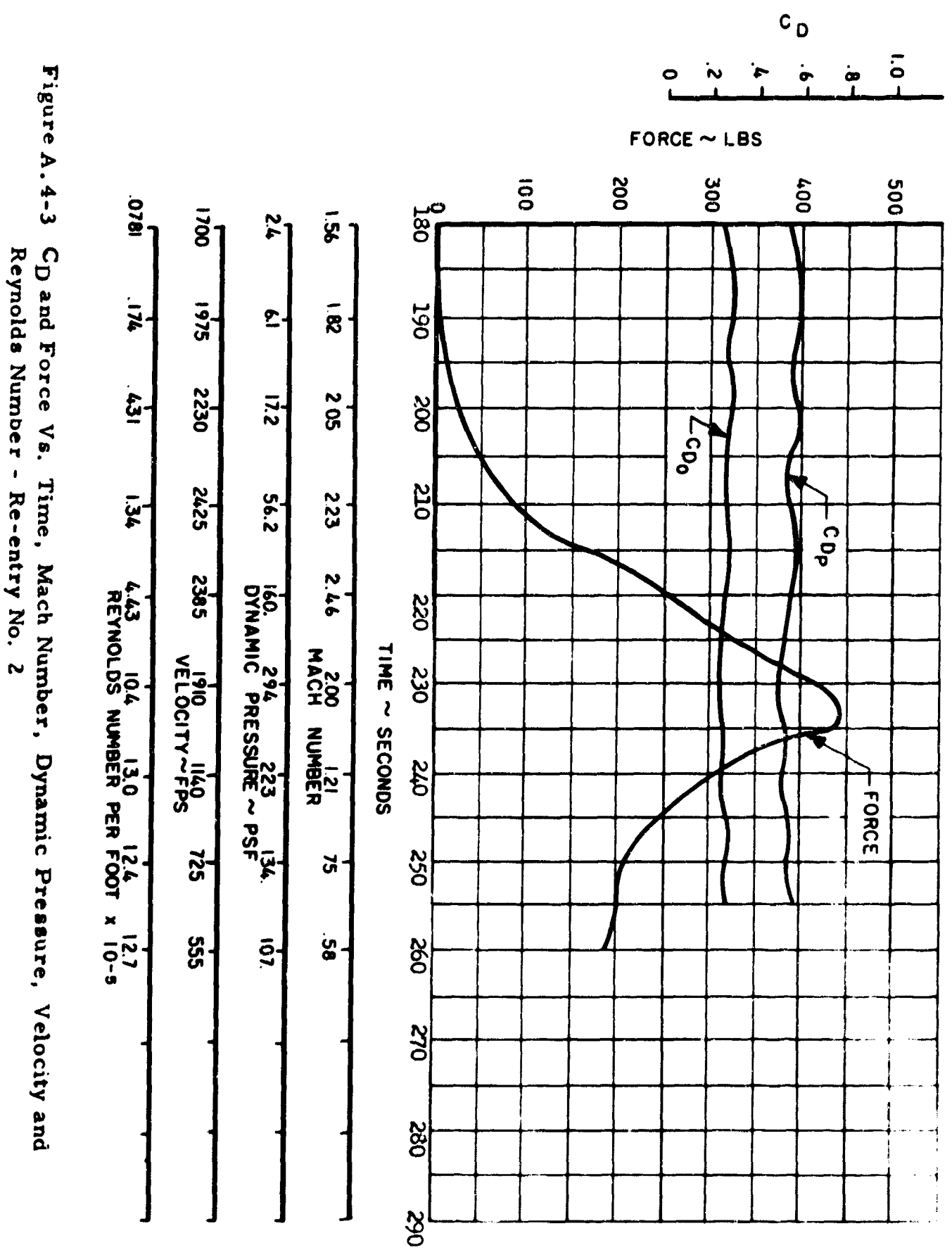
Figure A.4-3 C_D and Force Vs. Time, Mach Number, Dynamic Pressure, Velocity and Reynolds Number - Re-entry No. 2
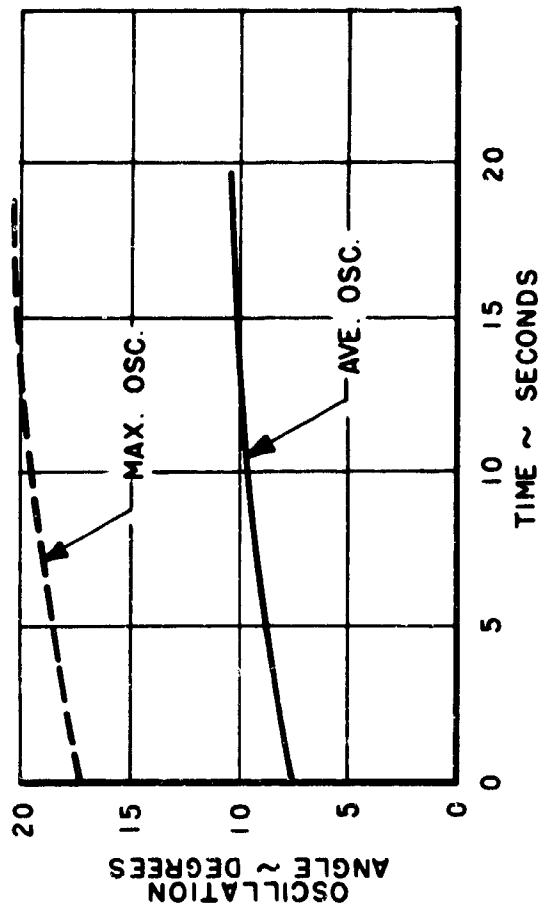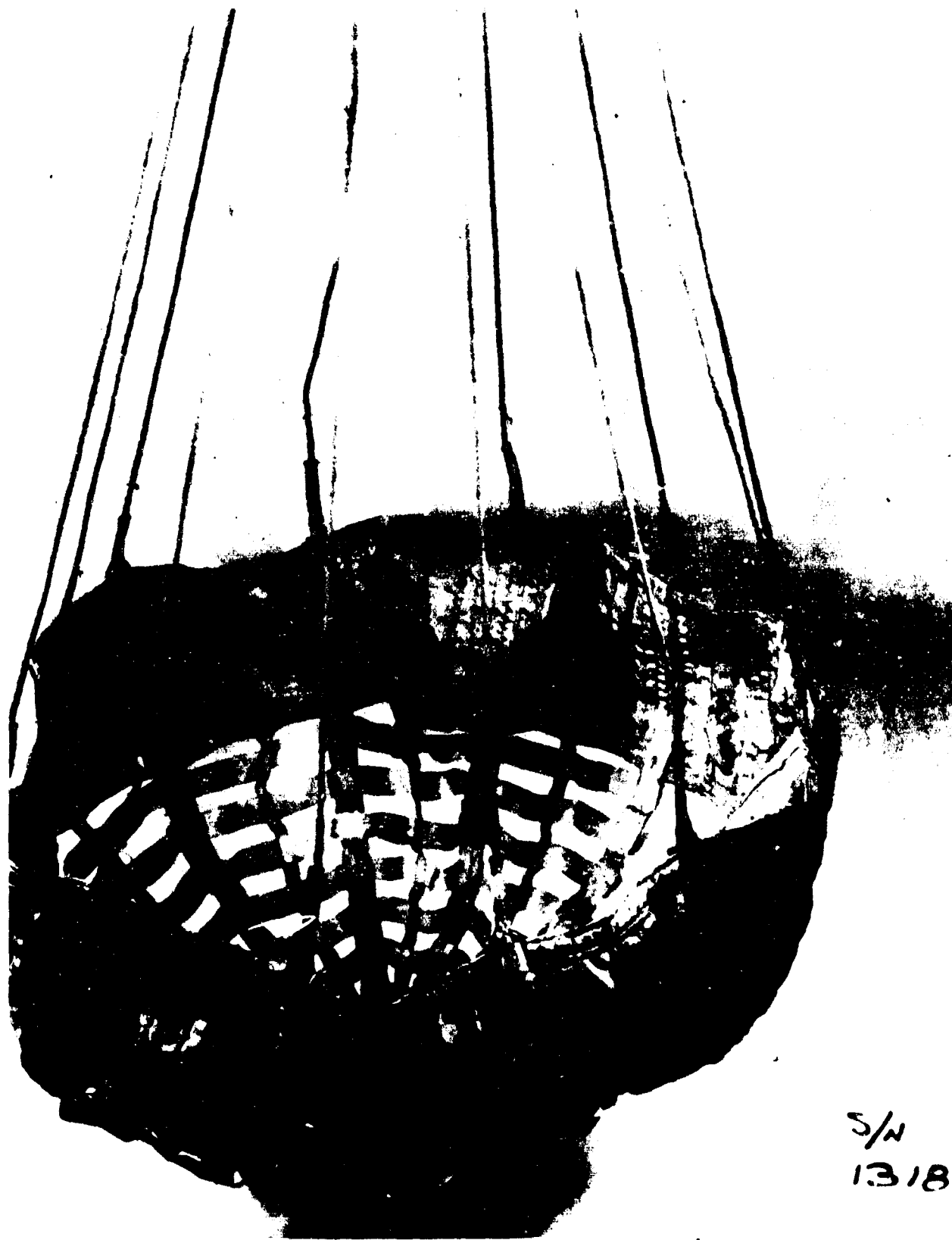
Figure A.4-4 Oscillation Angle Vs. Time
Test No. 2

S/N
1318

Figure A.4-5 Recovered Test Parachute - Test No. 2

57.

A.5   TEST MISSION 3

Date: 21 February 1963
Time: 07:10 CST

A.5.1   Objective and Test Setup

The objective of Test No. 3 was to test a Hyperflo parachute (Cook Electric P/N 596-8869) at a Mach number of 3.1 and an altitude of 110,000 feet. This 2.71 foot D_o parachute had its roof constructed using 12 gores of Perlon mesh. This mesh had a porosity of 35 percent. Roof porosity was 26 percent and total parachute porosity was 12.7 percent. The line length was 2.6 D_p, the D_p/d_B ratio was 2.5, the x/d_B was 7.8 and the W/S_o was 94,

$$\text{where} \quad D_p = 1.87 \text{ ft.} \quad S_o = 5.78 \text{ ft.}^2$$
$$d_B = 0.75 \text{ ft.} \quad S_p = 2.76 \text{ ft.}^2$$

A 1000 pound tensiometer and an accelerometer rated at ±1 g were used as part of the data gathering components.

The launch vehicle consisted of a 1st stage Honest John, a 2nd stage Nike and a 540 pound Cree payload with a 7.5 degree Nike to Cree Adapter. Ignition time for the second stage was 20 seconds. The booster fin angles of incidence were $1/2°$ and $0°$ for first and second stages, respectively.

A.5.2   Test Result Summary

The general test results are summarized below:

	Anticipated	Actual
Deployment Mach Number	3.1	2.1
Deployment Altitude (Ft.)	110,000	101,200
Deployment Dynamic Pressure (lbs/ft^2)	103	70
Vehicle Spin Rate at Deployment (rps)	-	1
Deployment Time (sec.)	47.5	48.0
Opening Shock (lbs)	225	-
C_{D_o} Ave. (1-5 sec.)	0.29	-
Max. Temperature (°F)	-	165

A.5.4   Test Discussion

This test was only partially successful in that the full objectives of the test were not achieved. The telemetry system went out at second stage burn-out and did not come back on again until in the subsonic regime

58.

of re-entry. The on-board camera functioned properly and good film data were obtained. Radar tracking was good and the trajectory is shown in Figure A.5.1.

Figure A.5.2 shows the subsonic force and C_D during re-entry. Figure A.5.3 shows the parachute oscillation. The test film showed the parachute to have good opening tendency and excellent inflation and oscillation stability. The general parachute performance has been judged to be very good. There was no tendency for line twist. The parachute was recovered without damage. The canopy maximum temperature of $165^\circ F$ was obtained from the on-board camera film. Figure A.5.4 shows the parachute after recovery.

The trajectory was satisfactory from launch until second stage burn-out. Then, the combination of second stage Nike plus Cree encountered what is believed to be a pitch-roll coupling condition. The net result of this condition was very high angle coning. It is believed that during the high "g's" caused by this coupling that the forward end of the nose spike together with the telemetry antenna broke off. Within several seconds, it is assumed that the Cree broke away from the Nike. The phototheodolite was very poor; however, it shows the Nike, at a later period, in what appears to be end-over-end tumbling. The Cree continued in a normal trajectory from approximately $T_0 + 27$ seconds. However, in the three seconds from second stage burn-out at $T_0 + 24$ seconds to $T_0 + 27$ seconds, the Cree lost one full Mach number over and above its planned Mach trajectory.

It was concluded that the change of direction shown in Tests 1 and 2 was in some way also linked to the pitch-roll coupling problem. In order to solve this, it was decided to increase the roll rate of the second stage well above the pitch frequency. The roll rate to pitch frequency ratio would be maintained at a minimum of 1.5 for future tests.

The vehicle was recovered undamaged except for the lost spike and antenna.

The telemetry came back on at $T_0 + 4$ minutes. The aerodynamic heating existing during re-entry apparently burned the insulation off that part of the antenna co-axial cable hanging out of the remaining portion of nose spike. With the insulation gone, the braided shield wire was exposed to the air flow and unbraided, exposing the center conductor. It was concluded that the telemetry signal came from this exposed center conductor.
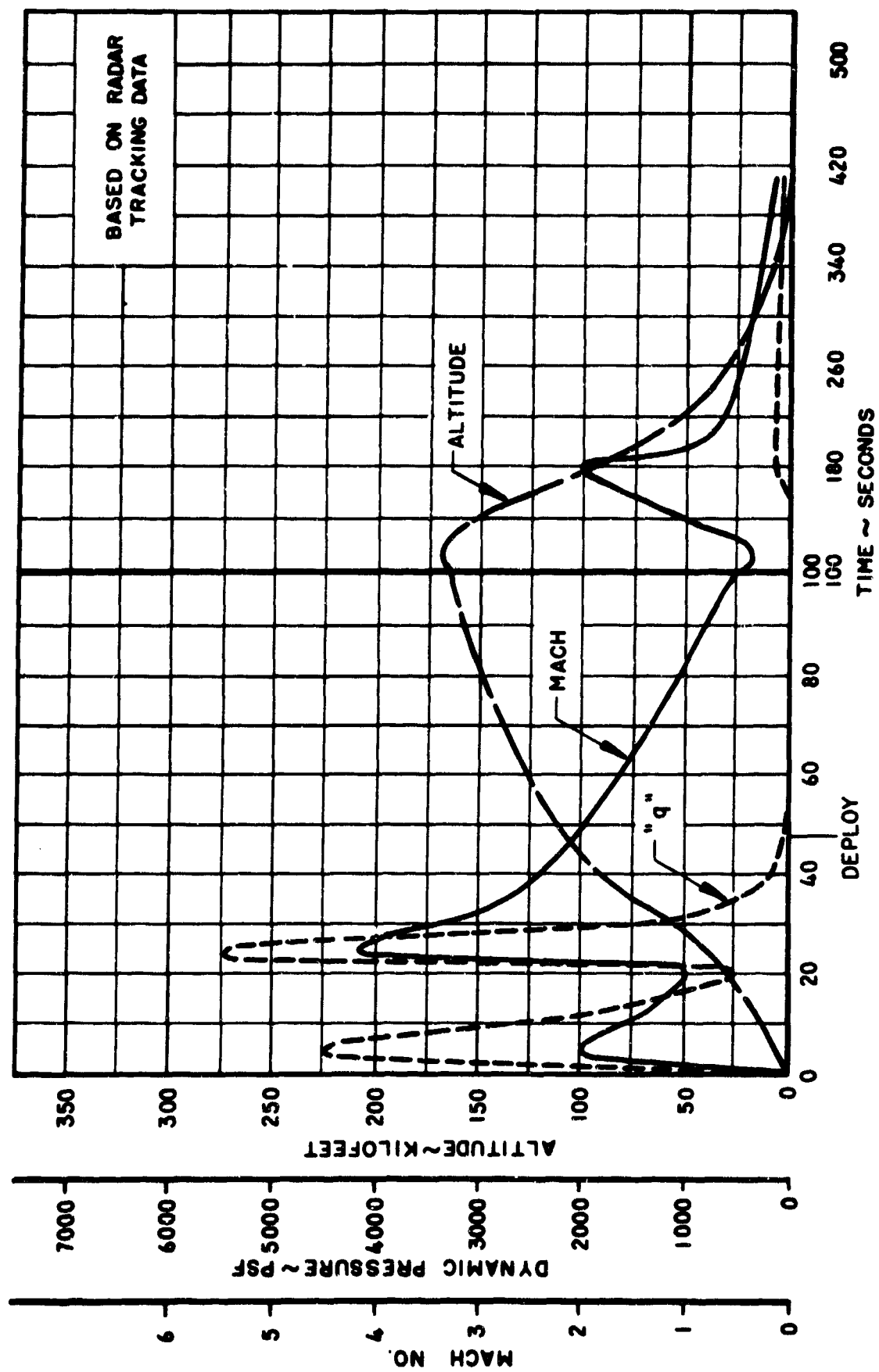
59.

Figure A.5-1   Missile Tracking Data - Test No. 3

60.
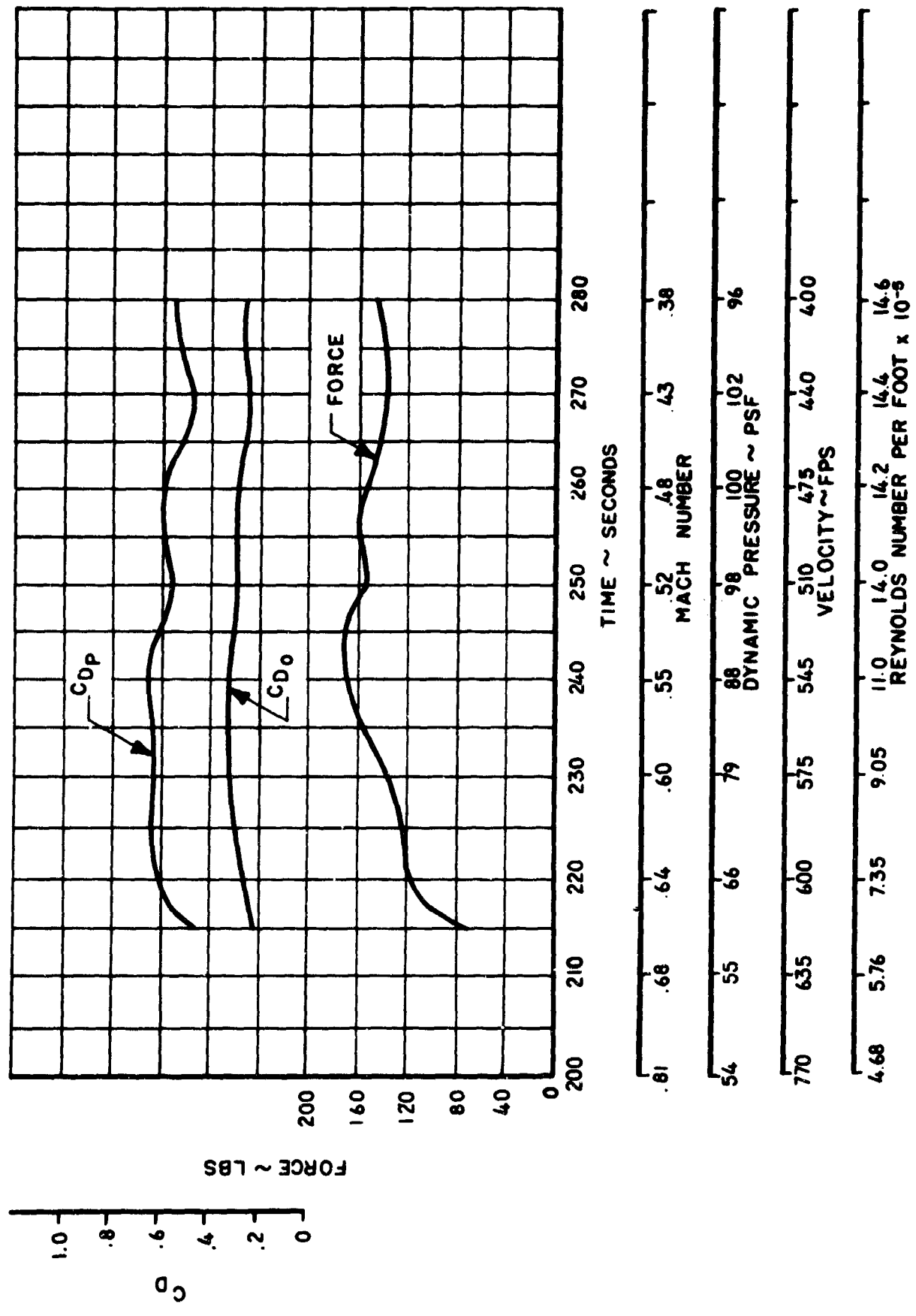
Figure A.5-2 C_D and Force Vs. Time, Mach Number, Dynamic Pressure, Velocity and Reynolds Number - Re-entry No. 3
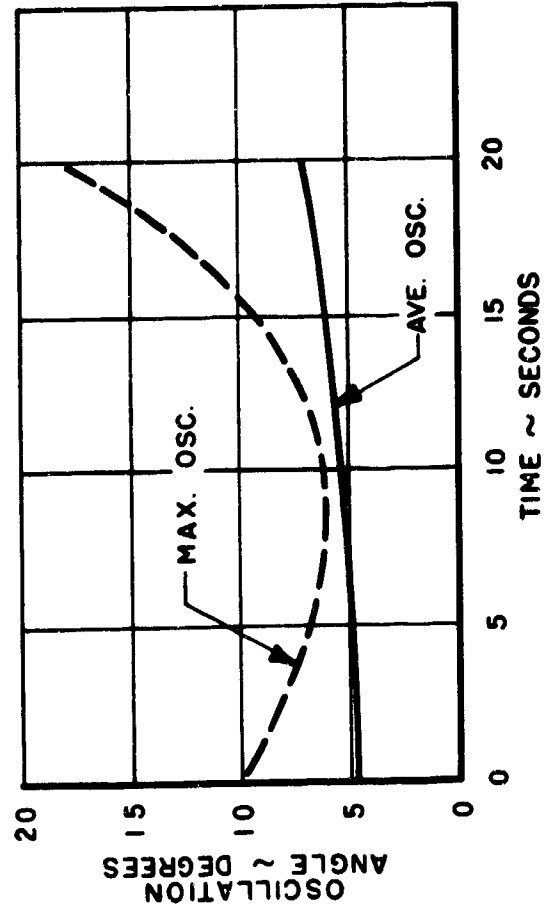
61.

Figure A.5-3   Oscillation Angle Vs. Time
                Test No. 3

Figure A.5-4 Recovered Test Parachute - Test No. 3

A.6   TEST MISSION 4

Date: 8 March 1963
Time: 07:00 CST

A.6.1   Objective and Test Setup

The objective of Test No. 4 was to test a Hyperflo parachute (Cook Electric P/N 596-7775) at a Mach number of 3.1 and an altitude of 140,000 feet. This 3.69 foot D_0 parachute had its roof constructed using 12 gores of 1-1/4 inch by 300 pound and 2 ply of 3/8 inch by 200 pound horizontal and vertical high temperature Nomex ribbons, respectively. Roof porosity was 27.5 percent and total parachute porosity was 13.7 percent. The line length was 2.6 D_p, the D_p/d_B ratio was 3.4, the x/d_B was 10.2 and the W/S_0 was 50,

where D_p = 2.55 ft. S_0 = 10.68 ft.^{2}
            d_B = 0.75 ft. S_p = 5.1 ft.^{2}

A 200 pound tensiometer and an accelerometer rated at ±1 g were used as part of the data gathering components.

The launch vehicle consisted of a 1st stage Nike, a 2nd stage Nike, a 3rd stage Nike, and a 540 pound Cree payload with a 7.5 degree Nike to Cree Adapter. Ignition times for the second and third stages were 5 and 20 seconds, respectively. The booster fin angles of incidence were 1°, 0.9^o, and 0.58^o for first, second and third stages, respectively.

A.6.2   Test Result Summary

The general test results are summarized below:

	Anticipated	Actual
Deployment Mach Number	3.1	2.83
Deployment Altitude (Ft.)	140,000	122,000
Deployment Dynamic Pressure (lbs/ft^2)	30	61.2
Vehicle Spin Rate at Deployment (rps)	-	4
Deployment Time (sec.)	50.0	49.70
Ejection to Full Line Stretch (sec.)	-	.23
Line Stretch to Full Open (sec.)	-	.07
Full Open to Max Load (sec.)	-	.180
Snatch Force (lbs)	-	240
Opening Shock (lbs)	120	200

Max. Load (lbs)	-	245
C_{D_o} Ave. (1-5 sec.)	0.29	0.30
Max. Temperature (°F)	-	350

A. 6. 3   Test Discussion

This parachute test was successful and all objectives of the test were met except that of recovering the test parachute. The telemetry and on-board film coverage were normal and good data were obtained. Radar tracking was good and is shown in Figure A.6.1.

Figures A.6.2 and A.6.3 show the force and C_D data for the test and re-entry regimes, respectively. Points 1, 2, and 3 on Figure A.6.2 are for snatch, full open, and maximum load, respectively. Parachute oscillation is shown in Figure A.6.4. The film showed the parachute to open quickly; however, once open, it exhibited poor inflation and oscillation stability. The parachute performance has been judged poor to fair. No canopy structural damage was noted during the 16 seconds of on-board camera coverage. Because of the low anticipated loads during the deployment test regime, a 300 pound tensiometer was used. This tensiometer has a breaking strength of about 950 pounds. During the re-entry phase of the trajectory, the tensiometer broke and the test parachute was lost. A maximum canopy temperature of 350 - 390°F was obtained from the on-board camera film.

The trajectory was normal and the Cree vehicle was recovered undamaged. The first stage Nike had not yet separated when the second stage ignited. When the second stage gases impinged upon the dome of the first stage, the first stage Nike suffered some structural damage. No effect in trajectory was noticed by this occurrence.

After the loss of the test parachute, it was concluded that a 10,000 pound nylon link across the tensiometer would eliminate further parachute losses due to over-loaded tensiometers.
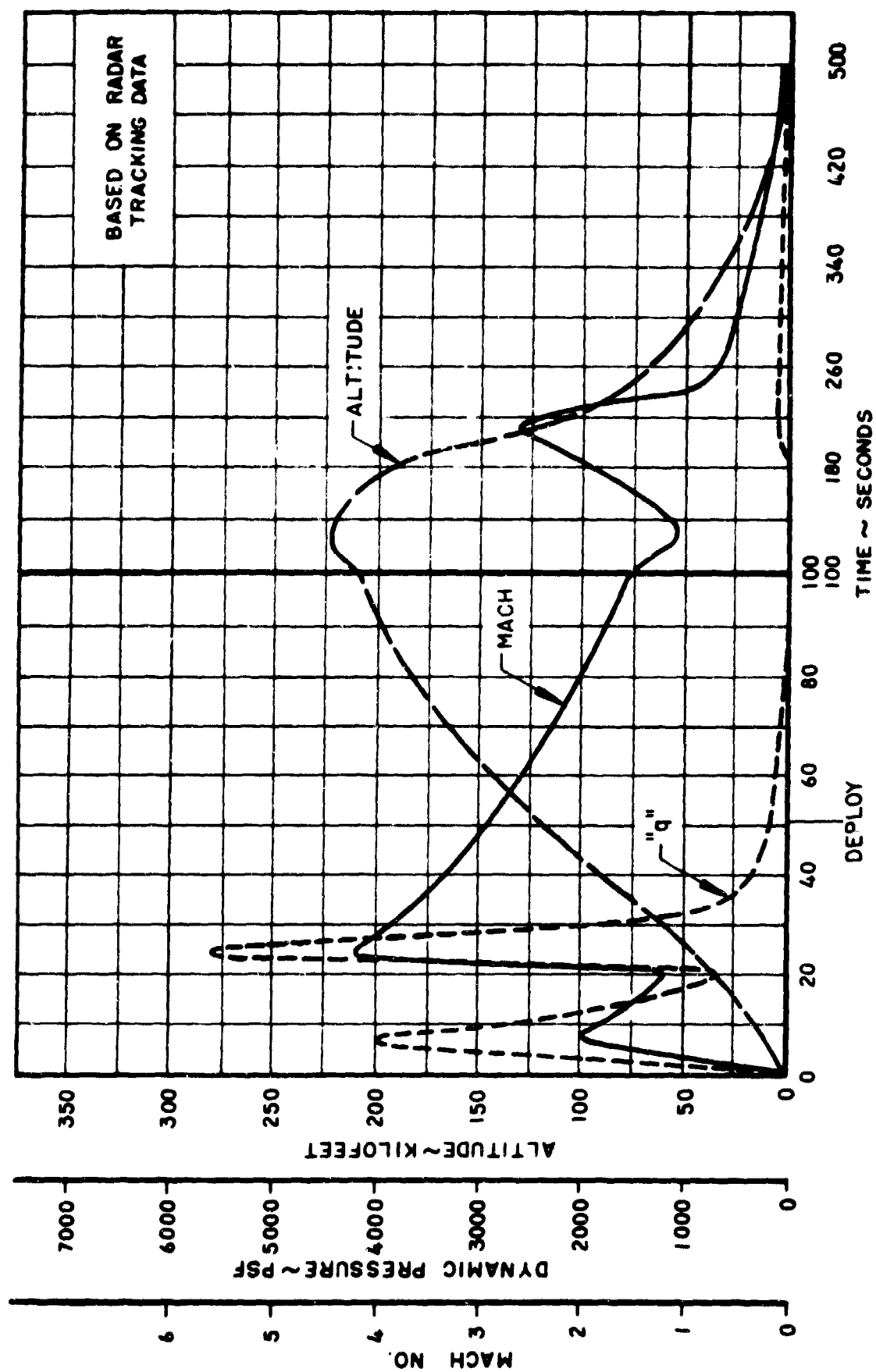
65.

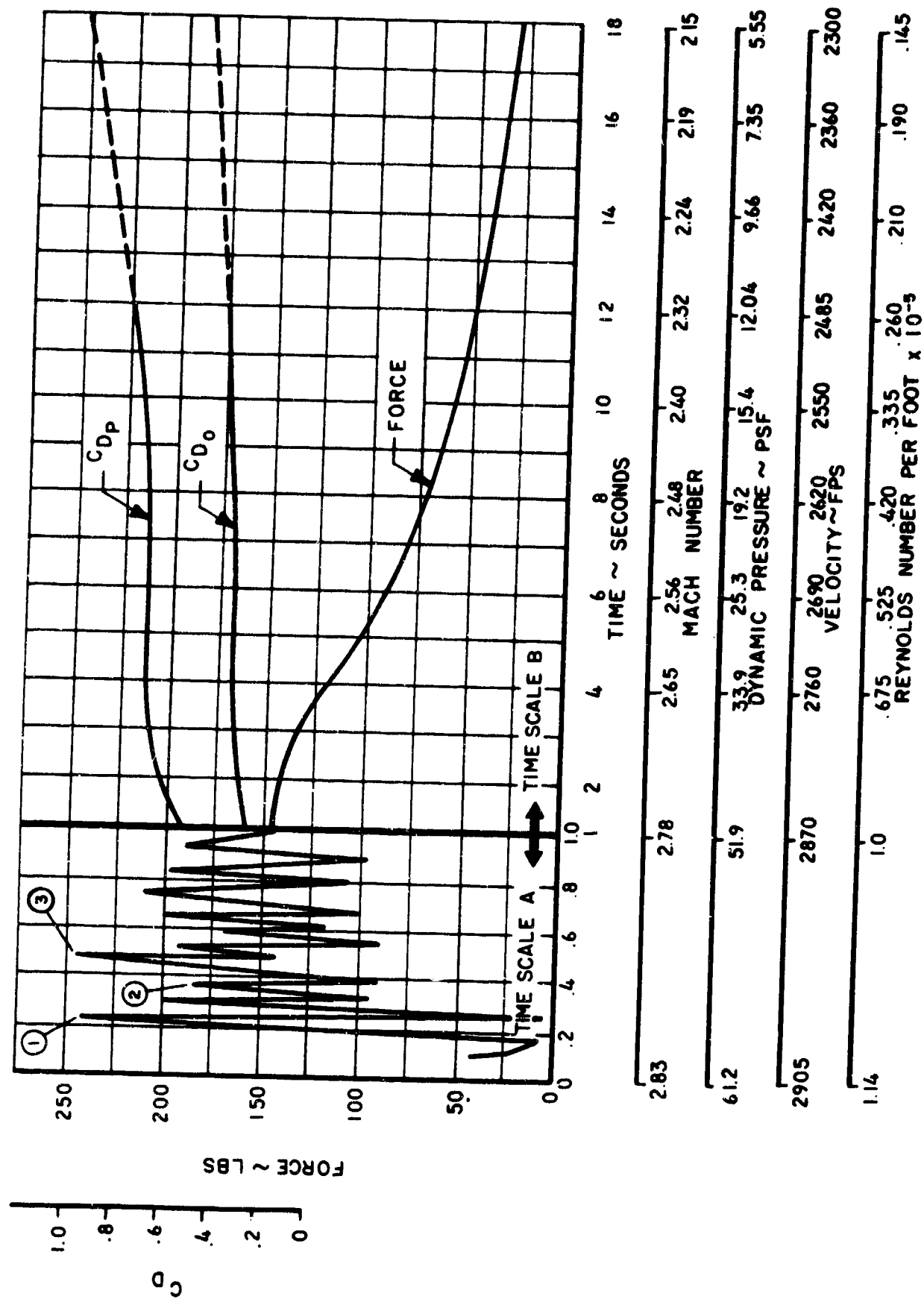Figure A.6-1 Missile Tracking Data - Test No. 4

Figure A.6-2 C_D and Force Vs. Time, Mach Number, Dynamic Pressure, Velocity and Reynolds Number - Test No. 4
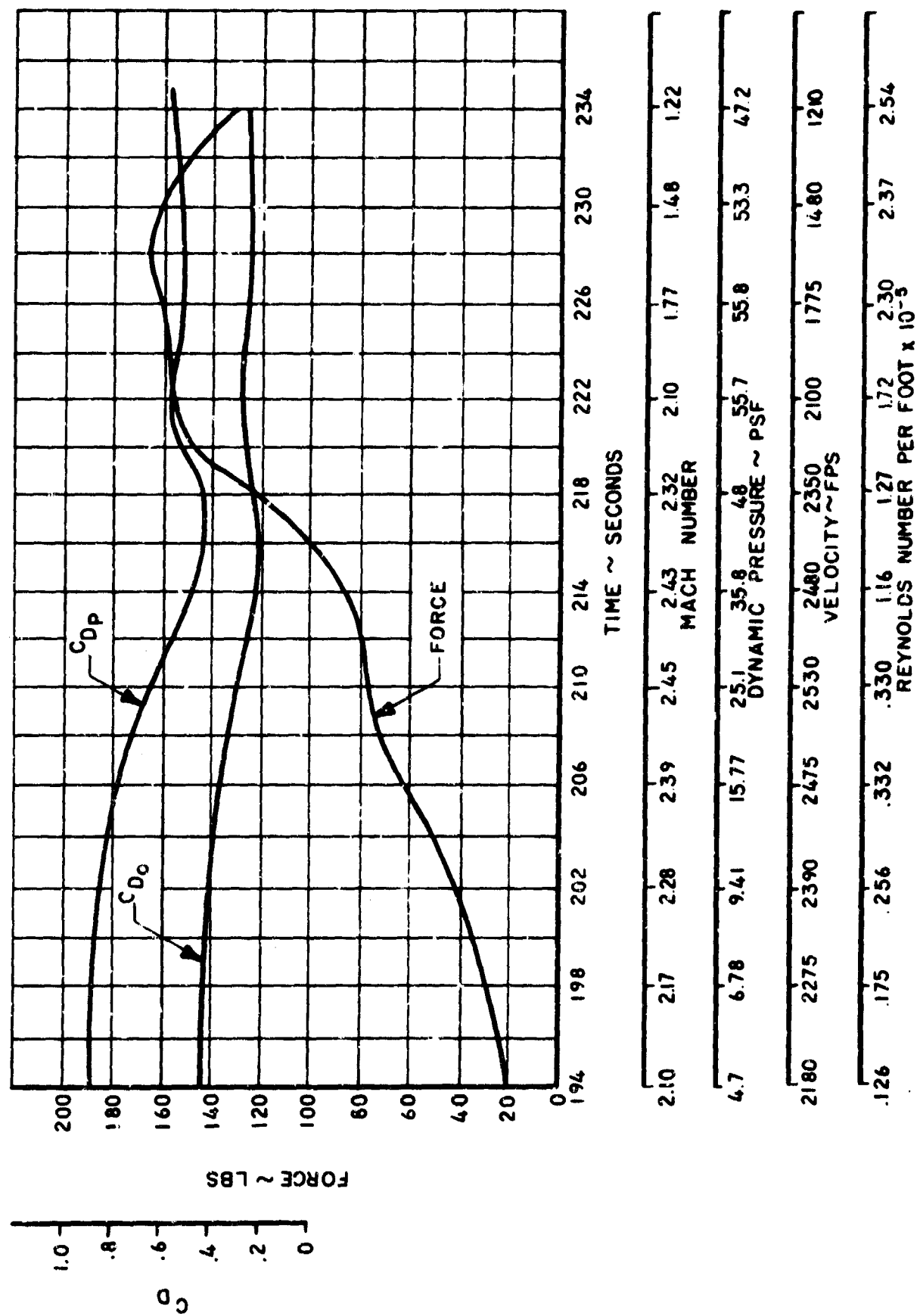
67.

Figure A.6-3 C_D and Force Vs. Time, Mach Number, Dynamic Pressure, Velocity and Reynolds Number - Re-entry No. 4
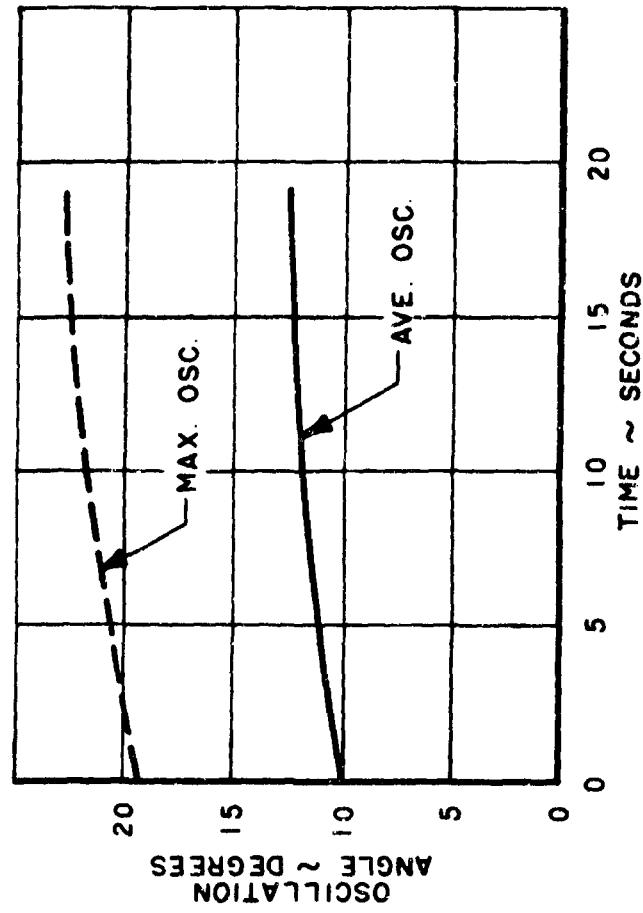
Figure A.6-4   Oscillation Angle Vs. Time
Test No. 4

69.

A.7   TEST MISSION 5

Date: 28 March 1963
Time: 07:45 CST

A.7.1   Objective and Test Setup

The objective of Test No. 5 was to test a Hyperflo parachute (Cook Electric P/N 596-8992) at a Mach number of 3.8 and an altitude of 100,000 feet. This 3.69 foot D_o parachute had its roof constructed using 12 gores of 3/8 inch by 200 pound and 2 ply of 3/8 inch by 58 pound horizontal and vertical high temperature Nomex ribbon, respectively. Roof porosity was 22 percent and total parachute porosity was 10.8 percent. The line length was $2D_p$, the D_p/d_B ratio was 3.4, the x/d_B was 8.45 and the W/S_o was 50,

where D_p = 2.55 ft. S_o = 10.68 ft.^{2}
         d_B = 0.75 ft. S_p = 5.1 ft.^{2}

A 1000 pound tensiometer and an accelerometer rated at ±5 g's were used as part of the data gathering components.

The launch vehicle consisted of a 1st stage Nike, a 2nd stage Nike, a 3rd stage Nike, and a 540 pound Cree payload with a 7.5 degree Nike to Cree Adapter. Ignition times for the second and third stages were 5 and 20 seconds, respectively. The booster fin angles of incidence were 1.0°, 0.9°, and 0.58° for first, second and third stages, respectively.

A.7.2   Test Result Summary

The general test results are summarized below:

	Anticipated	Actual
Deployment Mach Number	3.8	3.22
Deployment Altitude (Ft.)	100,000	86,400
Deployment Dynamic Pressure (lbs/ft^2)	235	345
Vehicle Spin Rate at Deployment (rps)	-	1/3
Deployment Time (sec.)	38.0	38.62
Ejection to Full Line Stretch (sec.)	-	.141
Line Stretch to Full Open (sec.)	-	.042
Full Open to Max Load (sec.)	-	.048
Snatch Force (lbs)	-	787
Opening Shock (lbs)	815	1125
Max. Load (lbs)	-	1732

70.

C_{D_0} Ave. (1-5 sec.)	0.25	0.30
Max. Temperature ($^\circ$F)		550

A.7.3   Test Discussion

This parachute test was successful and all objectives of the test were met except for Mach number. The telemetry data was good and the on-board camera provided good film coverage of the test. Radar tracking was good and is shown in Figure A.7.1.

Figures A.7.2 and A.7.3 show the force and C_D during the test and re-entry regimes, respectively. Points 1, 2, and 3 on Figure A.7.2 show snatch, full open, and maximum load, respectively. Figure A.7.4 shows the parachute oscillation. The film shows the parachute to open quickly, but once open, it exhibited poor inflation and oscillation stability. The temperature sensors indicated a maximum temperature of 550°F. The test parachute was recovered undamaged. Figure A.7.5 shows the parachute after recovery.

The first stage Nike did not fall away at burn-out and again broke apart upon second stage ignition as in Test No. 4. Several pieces of the first stage landed around the launch area. It was concluded that the $T_0 + 5$ second ignition time for second stage was too soon and that a minimum of 10 seconds should be provided for safety reasons. It was noticed on documentary film that the second stage burning time (as determined by the visible flame) was only one-half that of first and third stages. It is believed this is what accounted for the relatively poor trajectory performance as against that programmed.

The Cree vehicle was recovered undamaged and without incident.
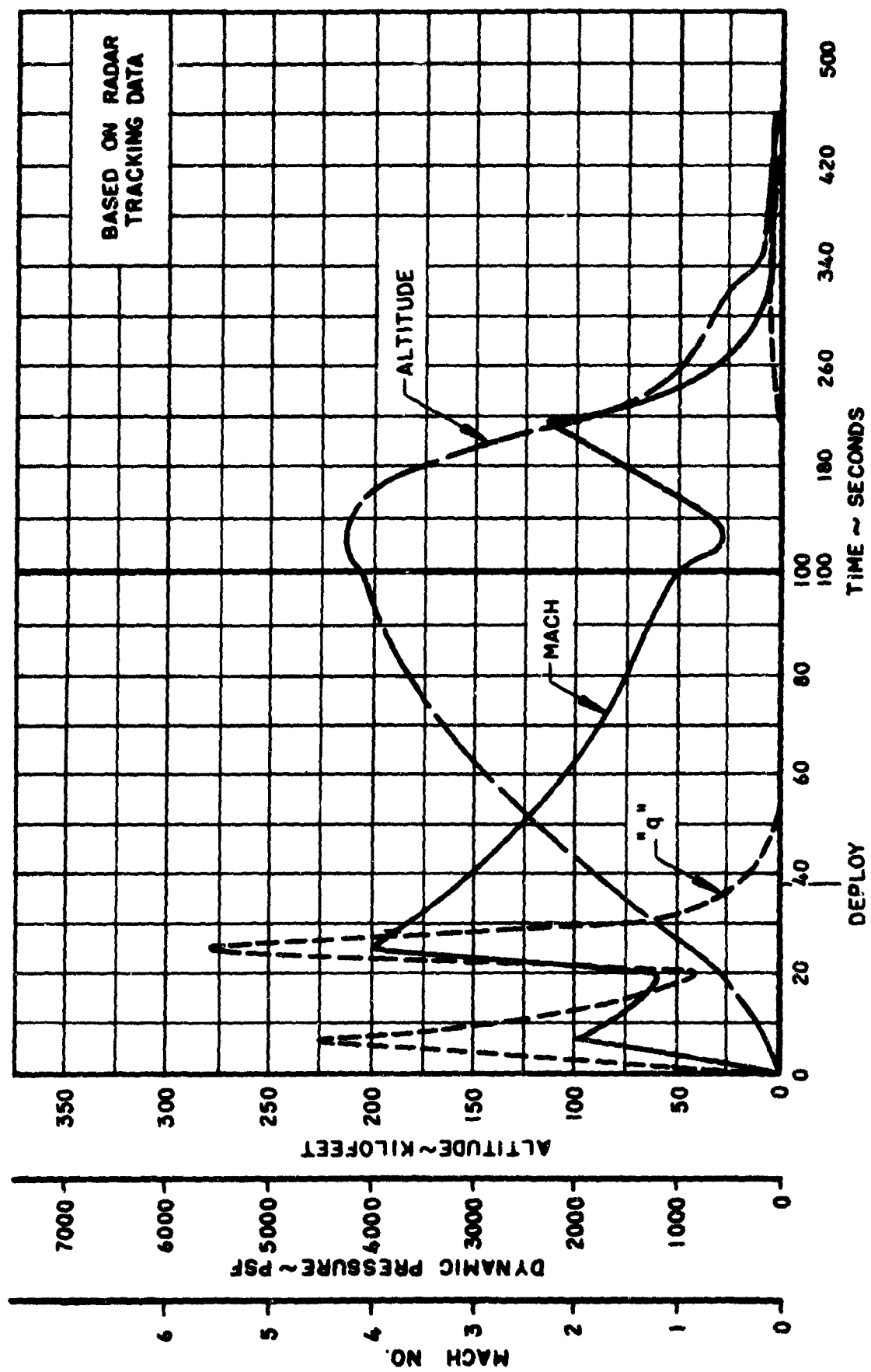
Figure A.7-1   Missile Tracking Data - Test No. 5

72.

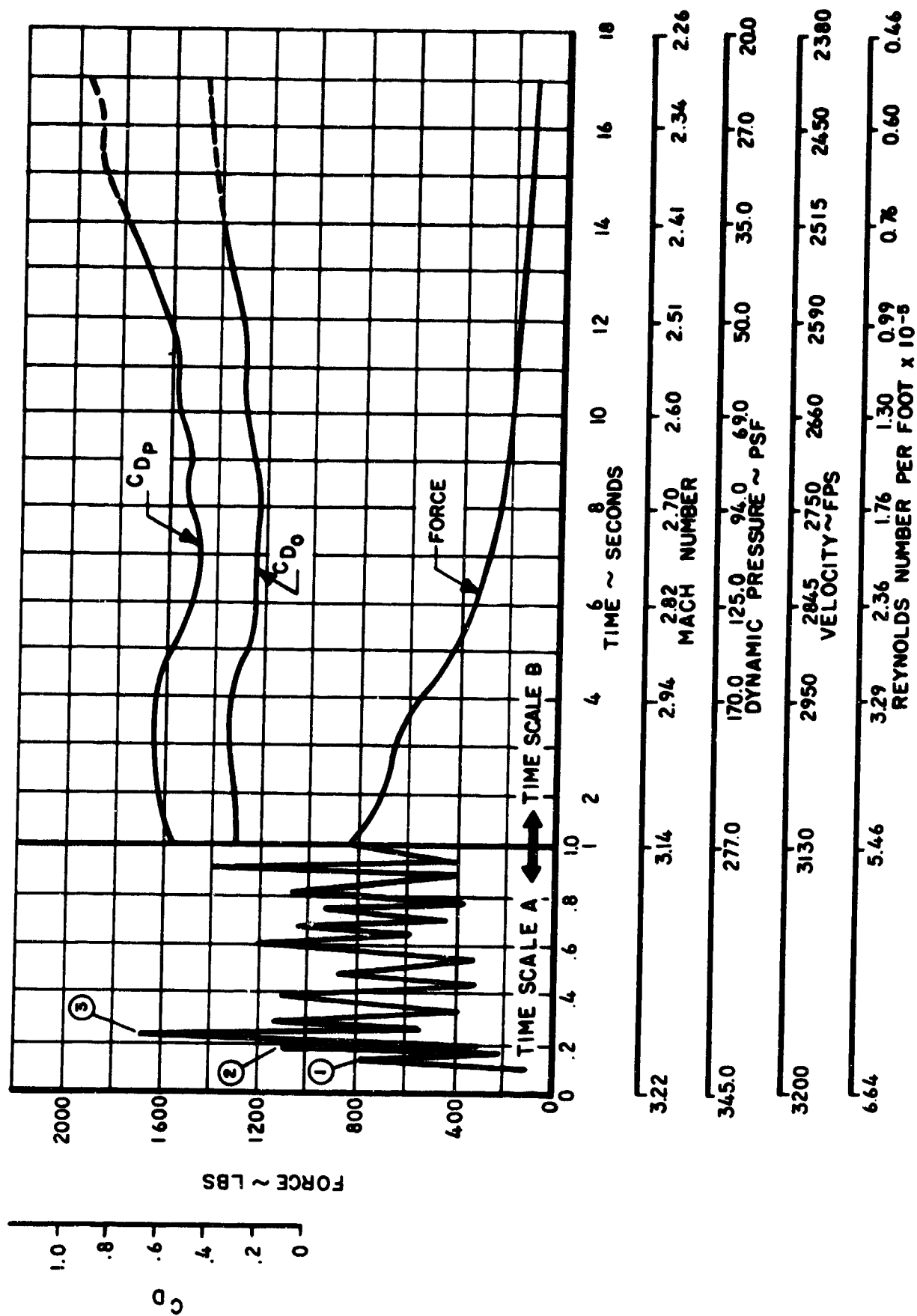Figure A.7-2 C_D and Force Vs. Time, Mach Number, Dynamic Pressure, Velocity and Reynolds Number – Test No. 5
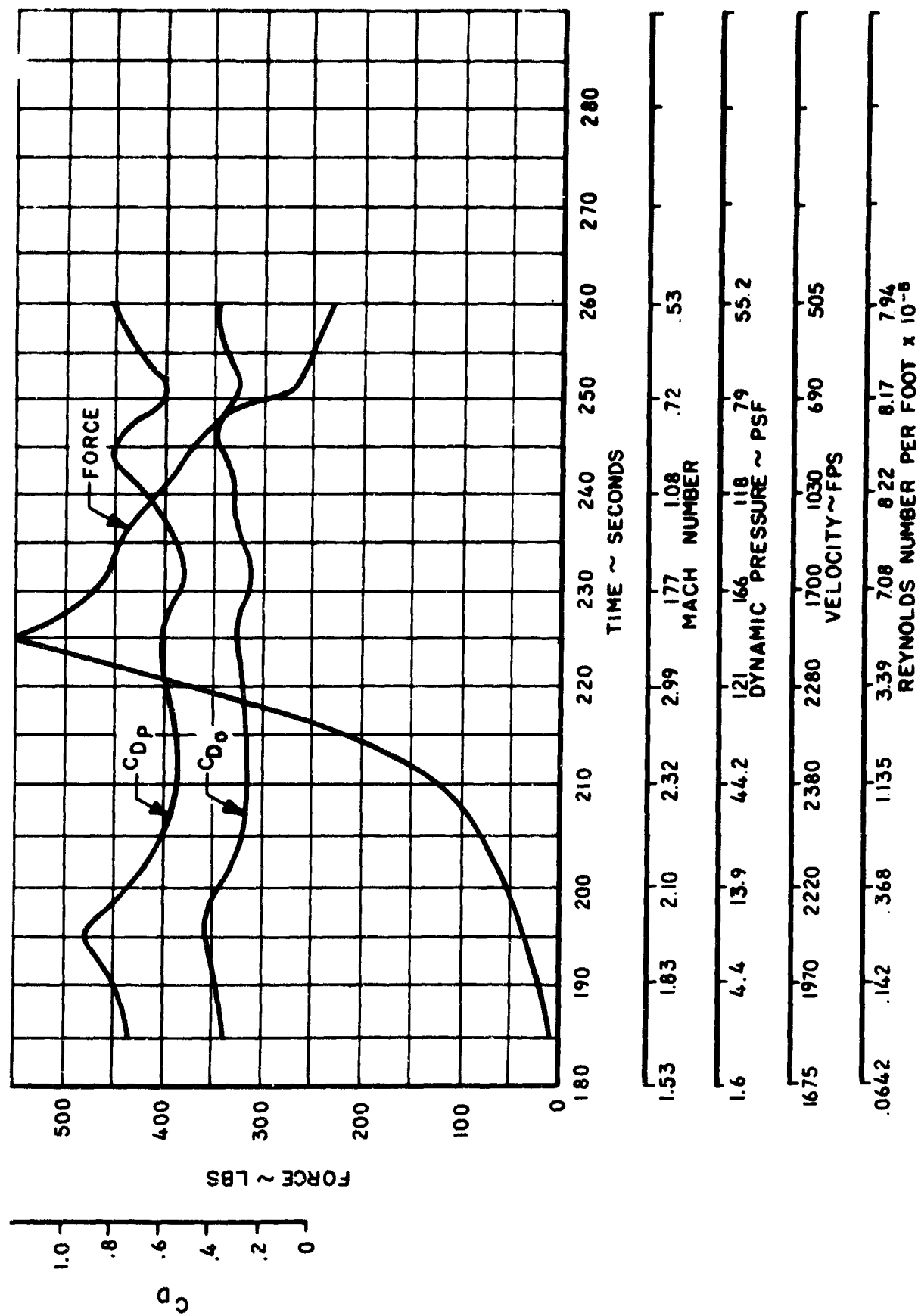
73.

Figure A.7-3 C_D and Force Vs. Time, Mach Number, Dynamic Pressure, Velocity and
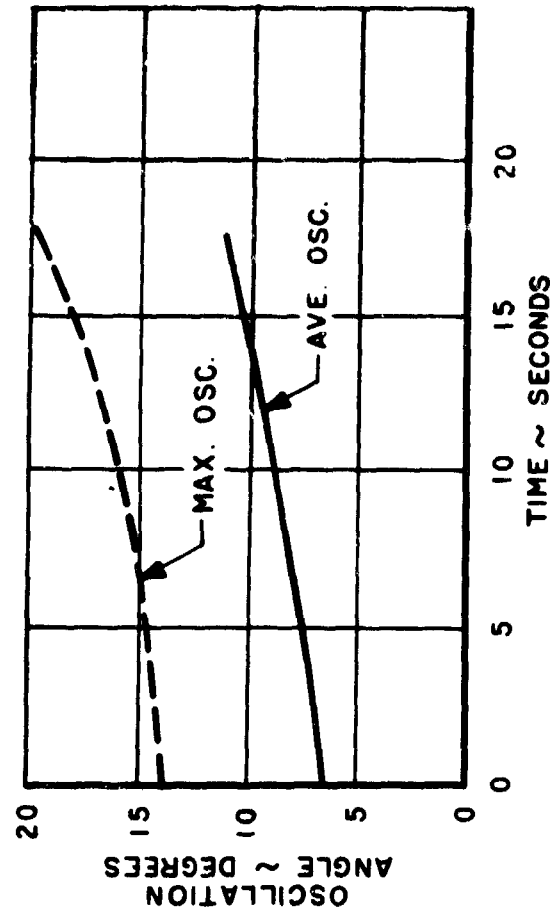Reynolds Number - Re-entry No. 5

74.

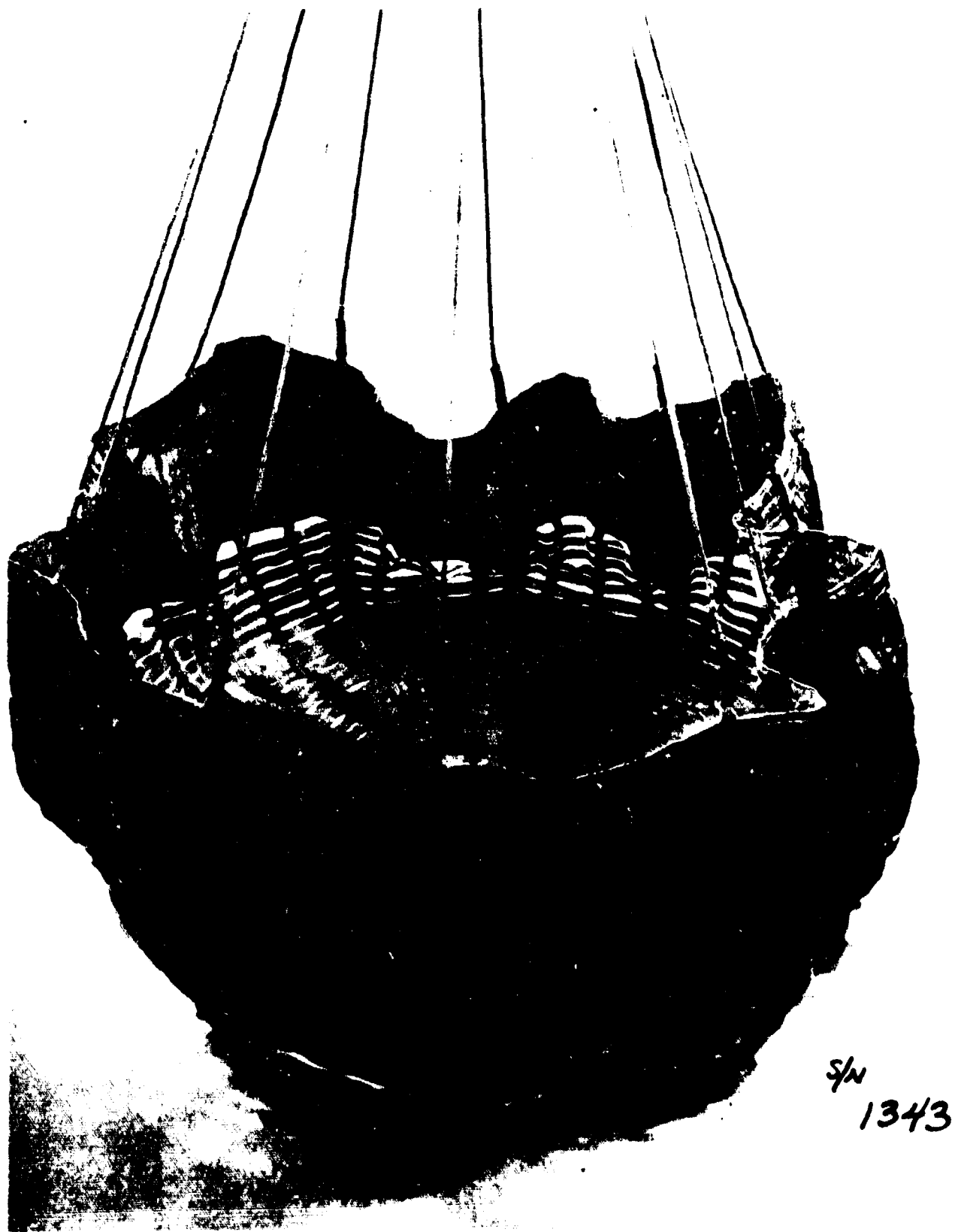Figure A.7-4   Oscillation Angle Vs. Time
                Test No. 5

75.

S/N
1343

Figure A. 7-5 Recovered Test Parachute - Test No. 5

76.

A.8   TEST MISSION 6

Date: 11 April 1963
Time: 15:21 CST

A.8.1   Objective and Test Setup

The objective of Test No. 6 was to test a Hyperflo parachute
(Cook Electric P/N 596-9024) at a Mach number of 4.25 and an altitude of
130,000 feet. This 3.69 foot D_o parachute had its roof constructed using
12 gores of 3/8 inch by 200 pound and 2 ply of 3/8 by 58 pound horizontal
and vertical high temperature Nomex ribbon, respectively. Roof porosity
was 14.9 percent and total parachute porosity was 7.5 percent. The line
length was 2 D_p, the D_p/d_B ratio was 3.4, the x/d_B was 8.45, and the
W/S_o was 50,

where D_p = 2.55 ft. S_o = 10.68 ft.^{2}
         d_B = 0.75 ft. S_p = 5.1 ft.^{2}

A 1000 pound tensiometer and an accelerometer rated at ±2.5 g's
were used as part of the data gathering components.

The launch vehicle consisted of a 1st stage Honest John, a 2nd
stage Nike, a 3rd stage Nike, and a 540 pound Cree payload with a 15 degree
Nike to Cree Adapter. Ignition times for the second and third stages were
10 and 30 seconds, respectively. The booster fin angles of incidence were
0.5°, 0.9°, and 0.58° for first, second and third stages, respectively.

A.8.2   Test Result Summary

The general test results are summarized below:

	Anticipated	Actual
Deployment Mach Number	4.25	3.98
Deployment Altitude (Ft.)	130,000	122,700
Deployment Dynamic Pressure (lbs/ft^2)	82	113
Vehicle Spin Rate at Deployment (rps)	-	1
Deployment Time (sec.)	47.0	47.29
Ejection to Full Line Stretch (sec.)	-	.26
Line Stretch to Full Open (sec.)	-	.09
Full Open to Max Load (sec.)	-	.31
Snatch Force (lbs)	-	220
Opening Shock (lbs)	262	280

77.

Max. Load (lbs)	-	385
C_{D_O} Ave. (1-5 sec.)	0.23	0.26

A.8.3 Test Discussion

This parachute test was successful and all objectives of the test were met except determining maximum canopy temperature and recovering the test parachute. The telemetry provided usable tensiometer data on the shock (70 Kc) channel only. The on-board camera obtained good coverage of the test. Radar tracking was good and the trajectory is shown in Figure A.8.1.

Force and C_D are shown in Figure A.8.2. The parachute oscillation is shown in Figure A.8.3. The on-board film shows the parachute to open quickly and the inflation and oscillation stability were fair to good with stability increasing with time. Points 1, 2, and 3 in Figure A.8.2 are snatch, full open and maximum load points, respectively.

The test parachute was not recovered. The tensiometer had about 2 feet of each suspension line attached to it. It is presumed that the Cree vehicle tumbled while going over the top (374,000 feet) of its trajectory and that the lines were worn and cut by the fin and dive brakes during re-entry. The force record gives no evidence of a parachute being present during the re-entry portion of the trajectory. Figure A.8.4 shows the recovered portion of the test parachute.

The quality of the on-board camera film was not good enough to make an accurate maximum temperature observation. The highest temperature sensor that could be seen change color was 329°F. It is felt that this is well below the actual maximum temperature which is believed to be of the order of 600°F.

This was the first time a boost combination of Honest John-Nike-Nike has been used to launch a Cree. The trajectory was near perfect and the Cree was recovered without damage or incident.
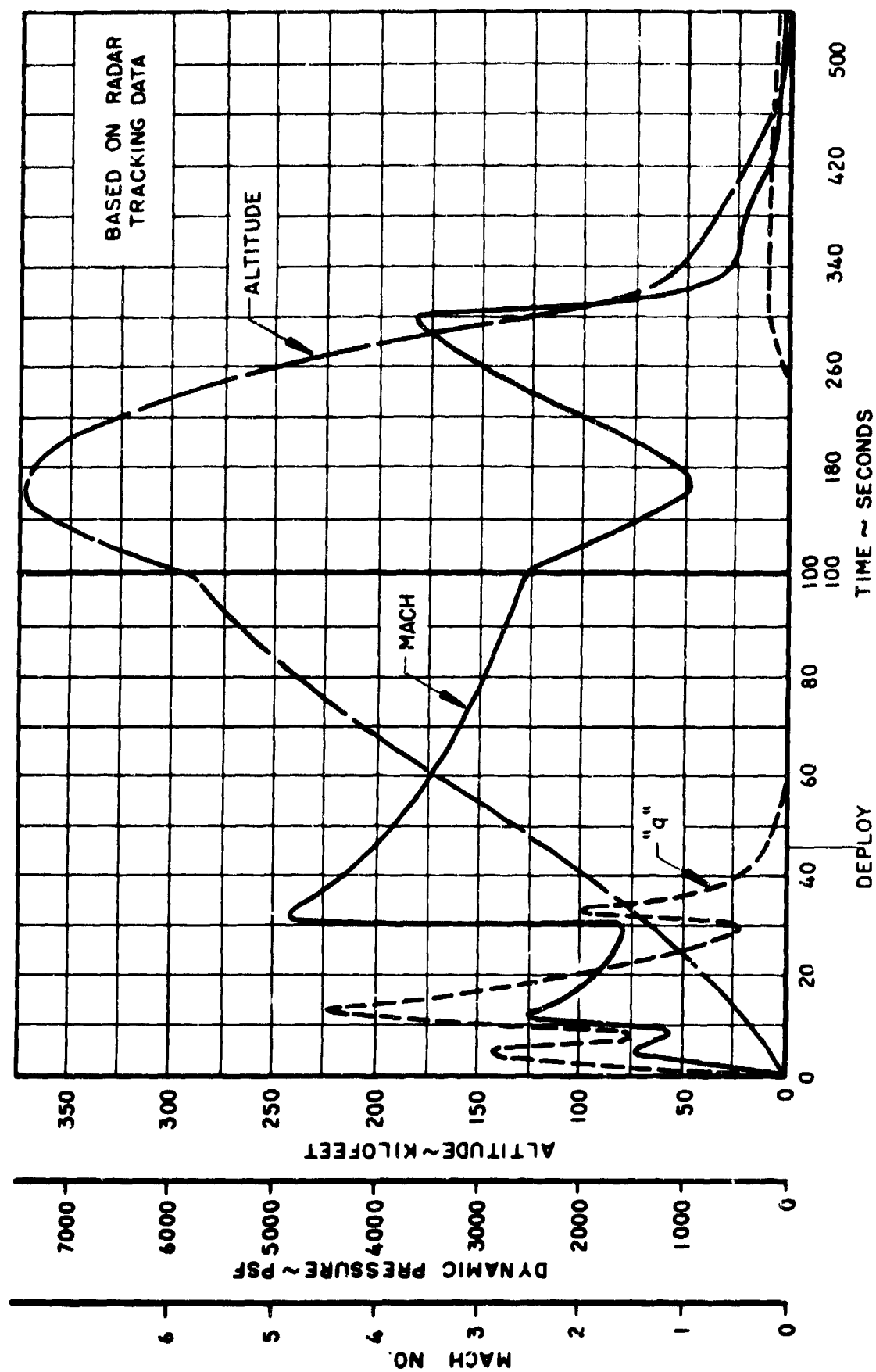
Figure A.8-1   Missile Tracking Data - Test No. 6
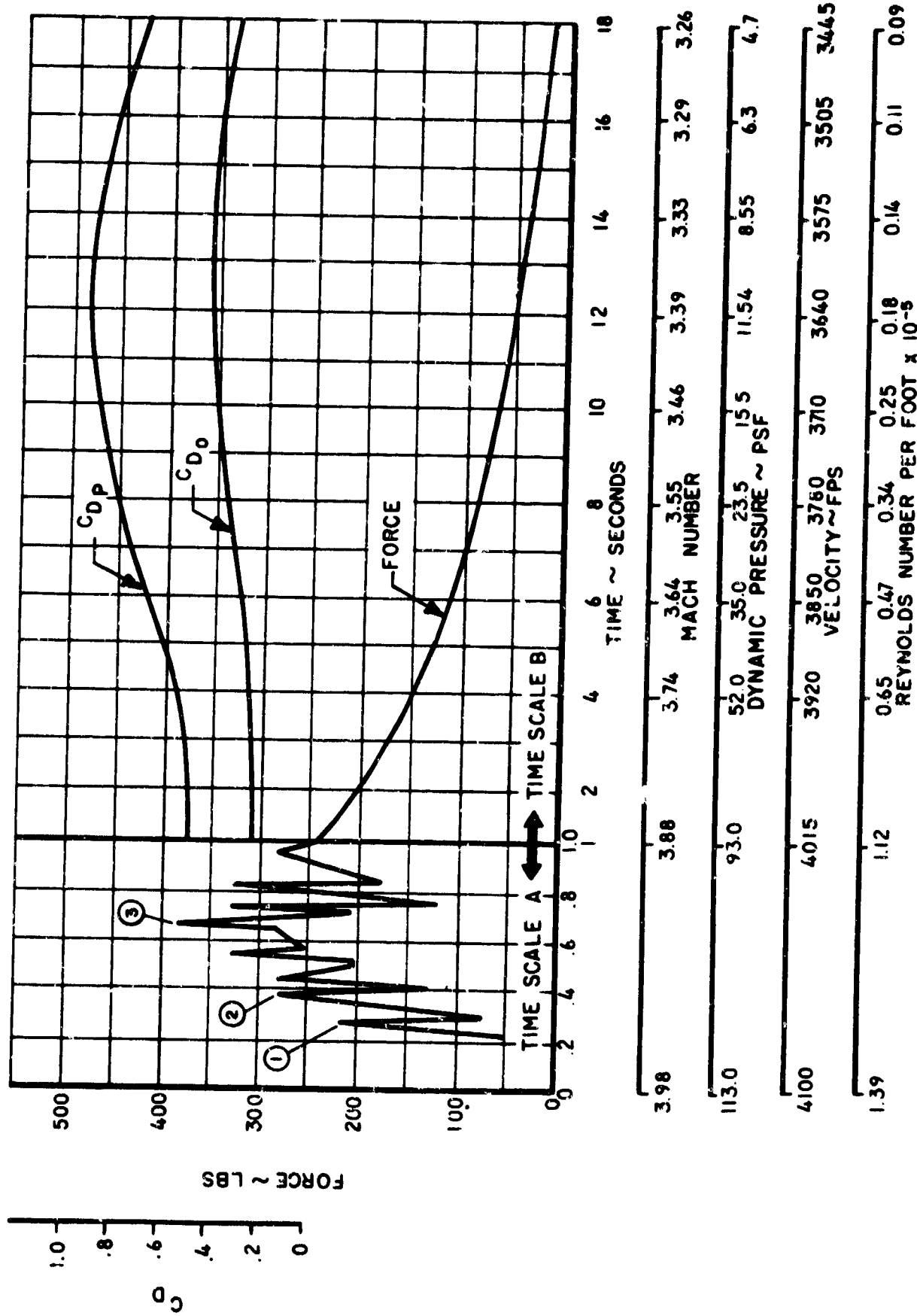
79.

Figure A.8-2 C_D and Force Vs. Time, Mach Number, Dynamic Pressure, Velocity and Reynolds Number - Test No. 6
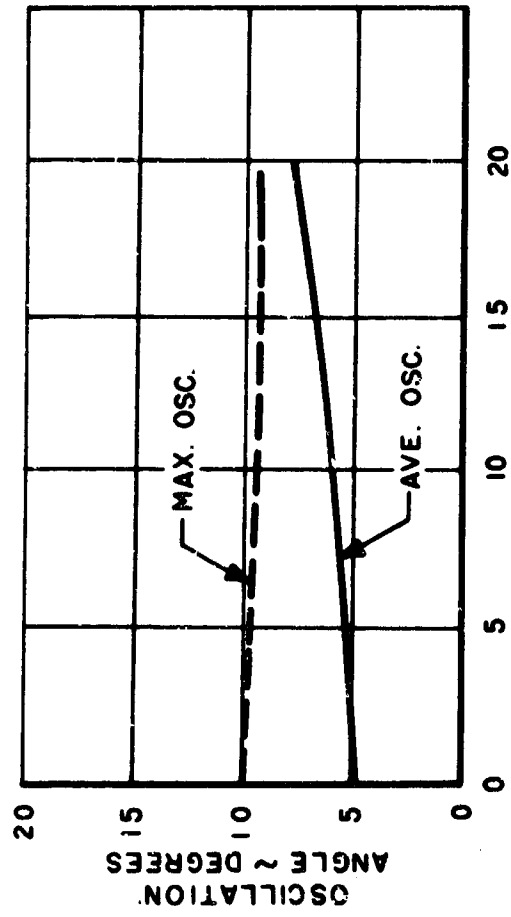
80.

Figure A.8-3   Oscillation Angle Vs. Time
Test No. 6

Figure A. 8-4 Recovered Test Parachute - Test No. 6

A.9 TEST MISSION 7

Date: 20 May 1963
Time: 11:30 CST

A.9.1 Objective and Test Setup

The objective of Test No. 7 was to test a Hyperflo parachute (Cook Electric P/N 596-9028) at a Mach number of 2.8 and an altitude of 100,000 feet. This 3.69 foot D_O parachute had its roof constructed using 12 gores of Perlon mesh. This mesh had a porosity of 45.2 percent. Roof porosity was 33.8 percent and total parachute porosity was 16.9 percent. The line length was 2 D_p, the D_p/d_B ratio was 3.4, the x/d_B was 8.45 and the W/S_O was 50,

$$\text{where} \quad D_p = 2.55 \text{ ft.} \quad S_O = 10.68 \text{ ft.}^2$$
$$d_B = 0.75 \text{ ft.} \quad S_p = 5.1 \text{ ft.}^2$$

A 3000 pound tensiometer and an accelerometer rated at ±5 g's were used as part of the data gathering components.

The launch vehicle consisted of a 1st stage Honest John, a 2nd stage Nike, and a 540 pound Cree payload, with a 15 degree Nike to Cree Adapter. Ignition time for the second stage was 25 seconds. The booster fin angles of incidence were 0.5° and 0.99° for first and second stages, respectively.

A.9.2 Test Result Summary

The general test results are summarized below:

	Anticipated	Actual
Deployment Mach Number	2.8	0.2
Deployment Altitude (Ft.)	100,000	44,200
Deployment Dynamic Pressure (lbs/ft^2)	115	8
Deployment Time (sec.)	47.0	47.12
Opening Shock (lbs)	480	-
C_{D_O} Ave. (1-5 sec.)	0.30	0.37

A.9.3 Test Discussion

This parachute test was unsuccessful because of a malfunction in the boost system. The telemetry operated satisfactorily and force data was obtained throughout the flight. The on-board camera functioned

properly and the film data was good. Radar tracking was good and the trajectory is shown in Figure A.9.1.

Force and C_D are shown in Figure A.9.2. The film shows the parachute to open slowly (but probably satisfactorily for a Mach number of 0.15) and once open, the parachute exhibits excellent inflation and oscillation stability. Figure A.9.3 shows the canopy oscillation.

The launch vehicle was an Honest John-Nike with a 540 pound Cree. The second stage Nike was programmed to ignite at $T_o + 25$ seconds; however, through a malfunction in the igniter, the Nike ignited within 1/4 second. The Nike and Honest John separated almost immediately and the payload trajectory was basically that achieved with a single stage Nike booster.

Many tests were performed in an effort to determine the exact cause of the malfunction but all efforts were fruitless. It was concluded to continue testing as before but that extra care should be given to the igniter modification and wiring insulation, and that the current to the igniter would be limited to 3 amps.

The Cree vehicle, together with the test parachute, was recovered without damage or incident.
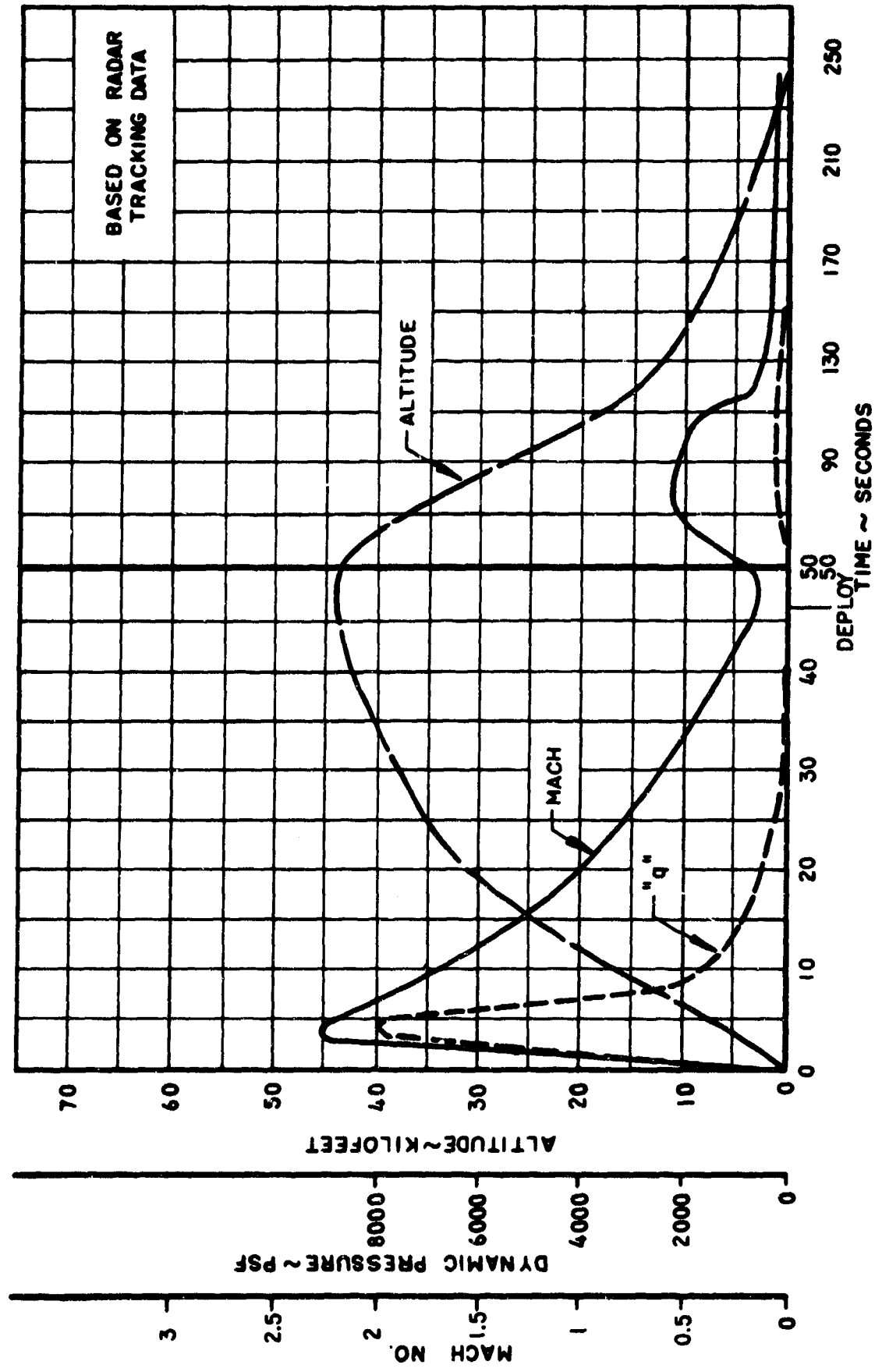
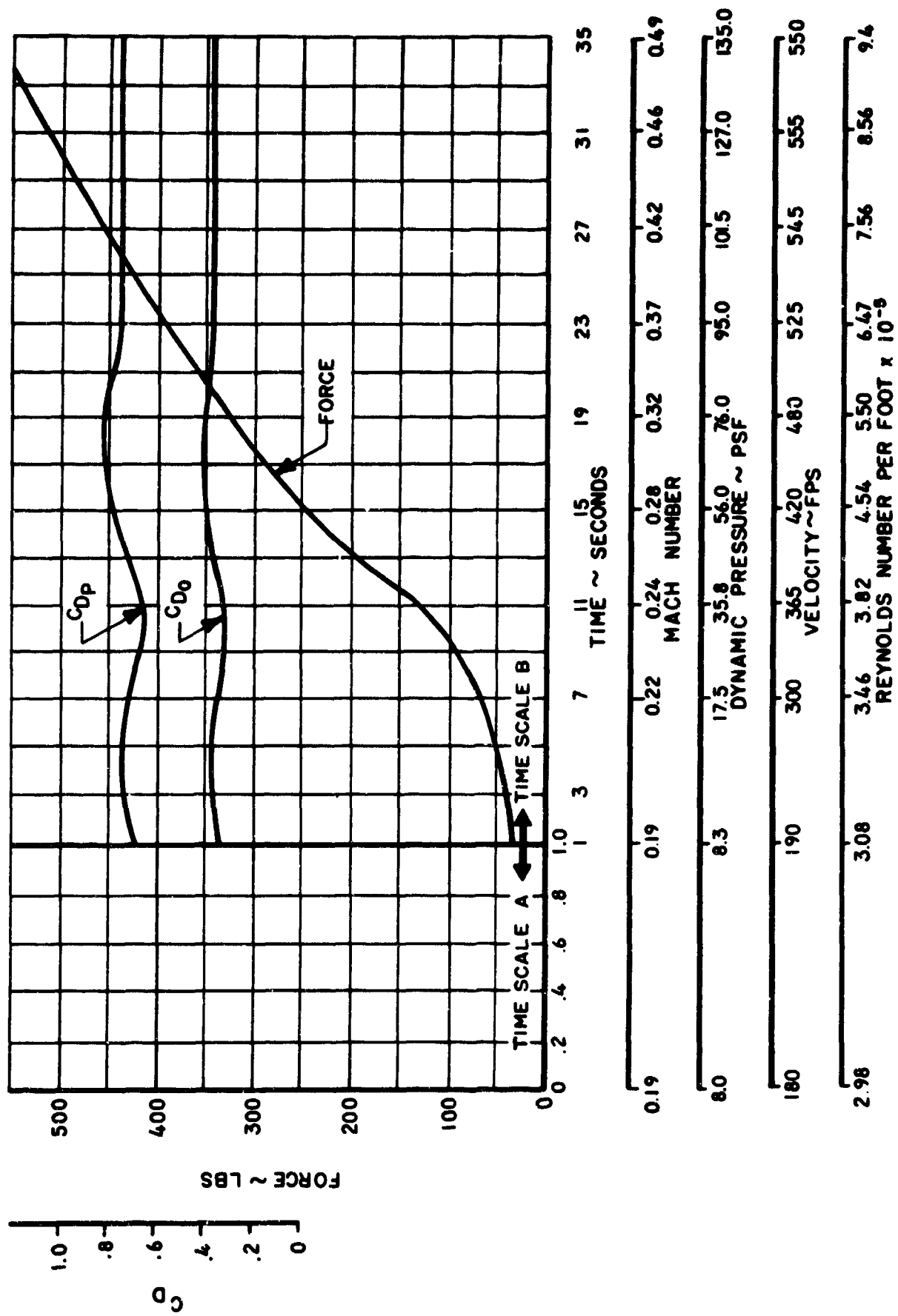Figure A.9-1   Missile Tracking Data – Test No. 7

85.

Figure A.9-2 C_D and Force Vs. Time, Mach Number, Dynamic Pressure, Velocity and
Reynolds Number - Test No. 7

86.
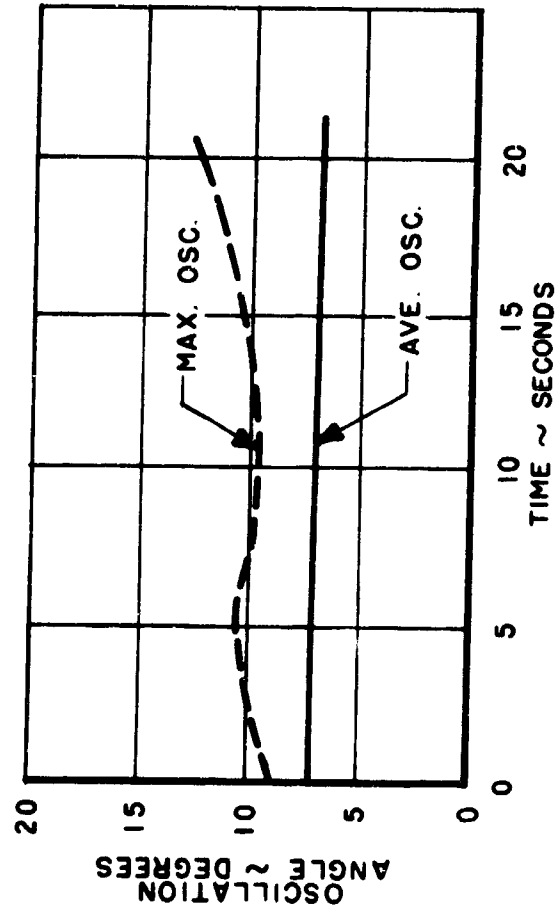
Figure A.9-3   Oscillation Angle Vs. Time
Test No. 7

87.

A.10 TEST MISSSION 8

Date: 27 June 1963
Time: 14:03 CST

A.10.1   Objective and Test Setup

The objective of Test No. 8 was to test a Hemisflo parachute (Cook Electric P/N 596-8151) at a Mach number of 3.5 and an altitude of 100,000 feet. This 4.12 foot D_o parachute had its roof constructed using 16 gores of 1-1/4 inch by 300 pound and 3/8 inch by 200 pound for the horizontals and verticals, respectively. All material was high temperature Nomex ribbon. Canopy porosity was 14.3 percent. The line length was 2 D, the D_p/d_B ratio was 3.4, the x/d_B was 12.0 and the W/S_o was 61,

$$\text{where} \quad \begin{aligned} D_p &= 2.55 \text{ ft.} & S_o &= 13.33 \text{ ft.}^2 \\ d_B &= 0.75 \text{ ft.} & S_p &= 5.1 \text{ ft.}^2 \\ D &= \frac{\pi}{2} D_p \end{aligned}$$

A 3000 pound tensiometer and an accelerometer rated at ±5 g's were used as part of the data gathering components.

The launch vehicle consisted of a 1st stage Honest John, a 2nd stage Nike, a 3rd stage Nike, and a 820 pound Cree payload with a 15 degree Nike to Cree Adapter. Ignition times for the second and third stages were 10 and 30 seconds, respectively. The booster fin angles of incidence were 0.5^o, 0.9^o, and 0.95^o for first, second and third stages, respectively.

A.10.2   Test Result Summary

The general test results are summarized below:

	Anticipated	Actual
Deployment Mach Number	3.5	3.44
Deployment Altitude (Ft.)	100,000	108,700
Deployment Dynamic Pressure (lbs/ft.^{2})	200	148
Vehicle Spin Rate at Deployment (rps)	-	1/2
Deployment Time (sec.)	46.03	46.96
Ejection to Full Line Stretch (sec.)	-	.39
Line Stretch to Full Open (sec.)	-	.09
Full Open to Max Load (sec.)	-	0
Snatch Force (lbs)	-	250
Opening Shock (lbs)	1730	1050
Max. Load (lbs)	-	1050

C_{D_0} Ave. (1-5 sec.)   0.50   0.34
Max. Temperature ($^{\circ}$F)   -   660

A.10.3   Test Discussion

This parachute test was successful and all objectives of the test were met. The telemetry and on-board film coverage were good. Radar tracking was good and the data is presented in Figure A.10.1.

Force and C_D for the test and re-entry regime are shown in Figures A.10.2 and A.10.3, respectively. Points 1, 2, and 3 in Figure A.10.2 are snatch, full open and maximum loads, respectively. The film shows the parachute to have a normal deployment and a reasonably good opening. The inflation stability was poor during the first several seconds but improved as both "q" and Mach reduced. The oscillation stability was fair and remains so throughout the 24 seconds of on-board camera coverage (see Figure A.10.4).

This was the same test parachute as used in Test No. 1. The test area C_D's are similar; however, the re-entry C_D on Test No. 8 is low. The telemetry record gave some evidence of a zero shift or malfunction during the re-entry phase. The force record appears to indicate a malfunction of the telemetry as the vehicle approached Mach 1. This evidence has greatly reduced the confidence of the data presented in Test No. 8 re-entry and thus has led to the use of the dashed data curves.

The test parachute was recovered intact and without damage. There was two types of temperature sensors used on this parachute. One type was the crayons left from Test No. 1, and the other was paints applied for this test. The paints showed a clear temperature change at 554°F while the crayons showed a definite change at 660°F. However, the crayons also showed a slight color change on the 930° sensor. Stagnation temperature at a Mach number of 3.5 at an altitude of 120,000 feet is about 1060°F. There were several paint sensors between 554°F and 930°F which did not show any color change. No definite conclusion has been reached upon the reliability of the crayon color change at 930°F; however, it is not felt to be good.

Two nylon strips, one a thin (2 inch by 300 pound) red and the other a heavy (1 inch by 600 pound) blue, were used for gore identification when viewing the on-board film. The thin red nylon was 95% burned away while the heavy blue nylon was slightly burned on the edges. Both strips were attached to a roof radial in a similar manner.

The launch and trajectory were normal and the Cree vehicle was recovered undamaged and without incident.

89.
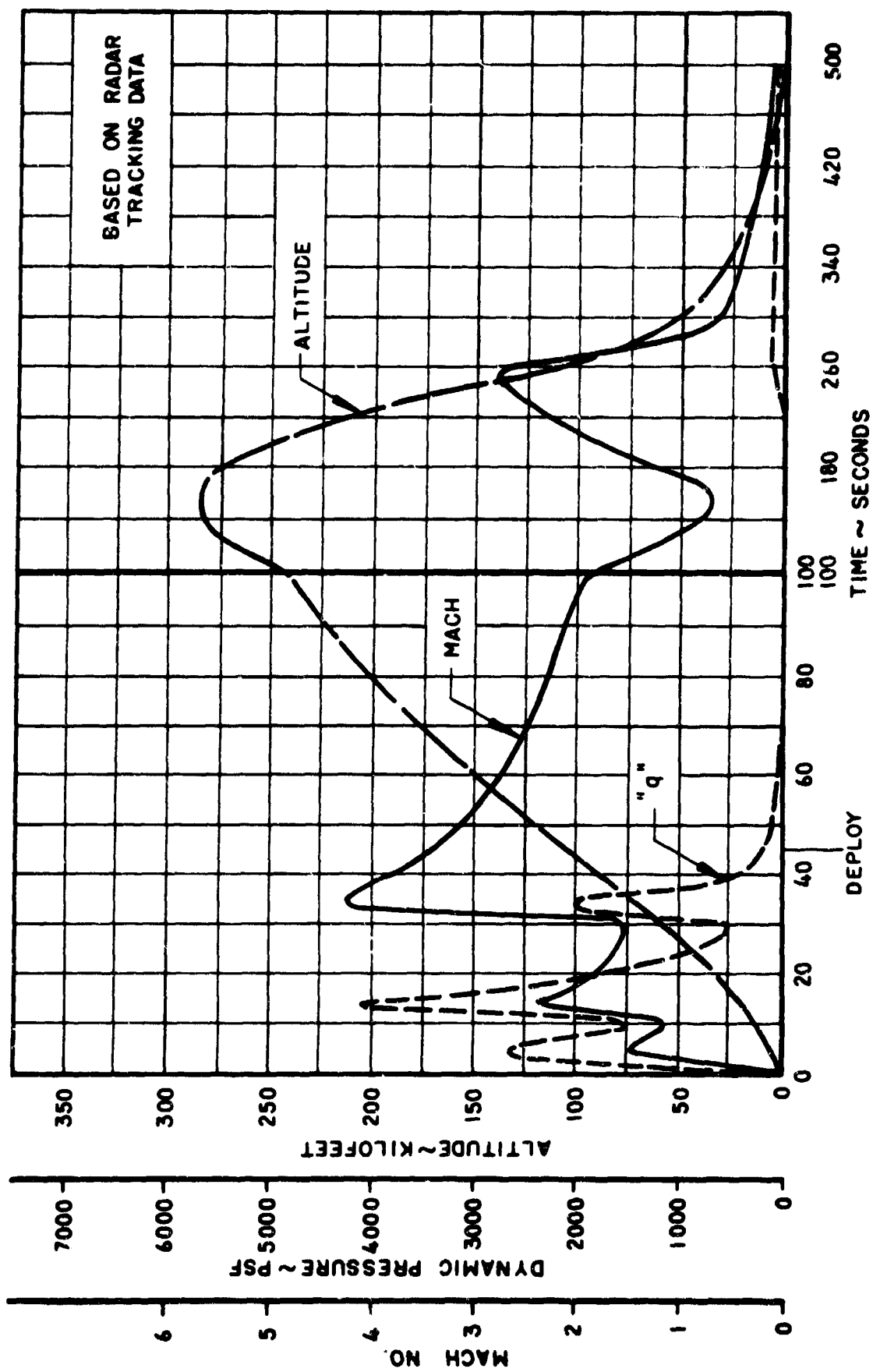
Figure A.10-1 Missile Tracking Data - Test No. 8

Figure A. 10-2 C_D and Force Vs. Time, Mach Number, Dynamic Pressure, Velocity and Reynolds Number - Test No. 8

91.

FORCE ~ LBS

400 300 200 100 0

C_D

1.0 .8 .6 .4 .2 0

C_{D_P}

C_{D_O}

FORCE

TIME ~ SECONDS

240   250   260   270   280   290   300

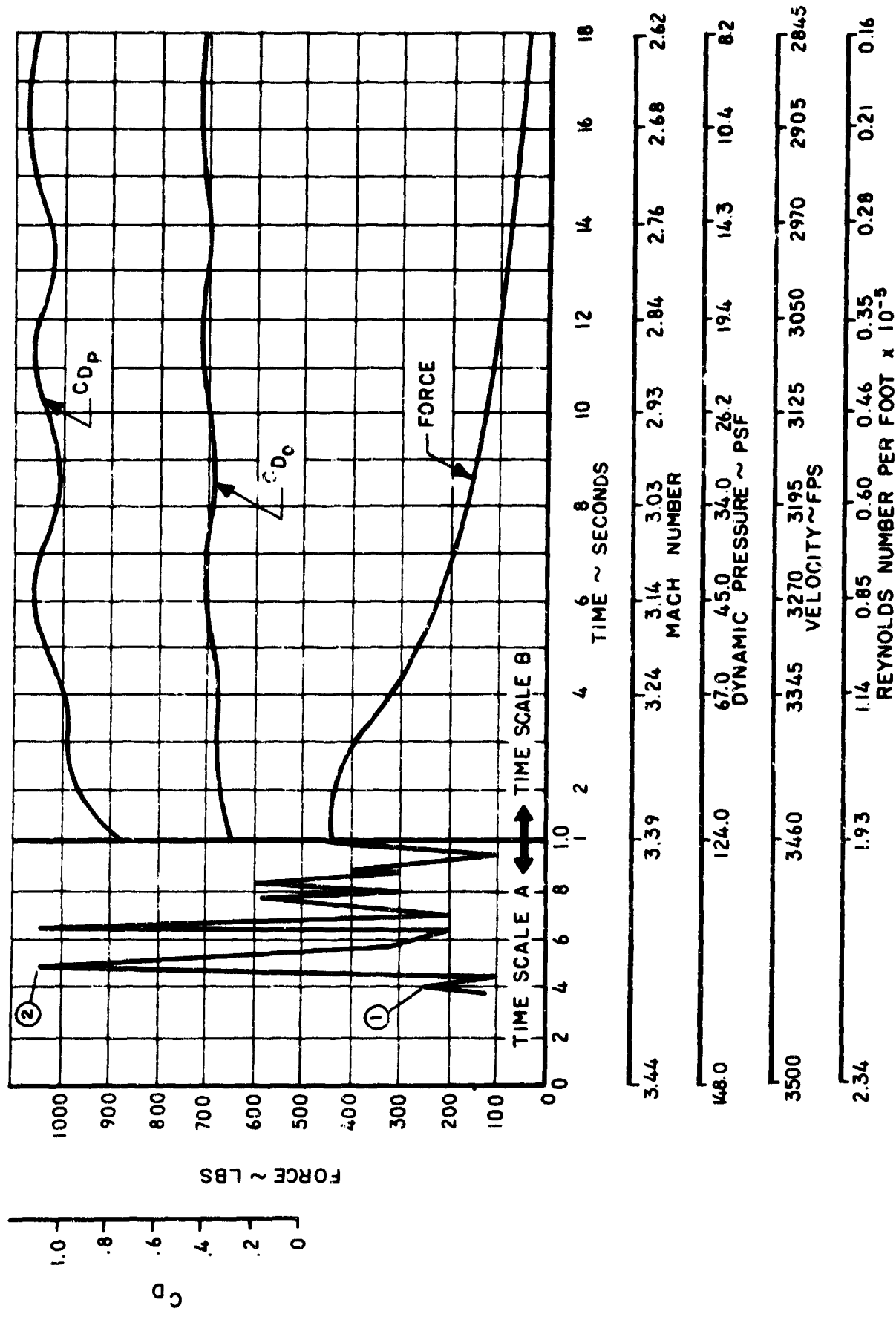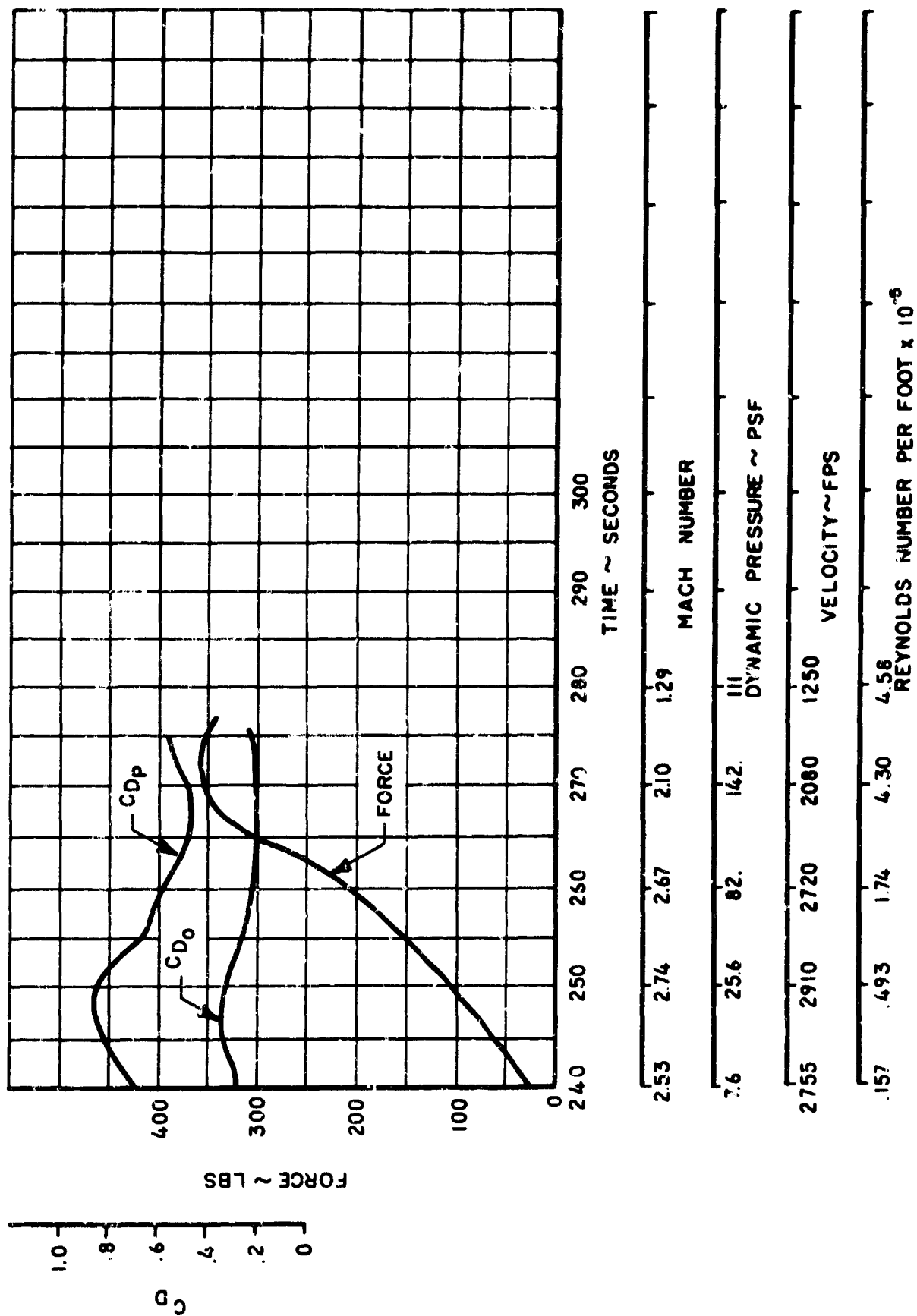| MACH NUMBER | 2.53 | 2.74 | 2.67 | 2.10 | 1.29 |
DYNAMIC PRESSURE ~ PSF	7.6	25.6	82.	142.	111
VELOCITY~FPS	2755	2910	2720	2080	1250
REYNOLDS NUMBER PER FOOT x 10^{-5}	.157	.493	1.74	4.30	4.58

Figure A.10-3 C_D and Force Vs. Time, Mach Number, Dynamic Pressure, Velocity and Reynolds Number - Re-entry No. 8
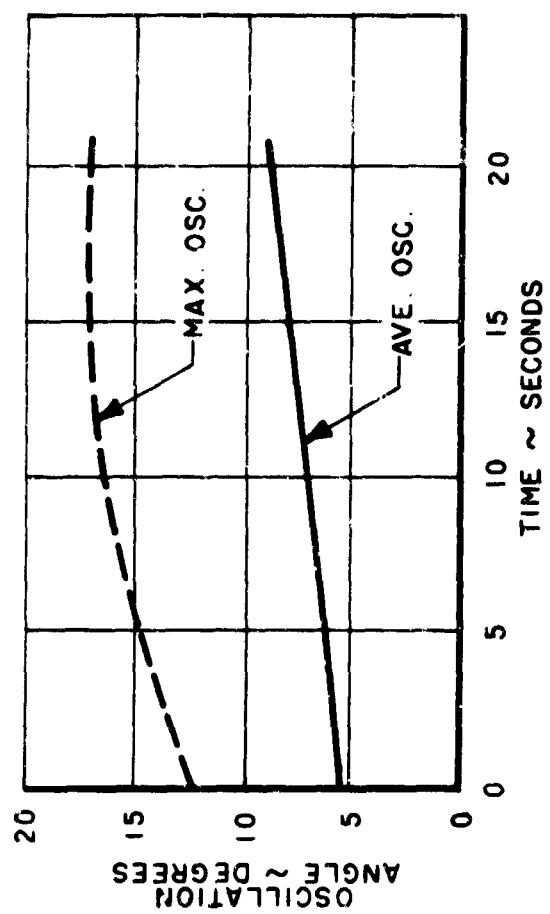
Figure A.10-4 Oscillation Angle Vs. Time
Test No. 8

A. 11 TEST MISSION 9

    Date: 31 July 1963
    Time: 11:30 CST

A.11.1   Objective and Test Setup

The objective of Test No. 9 was to test a Hyperflo parachute (Cook Electric P/N 596-9507) at a Mach number of 3.75 and an altitude of 140,000 feet. This 3.69 foot D_0 parachute had its roof constructed using a single disc of stainless steel mesh and 3/8 inch by 200 pound high temperature Nomex vertical tapes. Mesh porosity was 42.5 percent. Roof porosity was 29.1 percent and total parachute porosity was 14.5 percent. The line length was 2 D_p, the D_p/d_B ratio was 3.4, the x/d_B was 8.45 and the W/S_0 was 50,

    where D_p =   2.55 ft. S_0 =   10.68 ft.^{2}
             d_B =   0.75 ft. S_p =   5.1 ft.^{2}

A 1000 pound tensiometer and an accelerometer rated at ±1 g were used as part of the data gathering components.

The launch vehicle consisted of a 1st stage Honest John, a 2nd stage Nike, a 3rd stage Nike, and a 540 pound Cree payload with a 15 degree Nike to Cree Adapter. Ignition times for the second and third stages were 10 and 30 seconds, respectively. The booster fin angles of incidence were 0.5°, 0.9°, and 0.58° for first, second and third stages, respectively.

A.11.2   Test Result Summary

The general test results are summarized below:

	Anticipated	Actual
Deployment Mach Number	3.75	0.25
Deployment Altitude (Ft.)	140,000	29,200
Deployment Dynamic Pressure (lbs/ft^2)	42	75
Deployment Time (sec.)	50.5	49.9
Opening Shock (lbs)	146	-
C_{D_0} Ave. (1-5 sec.)	0.25	-

A.11.3   Test Discussion

This par. hute test was completely unsuccessful and none of the test objectives were me.. The telemetry and on-board film coverage were

good. Radar tracking was satisfactory and the trajectory is shown in Figure A. 11. 1.

The launch from the pad was normal. However, the first motion switch which provides power to the upper stage igniters did not function and the second and third stages did not ignite. With the second and third stages at their full weights, the $W/C_D A$ ratio between the Cree and the boosters is unfavorable for separation. Therefore, when the test parachute deployed, it was mortared into the Nike to Cree Adapter. The on-board film ran for slightly more than 1 second before daylight was seen. It was not until 3.5 seconds later that the parachute finally pulled free of the adapter. At this time, the parachute began to fail immediately and the roof was completely gone in several seconds. Although it cannot be seen on the film, it is believed that the test parachute was damaged prior to its complete release from the adapter. Figure A. 11.2 shows the parachute after recovery.

The vehicle impacted the water at about T_o + 90 seconds. Therefore, the recovery system was not activated and the recovery parachute was not deployed or inflation balloon inflated. The vehicle hit the water at about 700 fps and at a distance of one mile from shore. Navy Recovery Divers recovered the vehicle several days later. The Cree vehicle, together with all instrumentation was for all practical purposes completely destroyed. What was left of the test parachute was recovered, even though the tensiometer had failed.
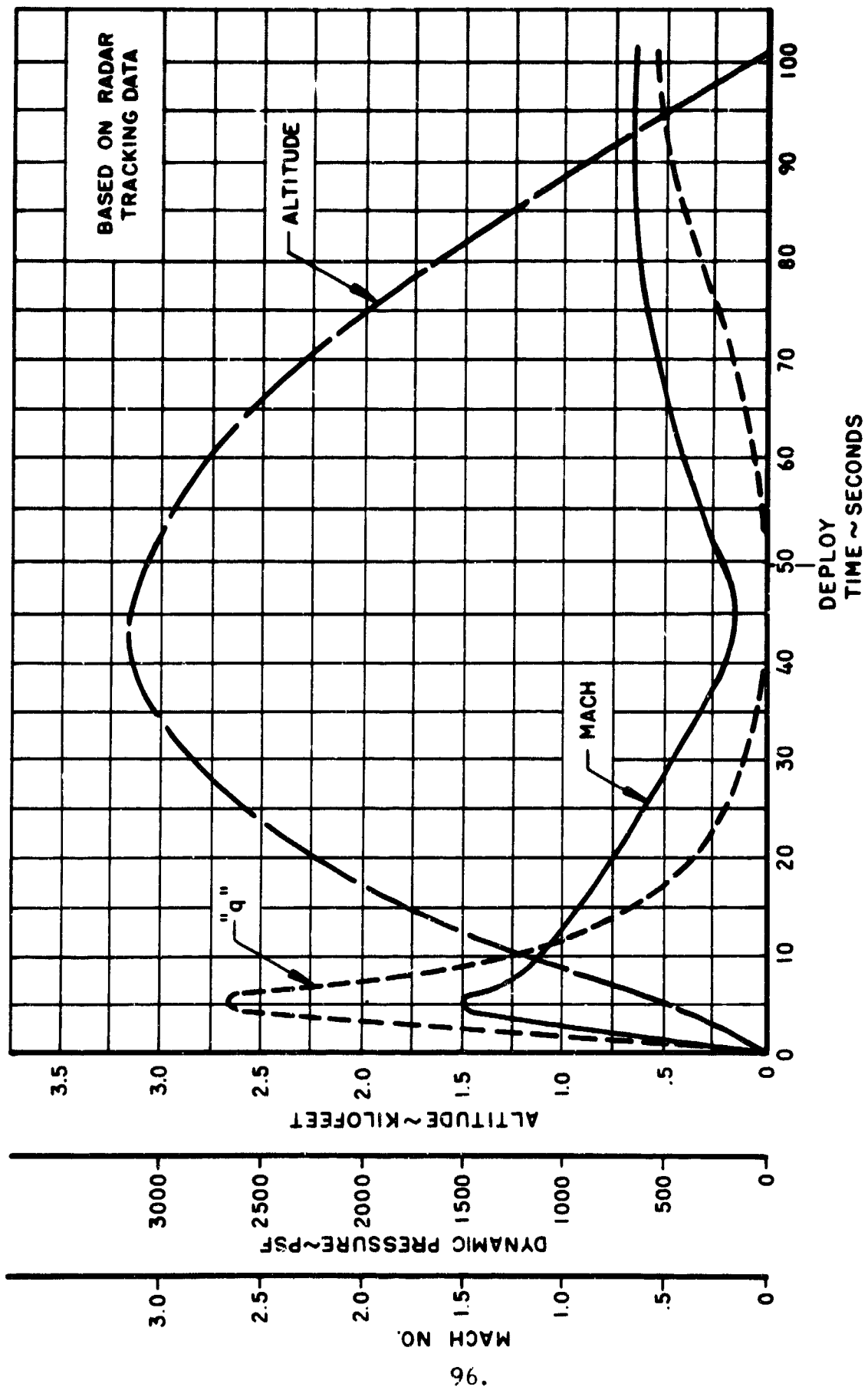
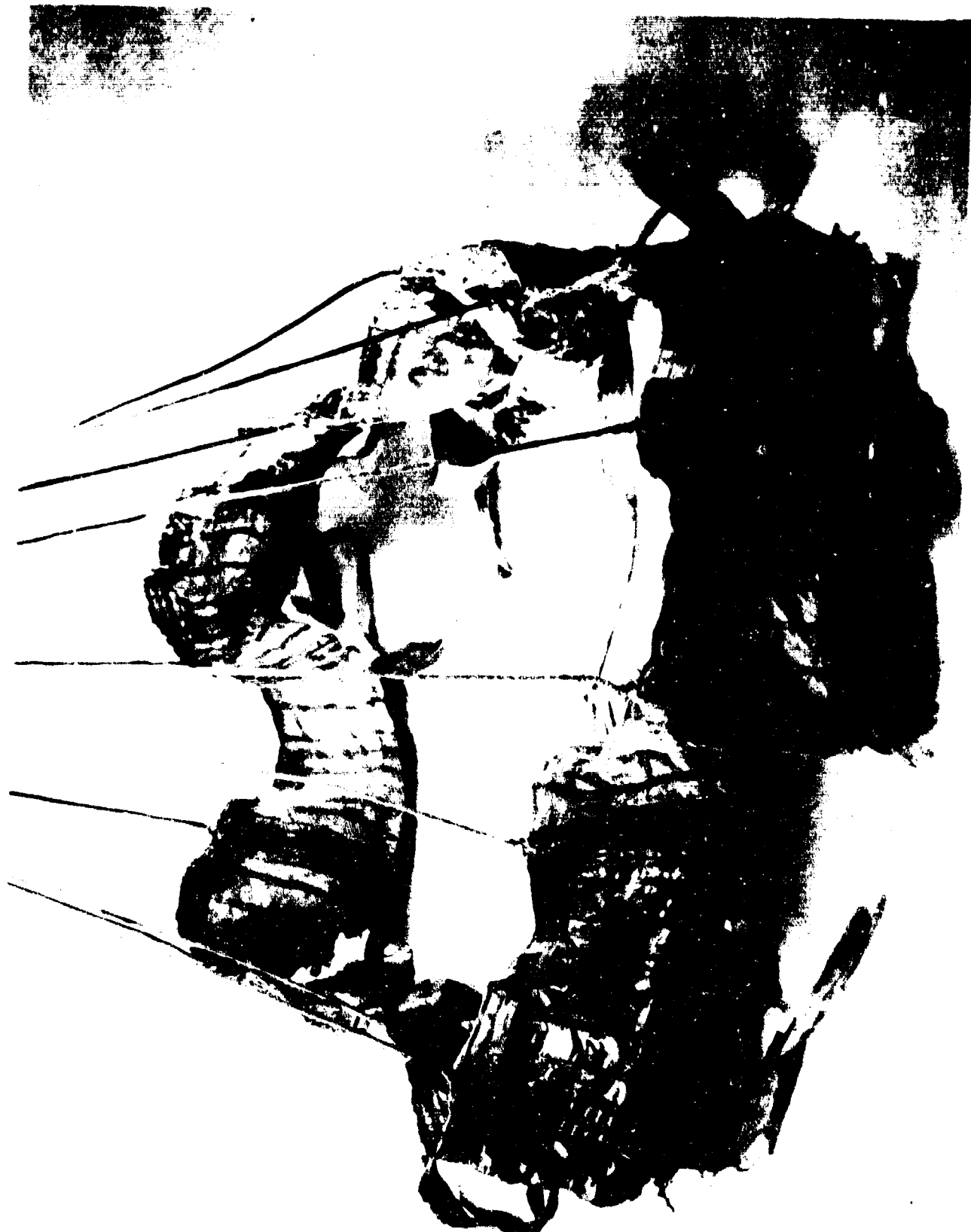Figure A.11-1 Missile Tracking Data - Test No. 9

Figure A.11-2 Recovered Test Parachute - Test No. 9

A.12 TEST MISSION 10

Date: 15 August 1963
Time: 11:01 CST

A.12.1   Objective and Test Setup

The objective of Test No. 10 was to test a Hyperflo parachute (Cook Electric P/N 596-9028) at a Mach number of 3.06 and an altitude of 200,000 feet. This 3.69 foot D_0 parachute had its roof constructed using 12 gores of Perlon mesh. This mesh had a porosity of 45.2 percent. Roof porosity was 33.8 percent and total parachute porosity was 16.9 percent. The line length was 2 D_p, the D_p/d_B ratio was 3.4, the x/d_B was 8.45 and the W/S_0 was 64,

where D_p = 2.55 ft. S_0 = 10.68 ft.^{2}
          d_B = 0.75 ft. S_p = 5.1 ft.^{2}

A 200 pound tensiometer and an accelerometer rated at ±1 g were used as part of the data gathering components.

The launch vehicle consisted of a 1st stage Honest John, a 2nd stage Nike, a 3rd stage Nike and a 680 pound Cree payload with a 7.5 degree Nike to Cree Adapter. Ignition times for the second and third stages were 10 and 30 seconds, respectively. The booster fin angles of incidence were 0.5°, 0.9°, and 0.8° for first, second and third stages, respectively.

A.12.2   Test Result Summary

The general test results are summarized below:

	Anticipated	Actual
Deployment Mach Number	3.06	2.98
Deployment Altitude (Ft.)	200,000	188,200
Deployment Dynamic Pressure (lbs/ft^2)	1.0	5.0
Deployment Time (sec.)	69.92	69.24
Opening Shock (lbs)	4.0	-
Max. Load (lbs)	-	16.0
C_{D_0} Ave. (1-5 sec.)	0.29	0.20

A.12.3   Test Discussion

This test was largely unsuccessful. The vehicle was not re-covered and therefore the on-board film was lost. The telemetry data was

good; however, because of the extremely low "q" in the test regime, the parachute loads were equally low. The force and C_D data is presented in Figure A. 12. 1; however, none of this data is considered to be very reliable. The problem is basically that "q" has had to be determined based upon standard atmosphere as well as a possible slight zero shift in the force record which would make a large percent change in that force. The graph then represents the best data available but should not be considered too strongly.

Data reduction performed for the re-entry phase of the trajectory definitely shows a C_{D_o} of around 0.05. This C_{D_o}, when compared to that obtained in Test No. 12, clearly shows that the test parachute had failed by this time. Both load and "q" were high enough during re-entry that their readings are considered accurate. The time and reason for test parachute failure are unkown. It is suspected that aerodynamic heating of the Perlon mesh may have caused canopy failure.

The launch and all phases of the trajectory were normal. The trajectory is shown in Figure A. 12. 2. Both the radar and telemetry data indicate that the recovery parachute was deployed as programmed and that it worked satisfactorily.

The vehicle could not be found in the impact area and is presumed to have sunk in 700 feet of water. No recovery was attempted because of the water depth.
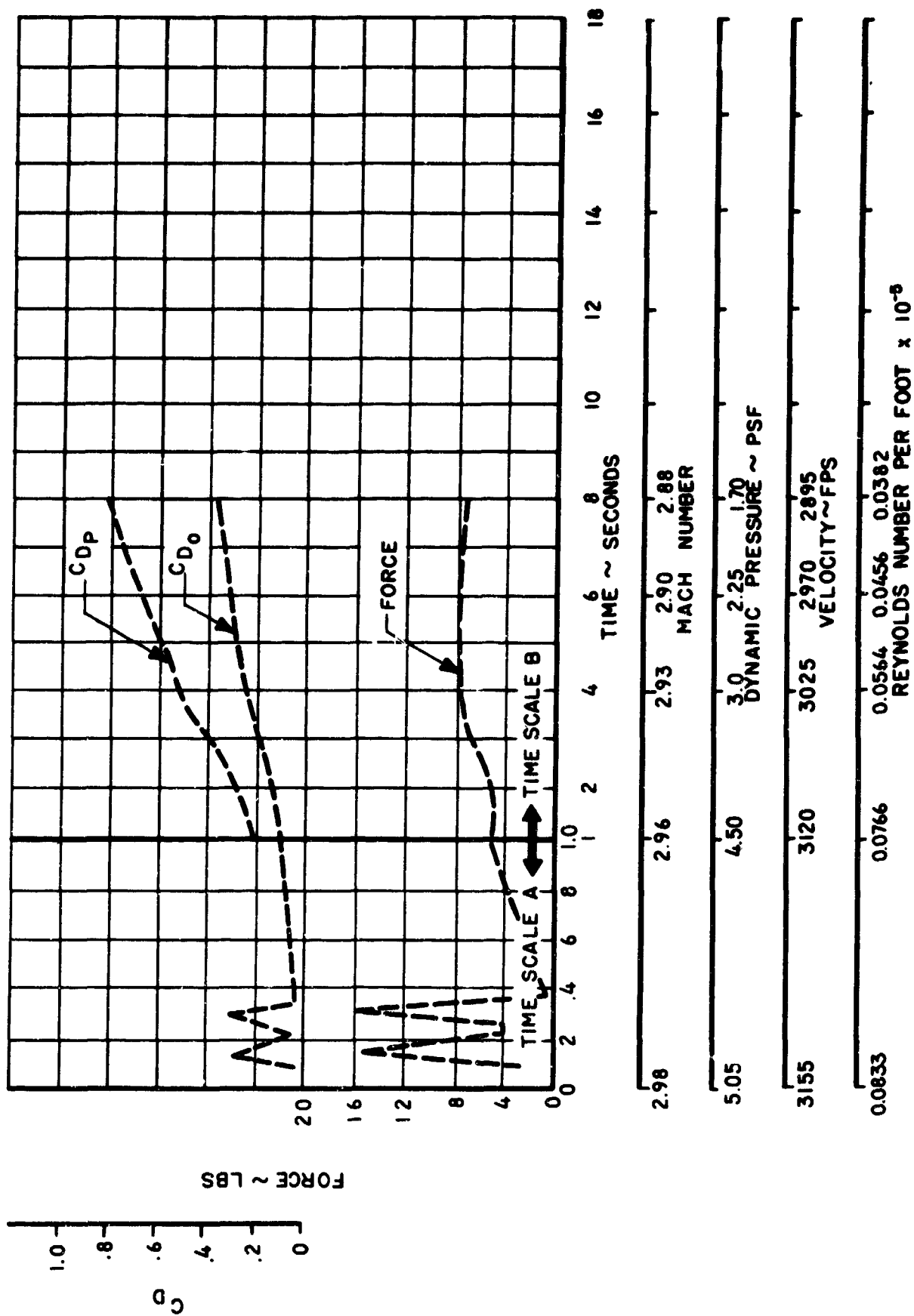
Figure A.12-10 c_D and Force Vs. Time, Mach Number, Dynamic Pressure, Velocity and Reynolds Number - Test No. 10
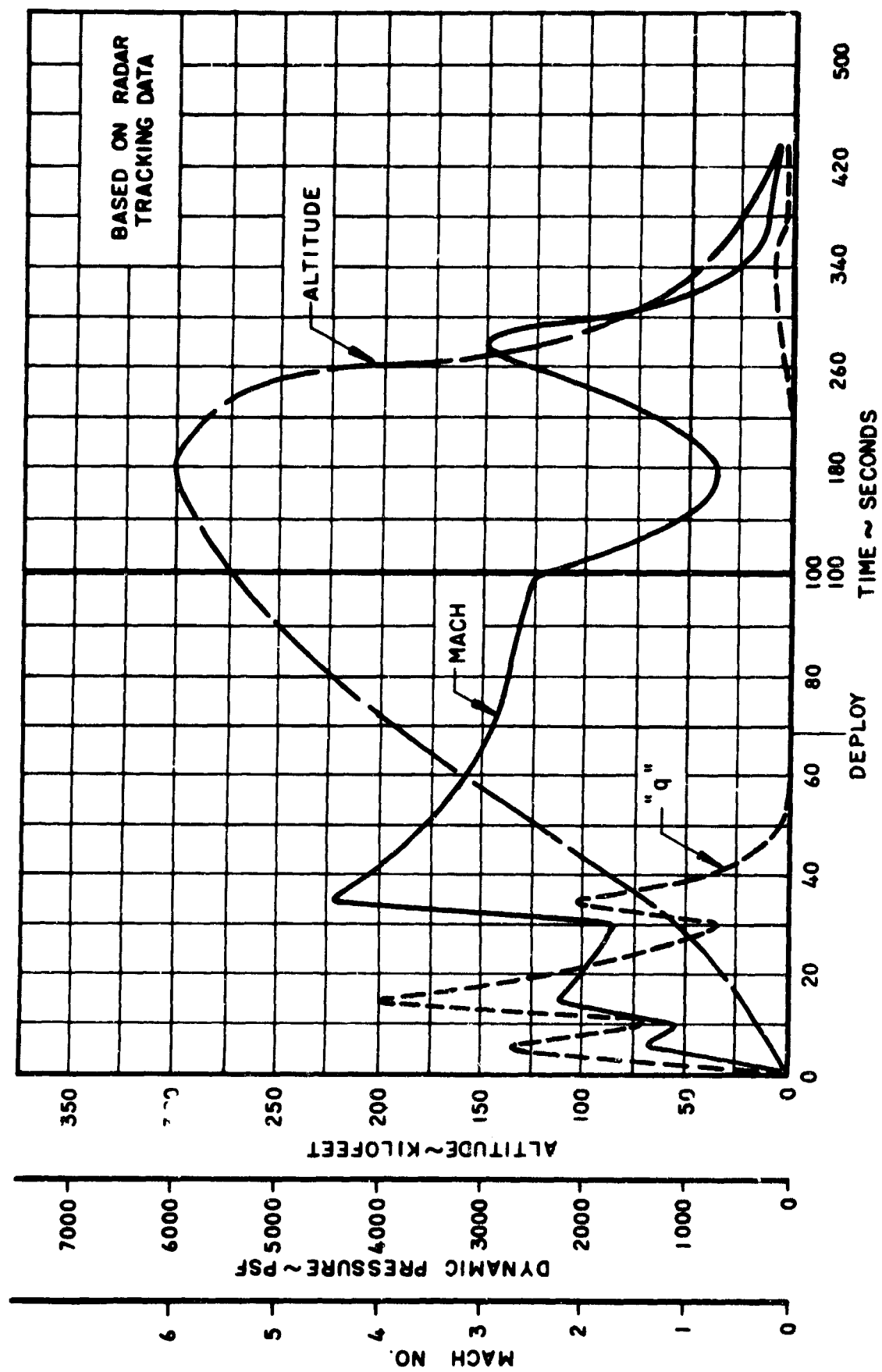
100.

Figure A.12-2 Missile Tracking Data - Test No. 10

101.

Date: 21 August 1962
Time: 14:07 CST

A.13.1   Objective and Test Setup

The objective of Test No. 11 was to test a Hyperflo parachute (Cook Electric P/N 596-9517) at a Mach number of 4.4 and an altitude of 100,000 feet. This 2.71 foot D_O parachute had its roof constructed using a single disc of stainless steel mesh and 12 Nomex ribbon radials. This mesh had a porosity of 35.4 percent. Roof porosity was 24.7 percent and total parachute porosity was 12.2 percent. The line length was 2 D_p, the D_p/d_B ratio was 2.5, the x/d_B was 7.0 and the W/S_O was 93,

where D_p = 1.88 ft. S_O = 5.78 ft.^{2}
         d_B = 0.75 ft. S_p = 2.76 ft.^{2}

A 1000 pound tensiometer and an accelerometer rated at ±2.5 g's were used as part of the data gathering components.

The launch vehicle consisted of a 1st stage Honest John, a 2nd stage Nike, a 3rd stage Nike, and a 540 pound Cree payload with a 15 degree Nike to Cree Adapter. Ignition times for the second and third stages were 10 and 20 seconds, respectively. The booster fin angles of incidence were 0.5^O, 0.9^O, and 0.58^O for first, second and third stages, respectively.

A.13.2   Test Result Summary

The general test results are summarized below:

	Anticipated	Actual
Deployment Mach Number	4.4	4.4
Deployment Altitude (Ft.)	100,000	94,200
Deployment Dynamic Pressure (lbs/ft^2)	330	430
Vehicle Spin Rate at Deployment (rps)	-	2
Deployment Time(sec.)	34.7	33.85
Ejection to Full Line Stretch (sec.)	-	.135
Line Stretch to Full Open (sec.)	-	.05
Opening Shock (lbs)	570	-
Max. Load (lbs)	-	333
Max. Temperature (^{O}F)	-	930
C_{D_O} Ave. (1-2 sec.)	0.23	0.1

A.13.3   Test Discussion

In this test, the test parachute was deployed at the required test regime, but the parachute failed structurally. The telemetry record was good and the on-board camera functioned normally. Radar tracking was good and the data is presented in Figure A.13.1.

Figure A.13.2 shows the force and C_D during the test. Figure A.13.3 shows a parachute opening and closing cycle prior to structural failure. No attempt has been made to show the extent to which the parachute opens or collapses during each cycle, but rather, the intent has been to show the cycling frequency. The last several cycles are longer in time than the others and probably indicates that an unobserved failure occurred at about 1.4 seconds.

The on-board film shows the parachute to deploy and open normally. However, once open, the parachute began a cycle of opening and collapsing until the steel mesh began to tear and rip out. The steel mesh was completely gone in about 3 seconds. The Nomex cone began to burn and melt away within 1 to 2 seconds after the canopy started to structurally fail.

The maximum parachute temperature recorded during this test was $930^\circ F$. This temperature was, however, for a non-operating parachute which would cause higher than normal heating effects.

The test parachute was recovered with its canopy almost completely destroyed. The Cree vehicle was recovered without damage or incident. Figure A.13.4 shows the parachute after recovery.
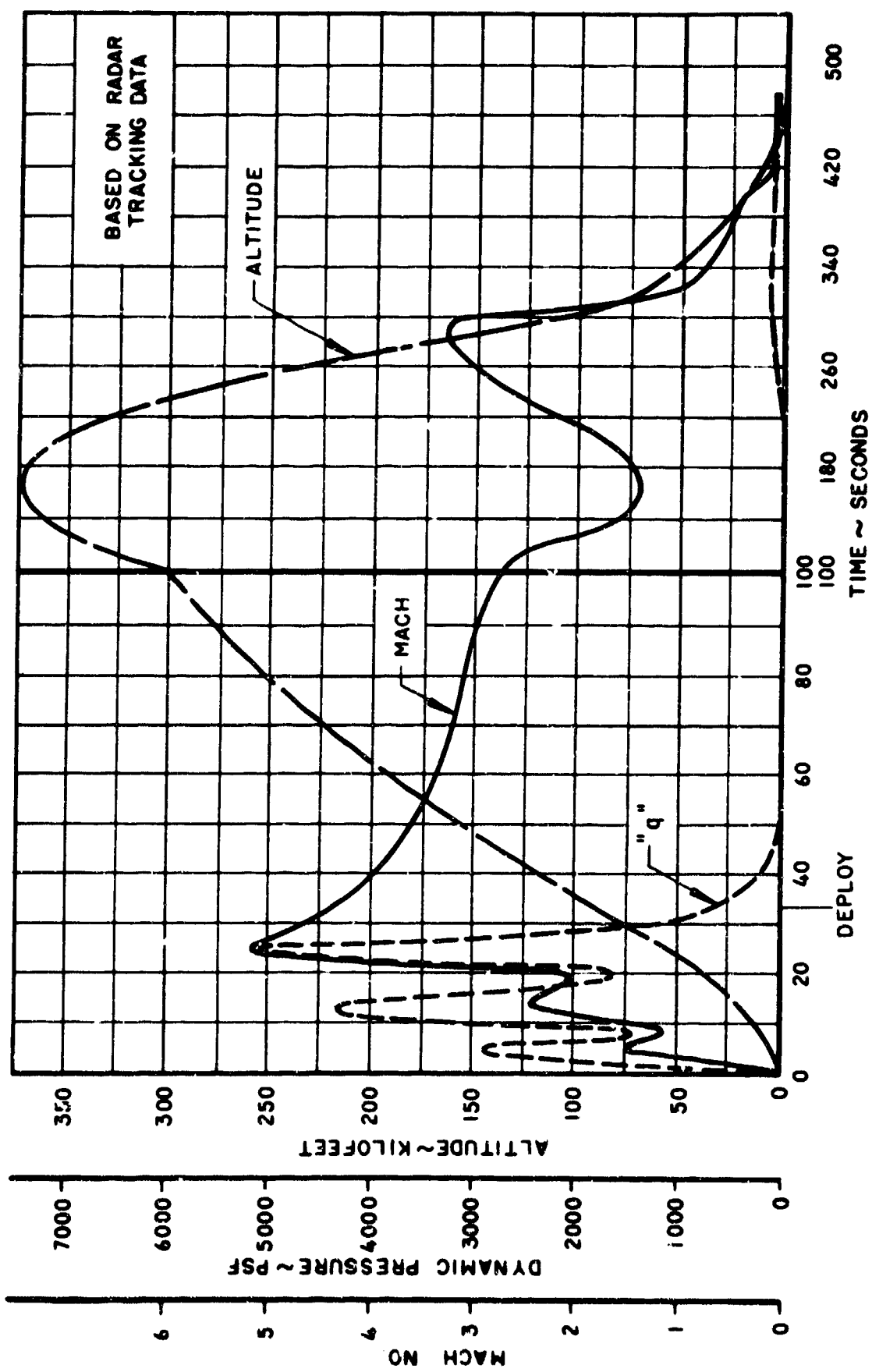
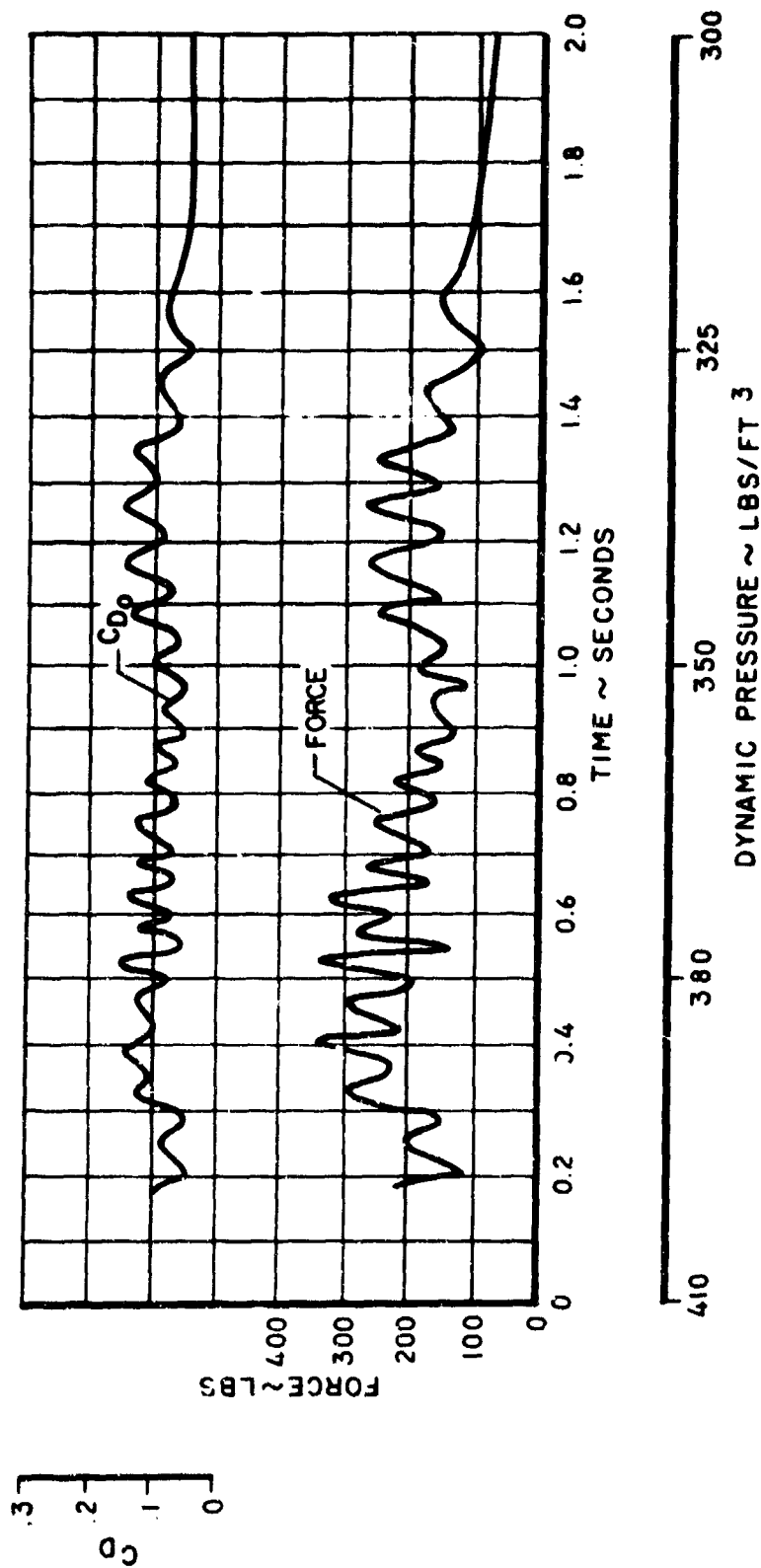Figure A.13-1 Missile Tracking Data - Test No. 11

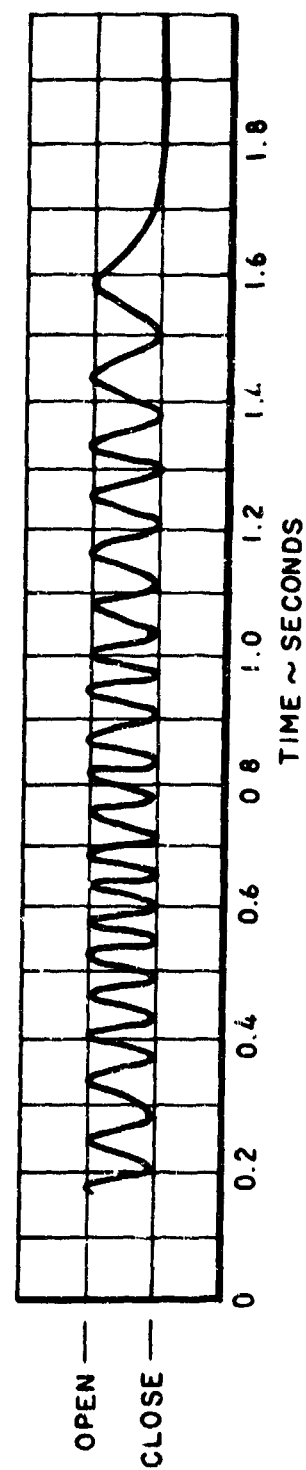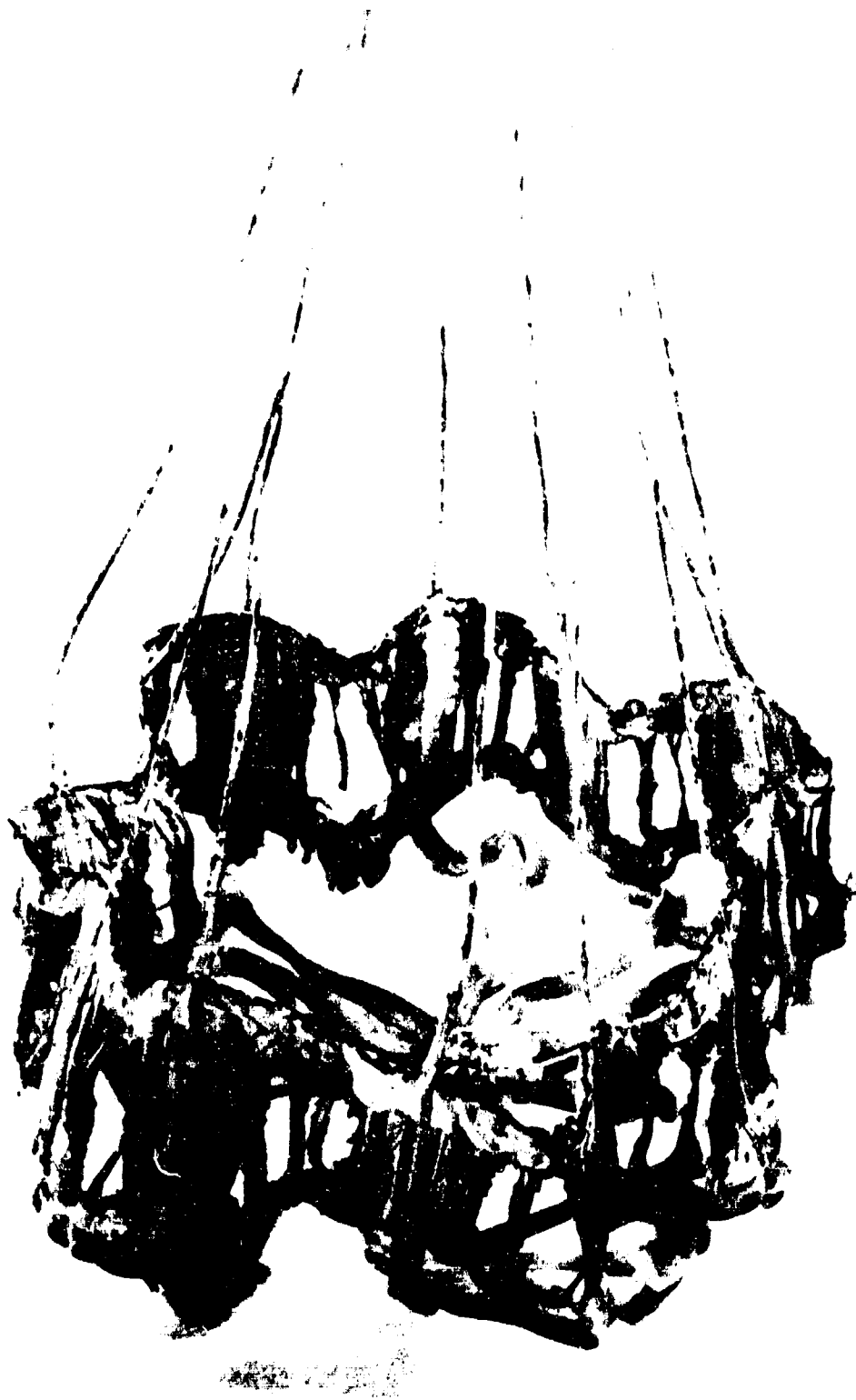Figure A.13-2 C_D and Force vs. Time and Dynamic Pressure - Test No. 11

Figure A.13-3 Parachute Opening Characteristics vs. Time - Test No. 11

S/N 1403

Figure A. 13-4 Recovered Test Parachute - Test No. 11

A. 14. 1   Objective and Test Setup

The objective of Test No. 12 was to test a Hyperflo parachute (Cook Electric F/N 596-9028) at a Mach number of 2.8 and an altitude of 100,000 feet. This 3.69 foot D_o parachute had its roof constructed using 12 gores of Perlon mesh. This mesh had a porosity of 45.2 percent. Roof porosity was 33.8 percent and total parachute porosity was 16.9 percent. The line length was 2 D_p, the D_p/d_B ratio was 3.4, the x/d_B was 8.45 and the W/S_o was 50,

where D_p = 2.55 ft. S_o = 10.68 ft.^{2}
         d_B = 0.75 ft. S_p = 5.1 ft.^{2}

A 3000 pound tensiometer and an accelerometer rated at ±2.5 g's were used as part of the data gathering components.

The launch vehicle consisted of a 1st stage Honest John, a 2nd stage Nike and a 540 pound Cree payload with a 15 degree Nike to Cree Adapter. Ignition time for the second stage was 30 seconds. The booster fin angles of incidence were 0.5° and 0.99° for first and second stages, respectively.

A. 14. 2   Test Result Summary

The general test results are summarized below:

	Anticipated	Actual
Deployment Mach Number	2.8	3.12
Deployment Altitude (Ft.)	100,000	77,000
Deployment Dynamic Pressure (lbs/ft^2)	115	494
Vehicle Spin Rate at Deployment (rps)	-	2
Deployment Time (sec.)	46.5	44.6
Ejection to Full Line Stretch (sec.)	-	.16
Line Stretch to Full Open (sec.)	-	.24
Opening Shock (lbs)	480	-
Max. Load (lbs)	-	350
C_{D_o} Ave. (1-5 sec.)	0.30	0.035
Max. Temperature (°F)	-	550

A. 14. 3   Test Discussion

In this test, the parachute was deployed in a test regime which was too severe for the materials used, due to programmer errors. The telemetry record was satisfactory and the on-board camera functioned normally. Radar tracking was good and the data is presented in Figure A. 14. 1.

Figure A. 14. 2 shows the force and C_D during test. Although the on-board camera film shows the parachute roof to completely fail within 0. 2 seconds after deployment, the force and particularly the C_D are shown for general information and as a guide for parachute performance for Tests 10 and 13 in which the test vehicles were not recovered. The C_{D_o} value obtained for the test parachute after the roof was completely destroyed was about 0. 04. Spot checks were also taken during re-entry and similar C_{D_o} values were obtained.

The maximum parachute temperature shown by the heat sensors was 550^oF, but as in Test No. 11, this temperature is greater than that which would be expected if the parachute had not failed structurally.

The test parachute together with the undamaged Cree were re-covered in a normal manner and without incident. Figure A. 14. 3 shows the parachute after recovery.

Although the "q" field in which the test parachute was deployed was almost 5 times that anticipated, a stress check of the canopy indicates that it should have had a safety factor of about 4, even at the higher "q". It appears that the only reasonable explanation for the parachute failure is aerodynamic heating effects on the low temperature materials used in the construction of this parachute.
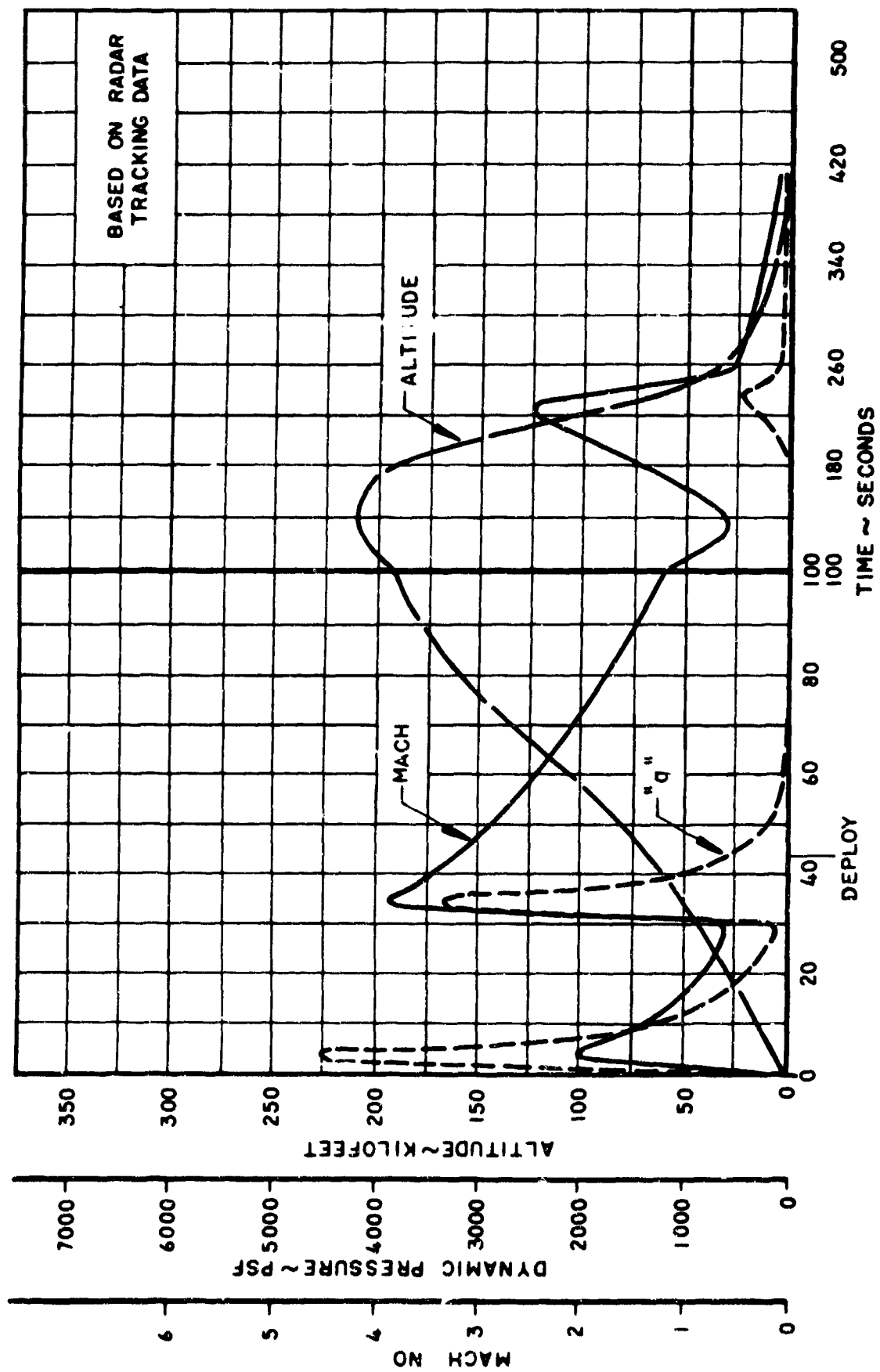
Figure A.14-1 Missile Tracking Data - Test No. 12
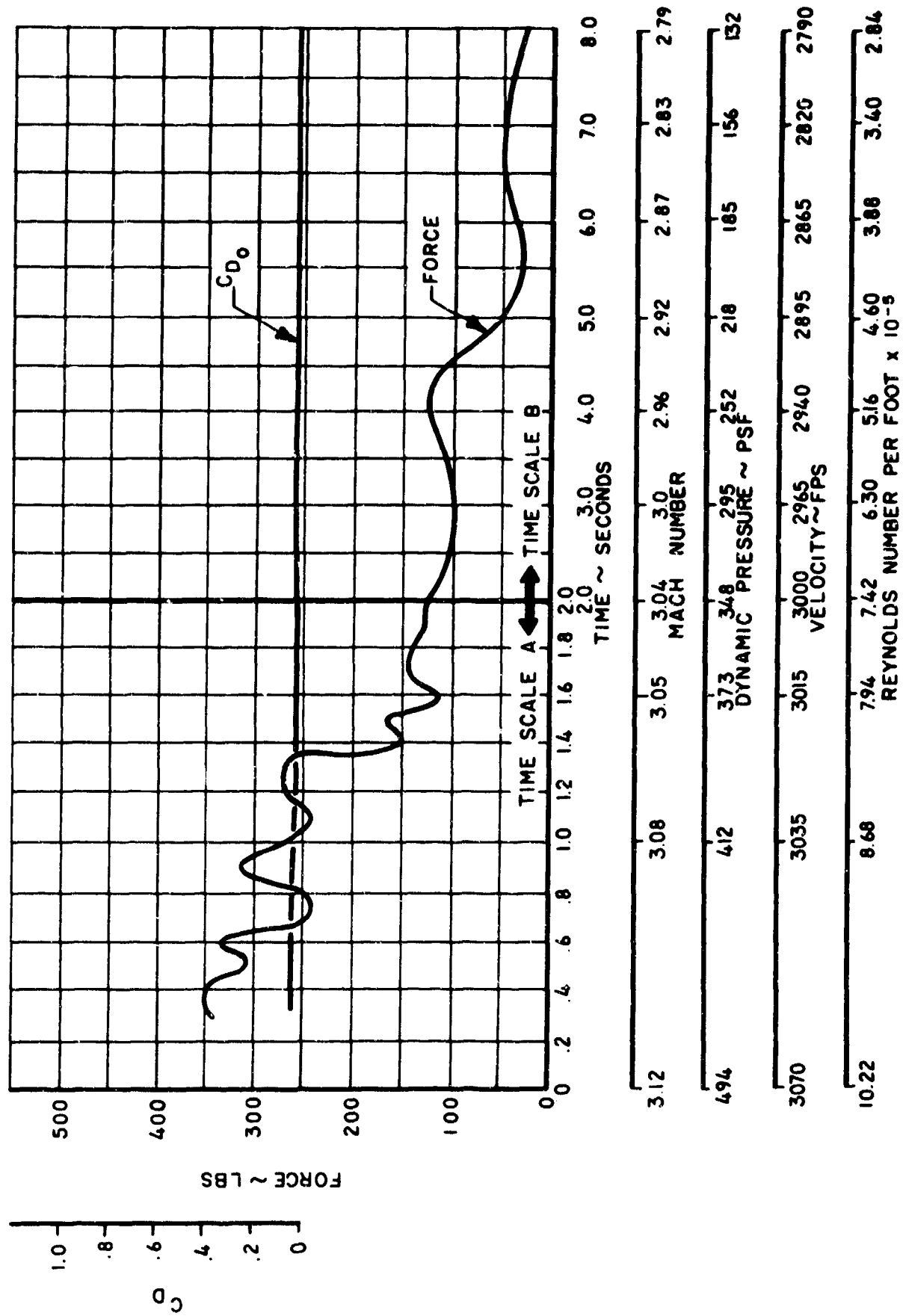
Figure A.14-2 C_D and Force Vs. Time, Mach Number, Dynamic Pressure, Velocity and Reynolds Number - Test No. 12

S/N
1419

Figure A. 14-3 Recovered Test Parachute - Test No. 12

111.

A.15 TEST MISSION 13

    Date: 12 September 1963
    Time: 05:54 CST

A.15.1   Objective and Test Setup

        The objective of Test No. 13 was to test a Hyperflo parachute (Cook Electric P/N 596-9522) at a Mach number of 3.3 and an altitude of 167,000 feet. This 3.69 foot D_o parachute had its roof constructed using 12 gores of Perlon mesh and 3/8 inch by 200 pound high temperature Nomex vertical tape. Mesh porosity was 45.2 percent. Roof porosity was 31.0 percent and total parachute porosity was 16.0 percent. The line length was 2 D_p, the D_p/d_B ratio was 3.4, the x/d_B was 8.45 and the W/S_o was 56,

        where D_p =   2.55 ft. S_o =   10.68 ft.^{2}
                     d_B =   0.75 ft. S_p =   5.1 ft.^{2}

        A 1000 pound tensiometer and an accelerometer rated at ±2.5 g's were used as part of the data gathering components.

        The launch vehicle consisted of a 1st stage Honest John, a 2nd stage Nike, a 3rd stage Nike and a 600 pound Cree payload with a 15 degree Nike to Cree Adapter. Ignition times for the second and third stages were 10 and 30 seconds, respectively. The booster fin angles of incidence were 0.5°, 0.9°, and 0.58° for first, second and third stages, respectively.

A.15.2   Test Result Summary

        The general test results are summarized below:

	Anticipated	Actual
Deployment Mach Number	3.3	2.95
Deployment Altitude (Ft.)	167,000	154,000
Deployment Dynamic Pressure (lbs/ft^2)	12.5	16
Deployment Time (sec.)	59	58.9
Opening Shock (lbs)	+9	-
Max. Load (lbs)	-	136
C_{D_o} Ave. (1-5 sec.)	0.28	0.22

A.15.3   Test Discussion

        This test was only partially successful because the vehicle and on-board film were lost. The radar data was good and the trajectory is

112.

shown in Figure A. 15. 1. The telemetry data was fair and the force and C_D curves are shown in Figure A. 15. 2.

It is felt that the reliability of the test data after the first 5 to 6 seconds is questionable. But is is definitely believed that the test parachute survived the first 2 to 3 seconds of test. Beyond this point, data is questionable.

The re-entry phase of the telemetry was analyzed and the C_{D_0} value was found to be about 0.05, thus indicating a failed parachute. Where this failure occurred is impossible to determine.

To minimize the heating to the low density roof, the Perlon mesh was dyed black in order to increase its emissivity. The object was to reduce the radiation equilibrium temperature of the Perlon mesh. This was felt feasible because with the low heat inputs at this altitude, correspondingly low equilibrium temperatures could be maintained. How effective this technique was in this case is, of course, unknown.

The vehicle performed as scheduled until the recovery parachute deployment time. The radar coverage for this test does not show the normal decrease in velocity that accompanies the successful deployment of the recovery parachute. The radar track indicates the vehicle hit the water at 300 fps. A search of the impact area was fruitless and it was presumed the vehicle sank in 180 feet of water.

Recovery efforts were made with commercial divers, but without success. The recovery operation was called off after two days of search because of increasing bad weather.
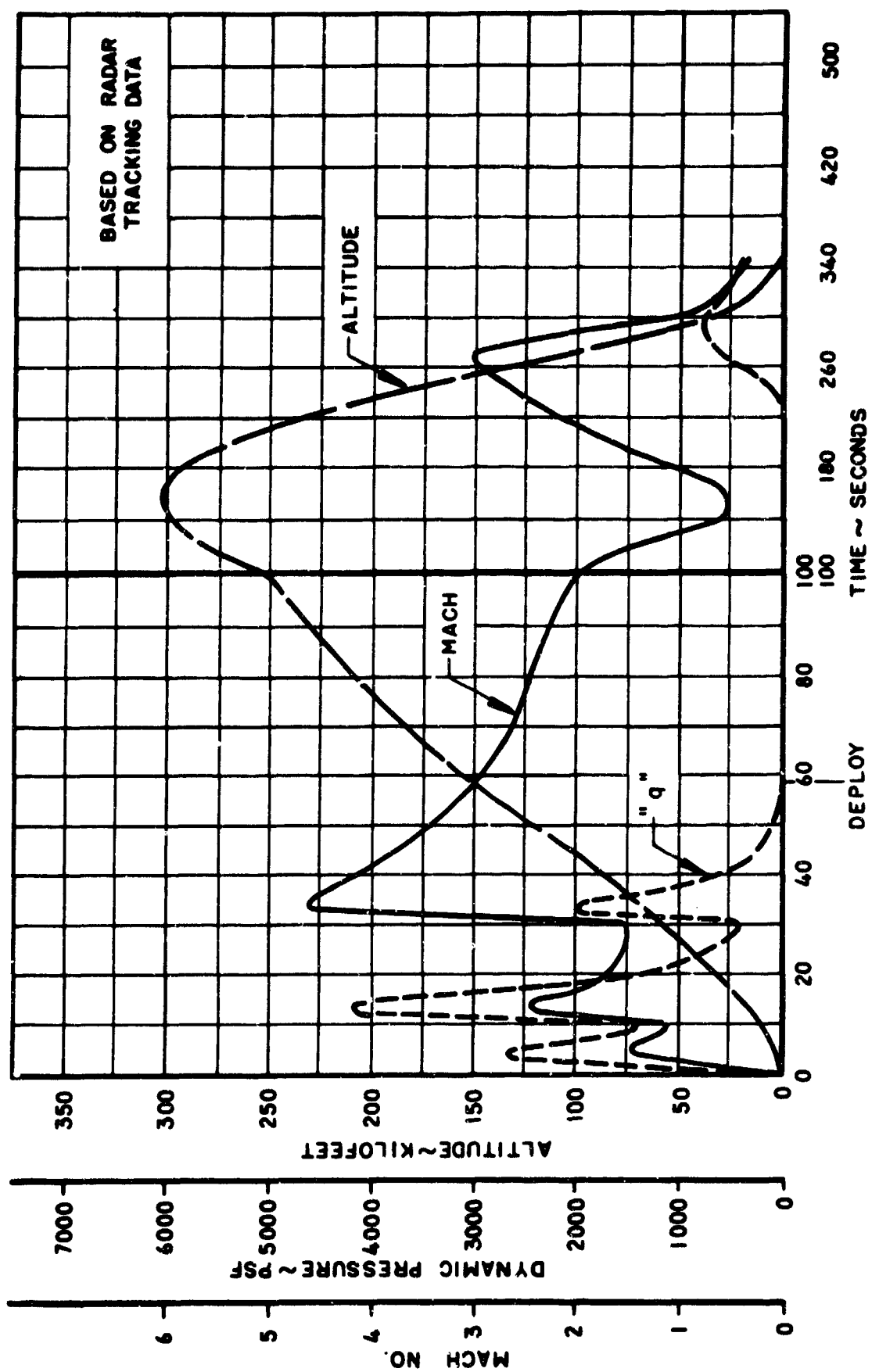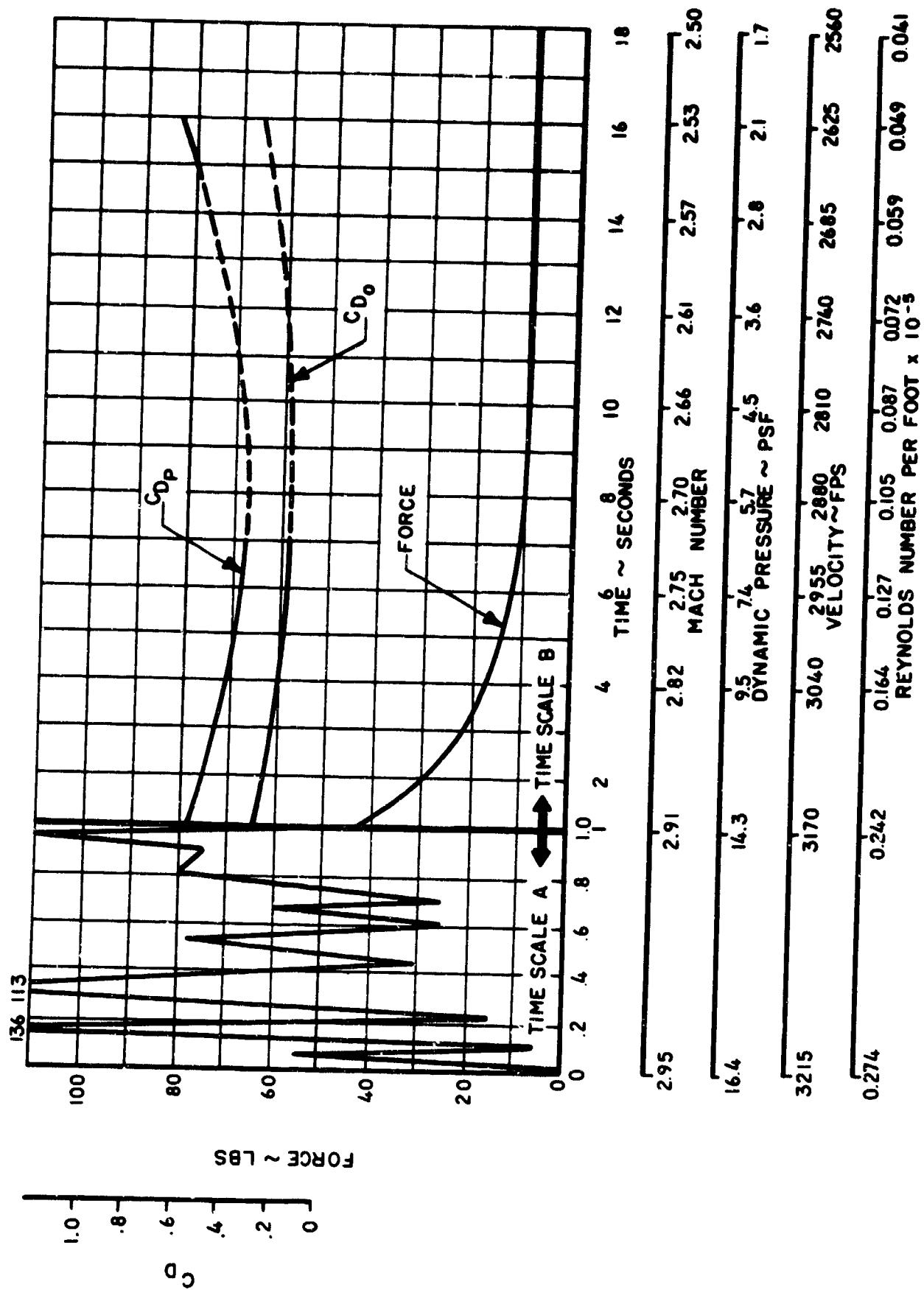
Figure A.15-1 Missile Tracking Data - Test No. 13

114.

Figure A.15-2 C_D and Force Vs. Time, Mach Number, Dynamic Pressure, Velocity and Reynolds Number – Test No. 13

115.

APPENDIX B

TEST VEHICLE DEVELOPMENT

B. 1   BACKGROUND

The Cree Decelerator test vehicle has been developed over the last seven years by the Tech-Center Division of Cook Electric Company. It was first designed for a land impact recovery. In 1959, Cree was redesigned to include a flotation system for water recovery.

In the beginning of this phase, a study of the performance and results of the past Cree phases was made. Effort was directed toward improving the reliability of the telemetry system (TM) and the quality of the recorded data. Other major areas of vehicle modification included the addition of dive brakes, strengthening of the vehicle above the flotation balloon compartment and removal of all unnecessary fasteners in the bulkheads. Figure B. 1 shows a cutaway view of a typical Cree vehicle.

B. 2   VEHICLE ELECTRONIC MODIFICATION

It was decided to keep the electronic modification effort at a reasonable level by maintaining the basic Cree electronic system concept. The major effort was then directed toward improved component quality and reliability. This component improvement would, in itself, provide a corresponding system improvement.

B. 2. 1   Component Equipment

The component equipment has been assembled into three units. These units have been called the instrumentation compartment, transducer compartment, and camera compartment. Figures B. 2, B. 3, B. 4 and B. 5 show the general component assembly within each compartment.

B. 2. 1. 1   Telemetry

The following redesign objectives were established for the Cree telemetry system:

(1)   Solid state circuits operating on a 28 V DC primary supply source

(2)   Two watts minimum output

117.

1. Pressure Probe and Antenna
2. Nose Spike
3. Nose Fairing
4. Ballast
5. Air Bottle
6. Fwd Bulkhead
7. Transducer Compartment
8. Spacer
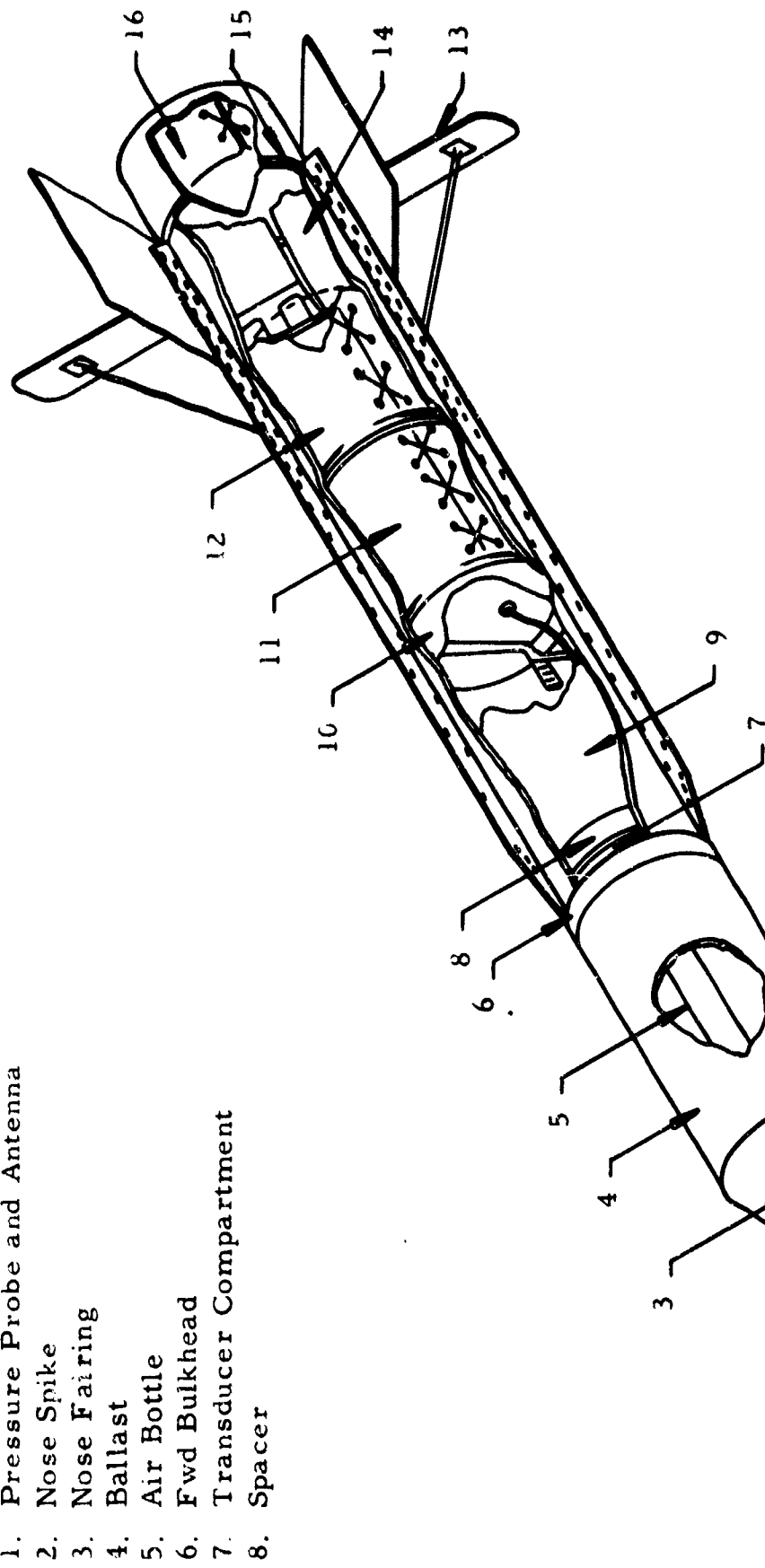
9. Instrumentation Compartment
10. Intermediate Bulkhead
11. Flotation Balloon
12. Recovery Parachute
13. Dive Brakes
14. Camera Compartment
15. Aft Bulkhead
16. Test Parachute

Figure B.1   Cutaway View of Cree Vehicle

118.

Figure B.3 Instrumentation Compartment
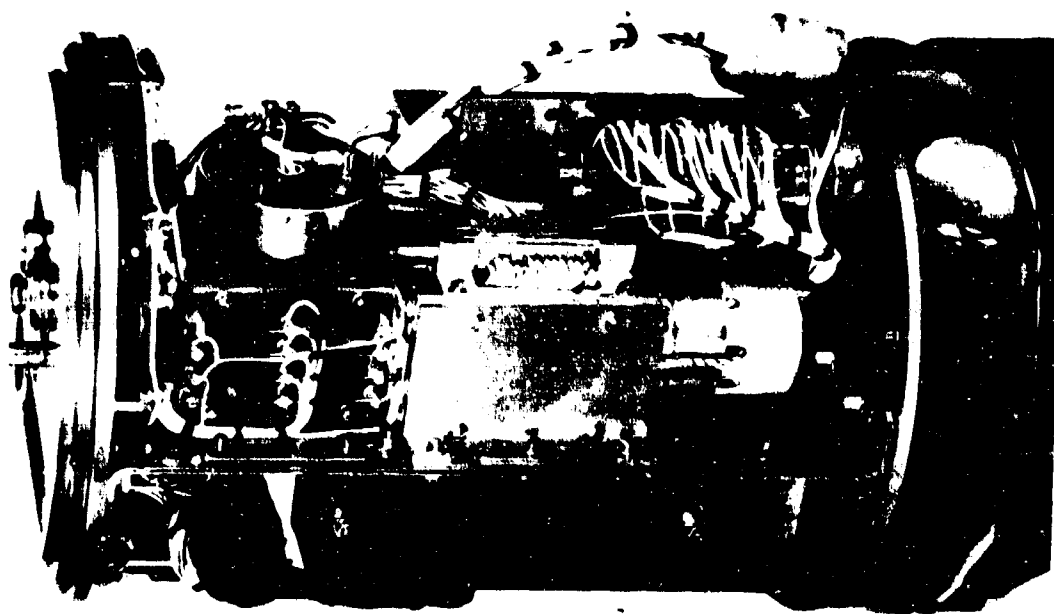
Figure B.2 Instrumentation Compartment

1. Pressure Probe and Antenna
2. Nose Spike
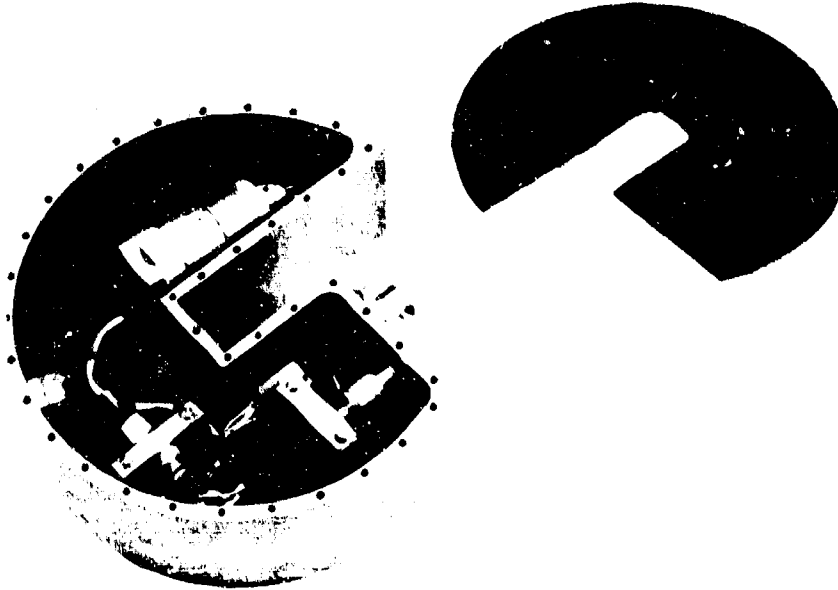
B. 4 Transducer Compartment
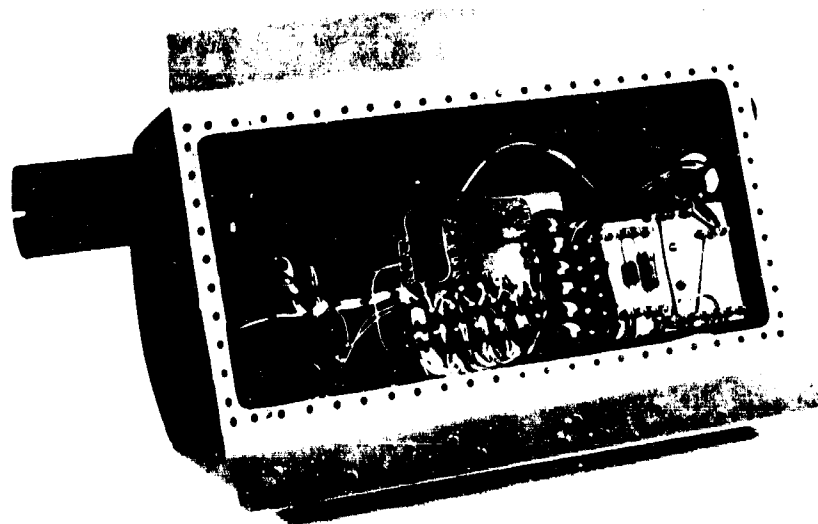
B. 5 Camera Compartment

(3) Improved voltage controlled oscillator
             (VCO) stability.

        The use of solid state circuits eliminated the need for high
voltage dynamotors or other DC or AC converters. With the present state-
of-the-art, 2 watts is the maximum practical output to be expected at 225 mc.
Calculations have shown that 2 watts is ample power for the application
required of the Cree.

        VCO stability has been a problem in earlier Cree TM
systems. VCO's from several sources were examined to determine their
stability under various combinations of environments. The TM system
selected is manufactured by Vector Manufacturing Company. The system
consists of the following components:

        (1) Transmitter type TRFP-2V

        (2) VCO type TL-61B

        (3) Summing amplifier TA-48.

B. 2. 1. 2   Pitot Static Antenna

        The TM antenna serves also as a pitot static tube. The
antenna used in earlier Cree models suffered from the following deficiencies:

        (1) As a pitot static tube, sealing and assembly were
   troublesome.

        (2) The temperature resistance of the phenolic insulator
             was marginal.

        A new design was adopted using an all-welded construction
technique which assures a reliable seal of the pressure lines. The insulator
itself is made from an asbestos wrap. This new antenna-insulator combina-
tion has proved very successful and a good antenna-to-telemetry system
impedance match was achieved.

B. 2. 1. 3   Beacon Radar Transponder

        On the recommendation of Eglin AFB, the radar beacon was
changed to the C-band from the S-band as used in earlier Crees. The track-
ing characteristics of the FPS 16 C-band radar are superior to the older
S-band radar. The Cree uses an Aero Geo Astro C/T-CV beacon. Its

121.

output is more than 100 watts with a receiver sensitivity of approximately 38 dbm. Two modified radar beacon scimitar antennas are used on the Cree. These antennas were designed and manufactured by the Engineering Services Branch of the Physical Science Laboratory at Eglin Air Force Base. The beacons are supplied and calibrated by the Special Devices Branch. Excellent results have been achieved with the above system.

B. 2. 1. 4   Timers

All functions within the Cree vehicle are initiated by two program timers; a main and an auxiliary unit. Earlier Crees used A. W. Haydon, Model J 3660, timers in both applications. Although no mission failures have been attributed to this timer, it was felt that improvement was called for. Tests conducted at the Inland Testing Laboratories of Cook Electric Company showed the Haydon timers to have erratic operation under certain environmental conditions. The result was a tendency of the cam assembly to rotate independently of the motor and thus cause timing errors. This was possible because of a clutch arrangement in the gear train. The J 3660 Haydon timer has been retained as the auxiliary timer in the Mod 62 Cree. However, it was modified by removing the clutch.

The main timer in the Mod 62 Cree is a model 4-23 manufactured by Acton Laboratories. This timer includes a voltage regulator and an RF filter as well as meeting the following requirements of MIL-E-5272C:

> Vibration : 5-200 cps, 0. 125 inch double amplitude,
> 30 g's, 3 planes
>
> Shock : 150 g's, 11 milliseconds, two directions,
> 3 planes, or 300 g's, 3 milliseconds, two
> directions, 3 planes.
>
> Acceleration : 125 g's, two directions, three planes.

B. 2. 1. 5   Timing Mark Generator

The timing mark generator used in the Mod 62 Cree is a specially designed solid state unit manufactured by the General Time Corporation as Model 208-4044. It operates on 28 V DC and produces marking pulses on both the on-board film and telemetry as follows:

> Frequency : 100 pps ± 1 percent

Environment :

Vibration : 15-20 g's, 15 to 2000 cps

Shock : 100 g's, 11 milliseconds

Acceleration : 75 g's

B. 2.2 Programming

The first movement of the Cree vehicle during launch pulls lanyard pins from the main and auxiliary system initiation switches. These switches energize the program timers and remove the transducer voltage. This latter function is intended to prevent the high-G conditions during launch from upsetting the TM recorders.

The first function of the program timers is the Nike to Cree booster separation. This is accomplished by firing an explosive ring in the transition cone after last stage burnout. After booster separation, the transducer voltage is restored. The calibration cam of the program timer has two notches. When the switch reaches these notches, the Ledex automatic stepping switch is energized to provide telemetry calibration immediately before and after the test point. The on-board camera is energized two seconds before the test point to allow the camera to build up speed. At the desired point in the trajectory, two mortars are fired by the timer to eject the can containing the test parachute. The ejection of the can removes a short on the time mark generator which now produces 100 pps marks on the on-board film and on one channel of the TM record. These marks help in the correlation between the film and TM, as well as providing accurate event times for parachute snatch and full open conditions.

At the end of the timer period, the recovery sequence is initiated by firing the dive brake squibs, by separating the nose weight and by arming the recovery parachute aneroid. At 10,000 feet the aneroid closes, firing the recovery door charge. The recovery chute is ejected after a 0.1 second delay. On water entry, salt water batteries open an explosive air valve, causing the balloon to inflate. To aid recovery, dye and shark repellent are attached to the balloon. A sonar devide is inserted in a bag in a recovery chute line as a location aid after water impact.

B. 3 VEHICLE STRUCTURAL MODIFICATION

As a result of the preliminary structural and aerodynamic investigations, the following Cree test vehicle improvements and additions were made. Figure B. 6 shows the Cree vehicle, less ballast.
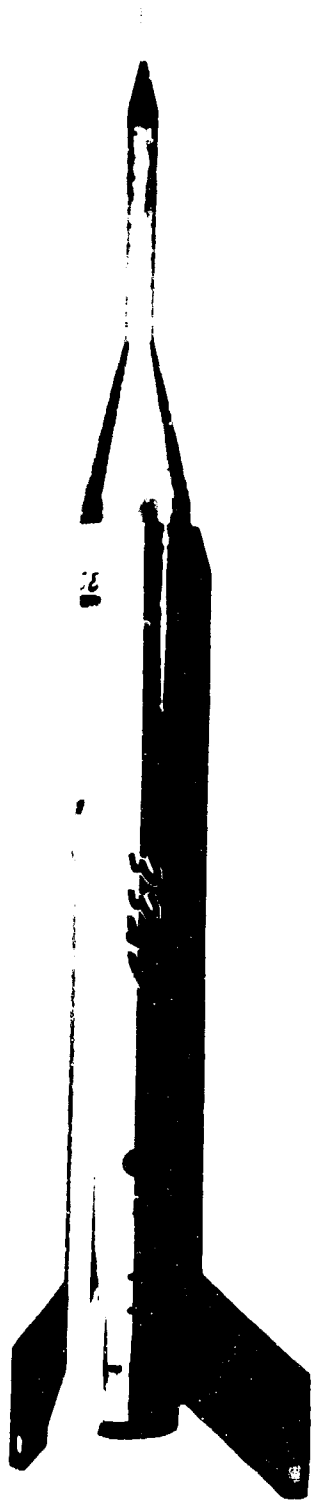
123.

Figure B.6 General Cree Vehicle

Figure B.7 Cree Vehicle With Dive Brakes Extended

B.3.1 Dive Brakes

A major structural change was the addition of dive brakes. The dive brakes were hinged at the rear bulkhead and opened with the air stream. The brake deployment was initiated by the program timer at approximately $T_o + 113$ seconds. Actuation was begun by a pyrotechnic device and augmented by a compression spring. The brakes were mechanically locked in the extended position to prevent their closure during the near-zero dynamic pressure encountered at the peak of most planned trajectories.

The addition of these 0.75 square foot dive brakes was calculated to reduce the re-entry velocity at 10,000 feet from 1200 fps to 600 fps. This reduction in velocity would allow a high reliability recovery with a proven 8 foot diameter FIST ribbon parachute at a deployment altitude of about 10,000 feet. Deployment of the recovery parachute was initiated by aneroids set to close a circuit at 10,000 feet. Figure B.7 shows the Cree vehicle with dive brakes extended.

B.3.2 Recovery Doors

Analysis of past Cree test data indicated the possibility of the structural failure of the forward portion of the recovery doors under high dynamic pressure ($q = 10,000$ psf) conditions. The recovery door backup and break strips were extended to cover the balloon compartment. The break strips were increased in thickness and changed from 7075-T6 aluminum to 2024-T3 aluminum. This change in material improves the notch sensitivity of the break strip and reduces the likelihood of inflight cracking due to vibration and loads. An aerodynamic fence was also added to divert the air flow over the leading edge of the recovery doors.

B.3.3 Antenna and Antenna Support

The telemetry antenna system was redesigned for ease of assembly and to incorporate high temperature materials. The support was made from rolled asbestos laminate and the antenna itself was made from a welded stainless steel assembly with an Inconel-X tip.

B.3.4 Cree Fins

The Cree fins were upgraded in material selection from a commercial Grade 1020 to an aircraft quality 4130 alloy steel. Slots were cut in each fin to provide a readily available location for the recovery boat personnel to attach a line to pull the vehicle from the water. Figure B.8 shows the Cree vehicle being lifted from the water.

B. 3. 5 Ballast

To simplify the problems of nose weight separation and possible tip-off damage to the telemetry antenna, an internal sleeve was welded into the nose ballast. In order to eliminate binding under flight-induced loads, a 1/4 inch clearance was provided between the sleeve and nose spike. The sleeve also simplified assembly procedures.
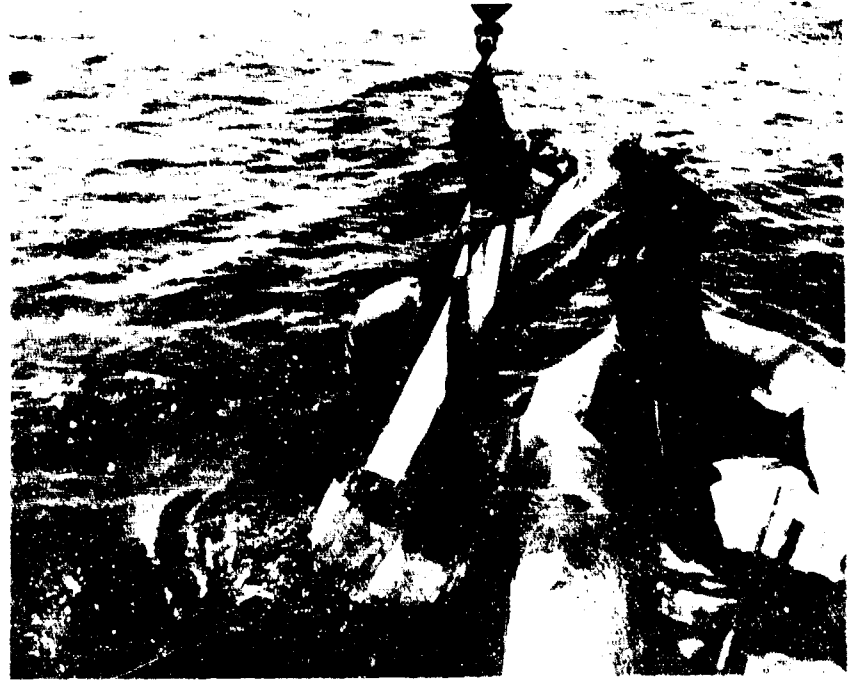
B. 3. 6 Fastener Reduction

The Cree test vehicle was originally designed for test parachute loads of 64,000 pounds; however, the maximum anticipated test parachute loads for this phase were 2,000 - 3,000 pounds. Careful recheck of the original stress analysis substantiated that one-half of the bulkhead and longeron fasteners could safely be removed. This reduction greatly simplified initial fabrication and in-field maintenance.

B. 3. 7 Cree Skins

The test vehicle skins were changed from 7075-T6 aluminum to 2024-T3 aluminum. This change was based upon reduced loads, simpler fabrication, and the reduced notch and scratch sensitivity of 2024-T3 alloy.

B. 3. 8 Nose Spike

The nose spike was reduced in length by 19 inches. This reduction in length increased the bending strength at water impact and also decreased handling problems. There was no effect on telemetry transmission.

B. 4 PYROTECHNIC SYSTEMS TESTING

Structural modifications as described in Section B. 2 and the aerodynamically induced high temperature requirements necessitated some modifications and additions to the Cree test vehicle pyrotechnic assemblies.

B.4.1 Recovery Doors

The extension of the backup and break strips over the balloon compartment on the recovery doors required that tests be made to establish that no fragments would enter the balloon area. Sheets of paper were stretched under the backup strip in the balloon compartment. In the first test, there were several 1/16 inch diameter holes in the paper. The backup strip was widened and additional tests were repeated with no more holes being made in the paper.

B.4.2 Screw Cutters

The pyrotechnic release for the dive brake door is a screw cutter. Tests were accomplished which increased the size of the cut screw from a previously designed No. 6 to a No. 10 screw. The cut screw was an AN 509-10 and the explosive was a duPont S-68, 4-grain squib. No malfunctions were found throughout the testing.

B.4.3 Test Parachute Ejection

The test parachute ejection system is identical to that used in the previous Cree phases. However, one full scale test was accomplished at Eglin Air Force Base as a precautionary step. This test was satisfactory.

B.4.4 Recovery Balloon Inflation

Three tests were accomplished at Eglin Air Force Base to test the Recovery Balloon inflation system. These tests were primarily done to check the breaking of the nylon line that holds the balloon cover in place. All tests were satisfactory. Figure B.9 shows the Cree vehicle floating in the water while Figure B.10 shows the position and relative size of the balloon.

B.4.5 Recovery Parachute Ejection

The recovery parachute ejection system failed during the first test and the Cree vehicle sank. Additional investigation showed that the wrong propellant had been procured and used. Since it was judged too late in the program to obtain the correct propellant, tests were performed to establish the correct charge weight with the new propellant. This weight was established at 3.5 grams. Failures that occurred later in the program tend to show that even this charge weight may have been too much and that future work should be done in this area. (The propellant used in previous Cree work was Hercules Powder Company M-9, 81 mm grain, while that used for the current program was M-9, 60 mm grain.)
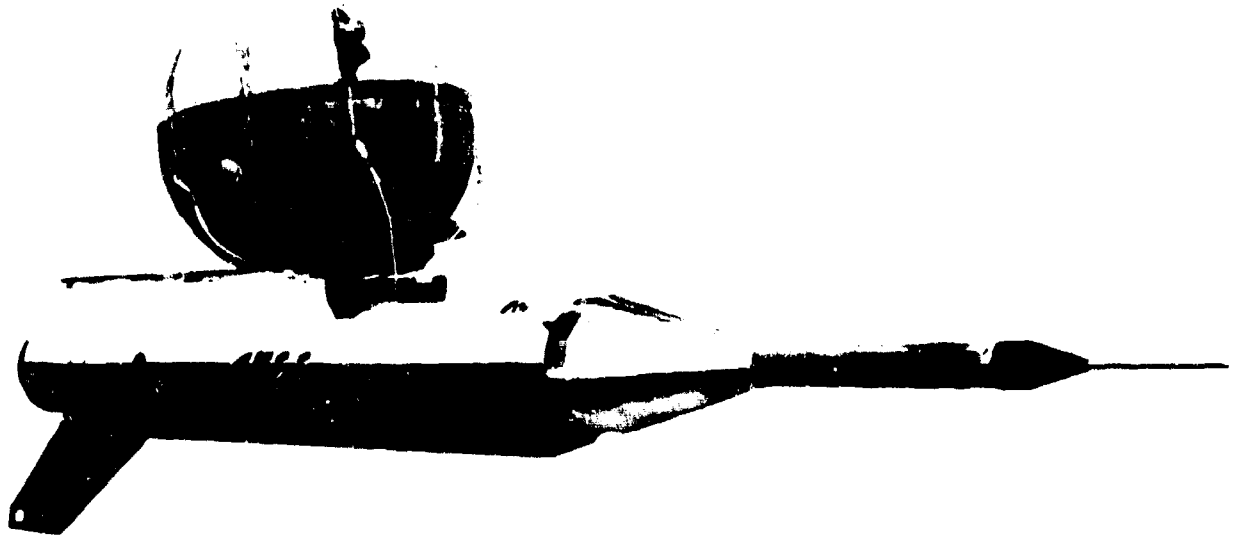
Figure B. 9 Floating Cree Vehicle

Figure B. 10 Cree Vehicle With Inflated Balloon

128.

B. 4. 6 High Temperature Explosives

High temperature Flexible Linear Shaped Charge (FLSC) and detonators were obtained from the Explosives Division of duPont. Due to time limitations, the charge sizes were based upon manufacturer's recommendations. It was apparent that the energy produced by the FLSC and detonator type used for the recovery doors was slightly above required level. However, no known failures can be attributed to this.

B. 5 AERODYNAMIC AND TRAJECTORY ANALYSIS

Trajectory studies were conducted with the aid of the Tech-Center Division Electronic Computer Facility. In order to perform these studies and to make final selection of booster-vehicle combinations for the various test points, estimates of drag and lift were required. The methods used for the determination of these aerodynamic characteristics are described below.

B. 5. 1 Drag

Estimates of the aerodynamic drag were made for the Cree vehicles, the booster-vehicle combinations and the recovery package.

The basic Cree vehicle configuration is the same as that used on previous programs, the primary differences being the addition of recovery brakes and the use of larger fins (12 inches by 14 inches) for the higher altitude, higher Mach number tests. Drag of the vehicle was estimated by using known values from the previous programs with corrections made for the recovery brakes and the larger fins. Since the fin planform was not changed, the drag contribution of the larger fins was estimated by the use of a direct area ratio. Recovery brake drag was estimated for both the closed and extended positions. For the closed position, the hinge was assumed to be equivalent to a flat plate and the aerodynamic force and projected brake area were assumed to be equivalent to that of a 20 degree half-angle wedge. Base drag was added to these values. The drag contributions of the extended drag brakes were assumed to be equivalent to 75 percent of the flat plate drag in supersonic flow and a drag coefficient of 0. 8 was assumed for subsonic flow.

For the booster-vehicle combinations utilizing the Nike booster, known drag values from previous programs were used with corrections for the increased contribution from the Cree vehicle due to the recovery brakes and larger fins as described above. For the boost configurations utilizing the Honest John, the drag contribution of the Honest John booster during thrust was obtained from Reference B. 1. Base drag during coast for the Honest John was estimated with the aid of Reference B. 2.

B.5.2 Lift and Center of Pressure

Lift curve slope pressure for the Cree vehicle and booster-vehicle combinations was estimated for the subsonic and supersonic flight regimes as follows:

B.5.2.1 Subsonic Flow

For the body, the normal force curve slope, C_N, was assumed to be 2.0 per radian and slender body theory was used to determine the center of pressure location. Reference B.3 was used to determine the lift curve slope of the fins, with the following corrections for compressibility and body upwash:

$$(C_{L_\alpha})_{comp} = \frac{(C_{L_\alpha})_{inc}}{\sqrt{1 - M^2 \cos^2 \Lambda}} \quad , \text{(Ref. B.2)}$$

Employing potential flow theory for body upwash on a trapezoidal fin:

$$C_{L_\alpha} = \left\{ \frac{Cr}{S}(b-a)(1 + a/b) - \frac{\tan \Lambda}{S} \right.$$

$$b^2 \left[1 + (a/b)^2 \right] \left[1/2 - a/b \right]$$

$$\left. - \frac{\tan \Lambda}{S} a^2 \, Ln \, (b/a) \right\} (C_{L_\alpha})_{comp}$$

where

M	=	Mach number
Λ	=	angle of sweep - degrees
C_r	=	Root cord - ft
a	=	body radius - ft
b	=	body radius plus semi-span - ft

130.

C_{L_α} = lift curve slope - per radian

S = planform area - ft^2

inc = refers to incompressible

comp = corrected for compressibility

Center of pressure was assumed to be at the quarter chord location.

B.5.2.2 Supersonic Flow

Center of pressure and lift curve slope for the body were determined by use of Reference B.4. Center of pressure of the fairings was assumed to be at their geometrical center and normal force slope was assumed to be that of an equivalent cone as given in Reference B.5. Lift curve slope and center of pressure for the fins were determined from Reference B.6.

B.5.3 Stability

Normal force contributions of the body, fins, adapters, and fairings were combined to determine the center of pressure location for the various booster-vehicle combinations used. These values were then compared with the center of gravity locations throughout the Mach number range to be experienced by these various combinations. For all cases, the minimum static margin of stability was 5 percent of the length of the configuration under consideration. This minimum margin occurred at lift-off for the three-stage Honest John-Nike-Nike-Cree 500 pound test vehicle. For all other cases, the static stability margin was much larger.

B.5.4 Booster Selection

Selection of booster combinations was limited to use of the Honest John and Nike motors. Trajectory studies were performed with the aid of the Tech-Center Electronic Computer Facility. Final selection of the booster combinations used was determined by the test point Mach number-altitude requirements, minimum Mach number during coast, maximum dynamic pressure encountered and the maximum time required for initiation of an event. The minimum Mach number during coast was limited to 0.5 due to stability considerations. The dynamic pressure was limited to a maximum of 8000 psf because of possible vehicle structural limits. The particular type of timers used limited the last sequencing to less than 120 seconds. The above limitations did not restrict the use of booster combinations that otherwise would have been selected.

131.

B. 5. 5 <u>Separation Dynamics</u>

A major problem associated with multistage boosters is that of assuring adequate separation between stages and between the last stage booster and test vehicle. Past experience with the booster combinations involved in the present tests has shown that adequate separation will be obtained upon release of the first and second stages involved. A complete study was made of the separation problems associated with the last stage booster-test vehicle separation.

Analysis shows that relative acceleration between two separating vehicles is given by:

$$\frac{\Delta a}{g} = \frac{q}{(W/C_D A)_1} \left[\frac{(W/C_D A)_1}{(W/C_D A)_2} - 1 \right]$$

where

Δa = relative acceleration, ft/sec^2

g = local acceleration due to gravity ft/sec^2

q = dynamic pressure, lb/ft^2

W = vehicle weight. lb

C_D = drag coefficient

A = reference drag area, ft^2

1 = refers to forward vehicle

2 = refers to rear vehicle

It is seen from this expression that the ballistic coefficient, $W/C_D A$, of the test vehicle must be greater than that of the empty last stage booster in order for positive separation to occur. For determination of the ballistic coefficient, the total drag of the Cree vehicle was used. For booster drag, contributions of the fairing, skin, fins and base drag were used The results of this investigation revealed that favorable separation conditions did not exist for the 250 pound Cree-Nike booster combination. For this reason, the 250 pound test vehicle was ballasted to a total weight of approximately 500 pounds.

Using this weight, it was found that conditions for test vehicle separation from the booster were favorable for all tests. Trajectory studies were made to insure that the separation distance was adequate at the time of test item deployment and that subsequent collision between the test vehicle and last stage booster would not occur. Based upon Ref. B.7, the drag contribution of the nose was added to the booster drag after initial separation of 3 test vehicle diameters.

B.6   FIELD PROGRAM TESTING AND FACILITIES

B.6.1   Pre-Flight Preparation

B.6.1.1   Calibration

All the transducers used in the Mod 62 Cree were low level strain gages. Parachute shock and drag strain gages were mounted on a single tensiometer. The shock channel was operated at one-half nominal input excitation to reduce its sensitivity. Calibration of the tensiometer was performed at the time of manufacture at the Tech-Center Division. In this test, the tensiometer was accurately loaded and the resulting output voltage from the gages was recorded.

The Mod 62 Cree used accelerometers in the 1-5 "g" range. In this range, the earth's gravitational field served as a check of the manufacturer's calibration. For this test, a Leeds and Northrup slide-wire voltmeter was used to record the transducer output voltage at 1 "g".

The air pressure transducers were calibrated by means of a Central Scientific Co. vacuum pump and manometer. Output voltage measured on the L&N slidewire voltmeter was recorded as the air pressure varied.

Each telemetry channel was provided with a calibration circuit which simulated approximately 40 and 80 percent outputs. The exact value was determined by measuring the output voltage in each calibrate position. This value was transferred to the curve of measured parameter versus output voltage to obtain the value of tension, "g", or pressure simulated by each calibrate position. The final step in the calibration of the Cree telemetry was to set up the Voltage Controlled Oscillators (VCO). The VCO's were adjusted to produce the lower and upper frequency limits as when zero and 20 millivolts, respectively are applied. The linearity was checked by plotting the output frequency as the input voltage was varied in 5 millivolt steps.

133.

The TM deviation was held to 100 ± 10 Kc. The sub-carrier taper and total deviation was set up using a New London Instruments Company Model 257 A Modulation Monitor.

B. 6. 1. 2   Squib Circuit Checks

Before final assembly of the Cree vehicle, the squib circuits were checked for operation and safety. In this test, the squibs were replaced by pilot lamps. The program timer was started by releasing the lanyard switches. The lamps lighted as the various squib voltages were applied. To assure the safety of the squib circuitry, a series of resistance, voltage and current measurements were made at each squib position. During this test, all systems of the missile were operated. This test was intended to discover any interaction between systems or any faults in the squib circuits capable of causing premature detonation or other malfunctions.

B. 6. 2   Pre-Flight Checkout

The first pre-flight check was referred to as the Horizontal Operational Readiness Check (HORC). For this test, the vehicle was not assembled to the boosters. The TM system was monitored by the TM receiving station at Site A-6. The signal strength, deviation and frequency were reported. The operating voltages and currents were measured. A recording of the sub-carriers was made during manual calibration. A vertical ORC was scheduled after all problem areas discovered in the HORC were corrected. In the vertical ORC, the Cree was mounted to the boosters and elevated to the launch position. The TM checks listed above were repeated and operation of the radar beacon was confirmed by Site A-20.

The pre-launch routine was the same as for the vertical ORC. At T_o-30 minutes, radar tracking (Site A-20) and TM tracking (Site A-6) were contacted. Initial checkout was performed using external power. When radar tracking and TM reception had been reported, the vehicle was switched to internal power. Monitor voltages and TM parameters were compared to values recorded during the vertical ORC. When proper operation had been confirmed, the radar beacon was switched back to external power and the TM system was turned off. At T_o-10 minutes, all systems were again checked on external power. At T_o-2 minutes, the Cree was switched to internal power. Recorders were started at Site A-6 at T_o-1 minute. The TM calibrate positions were manually stepped through as a pre-flight calibration. Figure B. 11 shows an Honest John-Nike-Nike 500 pound Cree being readied for launch.
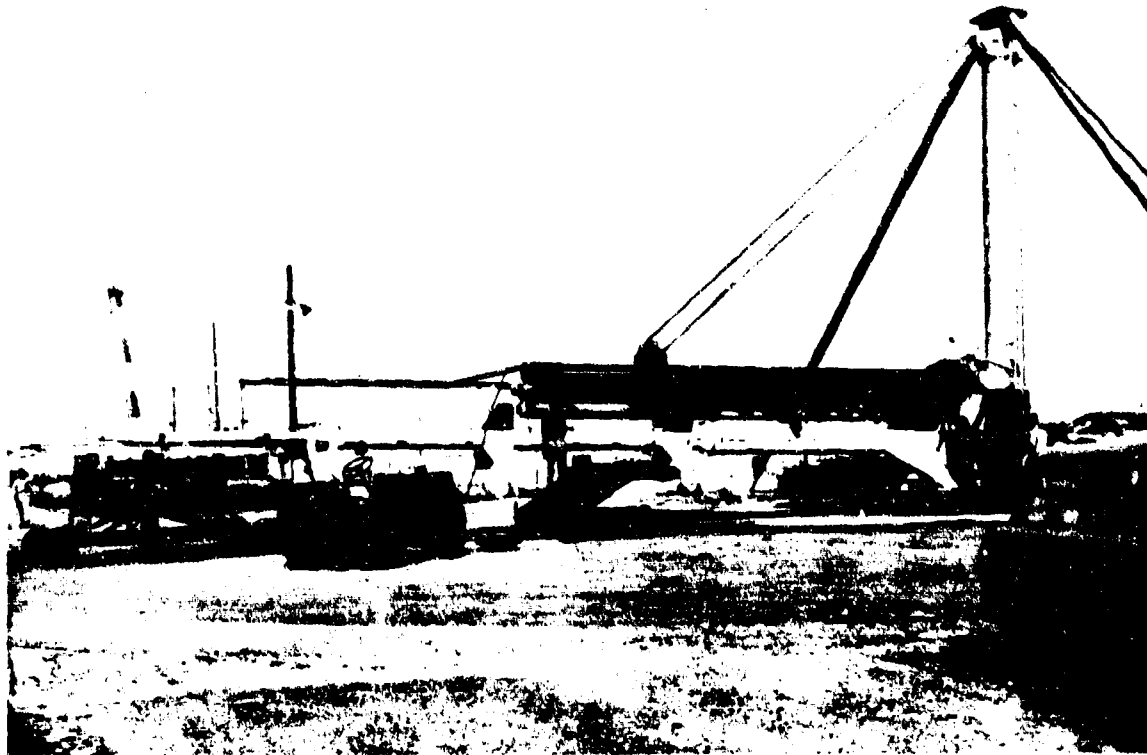
B . 11 Final Launch Preparations

B. 6. 3 Support Equipment

The Cree was visually tracked by Contraves phototheodolites. The quality of the Contraves record is affected by factors such as atmospheric conditions and site location. Good tracking was achieved through the test point on the lower altitude missions. Under hazy conditions, tracking was lost well below the test point. Under optimum conditions, the Contraves were considered the primary source of initial (0-120,000 feet) flight data.

The Cree was radar tracked from Site A-20 using two FPS-16 radars. One radar was used to track the AGA C/T CV beacon. The second radar was used to skin track. The skin tracking radar often followed the separating booster rather than staying with the Cree vehicle. To avoid this, a tracking aid called AGAVE was used. The AGAVE received the TM signal and was capable of reading out the approximate position of the payload by a direction-finding technique. If the position established by AGAVE diverged from the FPS-16 track, it was assumed that the skin tracking radar was following a booster. A new search was initiated by the FPS-16 in the area reported by the AGAVE.

135.

Telemetry was recorded at Site A-6 and D-3 on magnetic tape, a Sanborn recorder, and on a Midwestern recorder. The magnetic tape served as a permanent reproducible record of the flight. The Sanborn recorder operated at low speed and gave a quick-look capability for the entire flight. The Midwestern recorder operated at high speed and was suitable for data reduction. This recorder provides a non-fixed photographic type record which fades after long exposure to light. However, permanent records were obtained at a later period upon request.

B.7 FUTURE VEHICLE UPDATING

To correct the operational deficiencies and to provide for a better data gathering test vehicle, the following vehicle updating is strongly recommended should any future testing be done with the Cree as the test vehicle.

B.7.1 General Vehicle

Sufficient length (about 6 inches) should be added to the Cree vehicle to simplify assembly of the instrumentation packages and recovery equipment. In addition, this added length would provide an area where the dive brake hinge could be housed internally. This would also reduce drag and allow the design of a brake which would not be lost at water impact.

B.7.2 Pyrotechnic

Additional testing should be done with the high temperature explosives used on the recovery doors. In particular, the initiator holder should be "beefed up".

The recovery parachute ejection system requires a complete reanalysis, not involving the procedure used but rather the explosive used and its charge weight. The vehicle structure supporting the explosive should be "beefed up" and made from steel rather than aluminum. This will provide higher reliability, particularly when the same vehicle is reused many times. The nut supporting the test parachute ejector should have more thread engagement.

B.7.3 Telemetry an Electronic Systems

The telemetry system used was by and large very satisfactory. The addition of an event channel could, in the case of a malfunction, help to pinpoint the trouble. Several electrically actuated relays were used in the system; these should be eliminated because of possible chatter.

Power is removed from the transducers and tensiometer during the boost phase of the trajectory. It now appears it would be better to leave power on so that the strain gages do not cool off. This cooling off and then reheating may cause a zero shift. There should be no effect to the equipment caused by leaving the bridge voltage on. It does eliminate any evidence of a possible VCO zero shift. However, with the new VCO's, no zero shift was noted during this program that can be attributed directly to the VCO's.

The inter-vehicle wiring must be protected from the salt water. Teflon wiring was used because of anticipated heat; however, providing a salt water seal at connectors is almost impossible for teflon wire with present-day sealants. It might be better to return to ordinary wire and provide a separate heat-protecting sleeve.

A circuit should be added to cut off all power within the Cree vehicle upon water impact. This would greatly reduce battery damage from over-discharge and prevent salt water damage by electrolysis.

The initiation of nose weight separation, dive brake actuation and recovery system arming should be accomplished from two different cams on the program timer. Nose weight separation and dive brake actuation may be accomplished from the same cam, but recovery system arm should be separate. In addition, the nose weight and dive brake actuation should return to a power-off position after completion. This will eliminate the possibility of a short in these circuits draining the power required for recovery.

B. 7. 4 Instrumentation

The re-entry test results were in many ways of as much interest as the planned test regime data. To help enhance the value of the re-entry data, the on-board camera should be stopped after about 10 seconds and then restarted during re-entry at slow speed.

A very low range (50 pounds) tensiometer should be developed for use at low dynamic pressures. It should be recognized that this tensiometer will break during re-entry and that a higher range tensiometer should be placed in series so that the re-entry loading data will not be lost.

B. 7. 5 Location Aids

A reliable sonar beacon should be acquired and a suitable location found for it on the vehicle. What is most necessary, is to find a place where the beacon can survive the water impact.

APPENDIX B

REFERENCES

B.1 Clarence A. Brown, Jr., Performance Analysis of Six Solid-Fuel Rocket-Motor Boost Systems with Payloads of 300 to 2000 Pounds, NASA TMX-131, December 1959

B.2 S. F. Hoerner, Fluid Dynamic Drag, August 1957

B.3 F. W. Diederich, A Plan Form Parameter for Correlating Certain Aerodynamic Characteristics of Swept Wings, NACA TN 2335, April 1951

B.4 W. H. Dorrance and Robert C. Norell, Correlation of Cone-Cylinder Normal Force and Pitching Moment Data by the Hypersonic Similarity Rule, JAS Vol. 24, No. 5, May 1957

B.5 Equations, Tables and Charts for Compressible Flow, NACA Report 1135, 1953

B.6 Martin, Margolis, and Jeffreys, Calculation of Lift and Pitching Moments Due to Angle of Attack and Steady Pitching Velocity of Supersonic Speeds for Thin Sweptback Tapered Wings with Streamwise Tips and Supersonic Leading and Trailing Edges, NACA TN 2699, June 1952

B.7 Cook Research Laboratories, Recovery System Design Study for a Ballistic Re-entry Vehicle, Final Summary Report, November 1960